January 1983

Alteration of Availability of Heavy Metals to Aquatic Microflora by Complexation with Organics Associated with Oil Shale Development

Bruce S. Mok

Jay J. Messer

Alteration Of Availability Of Heavy Metals To Aquatic Microflora By Complexation With Organics Associated With Oil Shale Development

Bruce S. Mok and Jay J. Messer

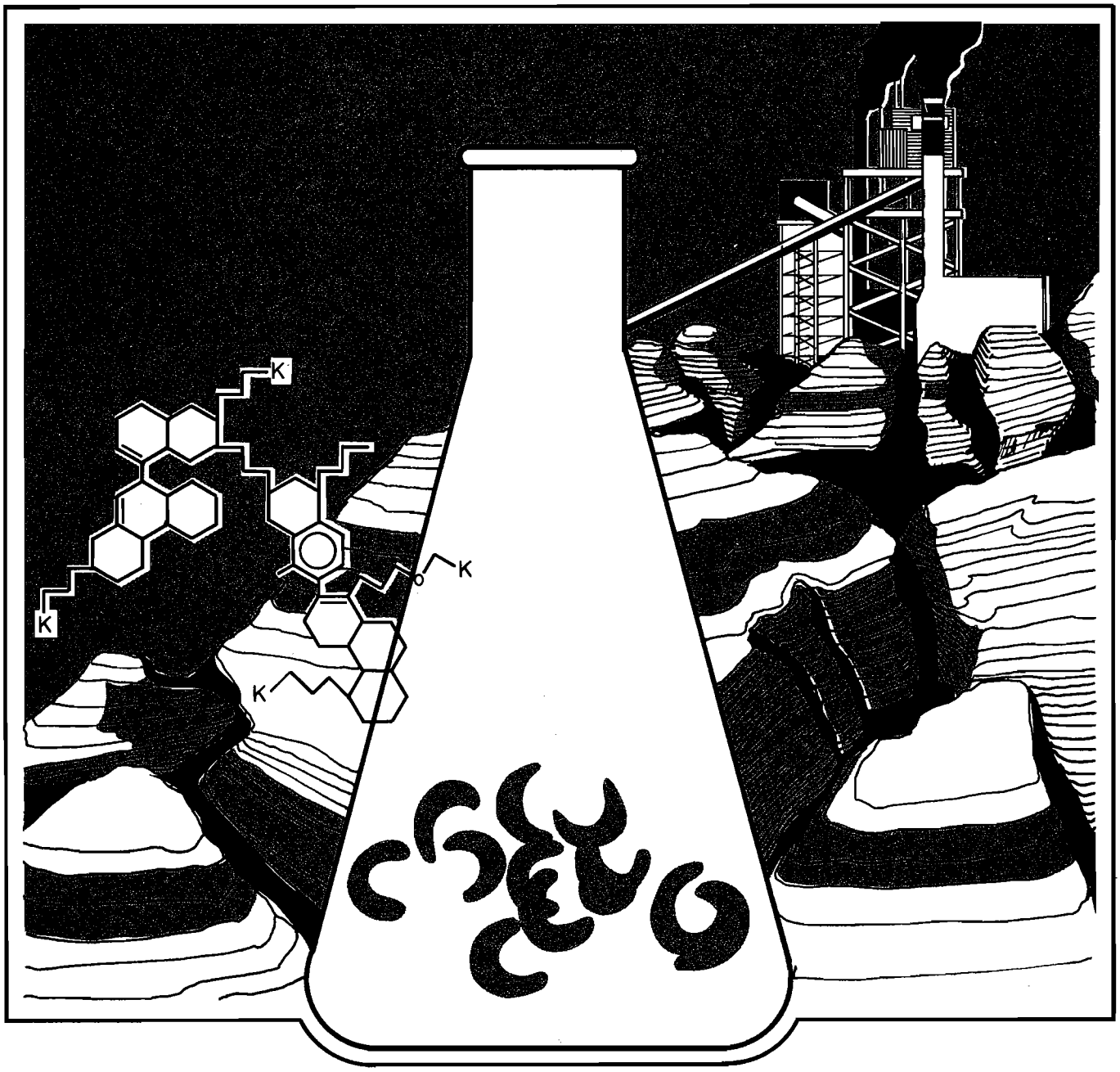

Utah Water Research Laboratory
Utah State University
Logan, Utah 84322

WATER QUALITY SERIES
UWRL/Q-83/05

May 1983

ALTERATION OF AVAILABILITY OF HEAVY METALS TO AQUATIC MICROFLORA BY COMPLEXATION WITH ORGANICS ASSOCIATED WITH OIL SHALE DEVELOPMENT

by

Bruce S. Mok
Jay J. Messer

The research on which this report is based was financed in part by the U.S. Department of the Interior, as authorized by the Water Research and Development Act of 1978 (P.L. 95-467).

Project No. A-051-UTAH, Contract No. 14-34-0001-1147

WATER QUALITY SERIES
UWRL/Q-83/05

Utah Water Research Laboratory
Utah State University
Logan, Utah 84322

May 1983

ABSTRACT

Leachates from both raw (unretorted) and Paraho retorted oil shale show the ability to bind copper, and perhaps cadmium, strongly enough to mitigate the inhibitory effects of these metals on the growth of the test alga, Selenastrum capricornutum. No detoxification of nickel was observed. The organic fraction of both leachates large enough to be retained by a UM2 ultrafilter were stimulatory to algal growth both in the presence and absence of added metals, possibly because of their ability to supply trace metal nutrients (e.g. iron) or to detoxify trace metal toxicants (e.g. copper) through complexation equilibria. The smallest size fraction of raw shale leachate, including inorganic ions and small organic ions capable of passing a UM2 ultrafilter, was highly toxic to the test alga. This corresponding fraction of Paraho retorted shale was also toxic, but to a lesser extent.

The nature of copper complexation by the oil shale leachate organics is suggestive of the binding of this metal by natural humic and fulvic acids in aquatic systems, although complexation capacities and conditional stability constants appear to be somewhat lower on an organic carbon basis. Complexation does not appear to be caused by the low-molecular weight ring-N compounds characteristic of retort water. Oil shale leachates are only likely to significantly increase copper and cadmium binding and transport in receiving waters if the corresponding TOC concentrations become similar to or greater than that contributed by natural humic and fulvic materials.

ACKNOWLEDGMENTS

We sincerely thank the following people for their assistance: Dr. Patrick L. Brezonik, Dr. L. Douglas James, Dr. Fredrick J. Post and Dr. Ronald C. Sims for their comments on the manuscript, Dr. John R. Tuschall, Jr., for his advice during the research, and Charles Liff for his assistance in computer programming and graphics. In addition we would like to acknowledge the staff at the Utah Water Research Laboratory, particularly, Leslie Johnson for typing and Donna Falkenborg for editing the manuscript.

This research was supported by the U.S. Department of the Interior, Project No. A-051-UTAH, Contract No. 14-34-0001-1147 (JER051).

TABLE OF CONTENTS

TABLE OF CONTENTS (CONTINUED)

LIST OF FIGURES

LIST OF FIGURES (CONTINUED)

LIST OF FIGURES (CONTINUED)

LIST OF TABLES

LIST OF TABLES (CONTINUED)

CHAPTER I

INTRODUCTION

Western Oil Shale

Redente et al. (1981) summarized the likely development of the Western U.S. oil shale industry in the following way. Known high-grade oil shale in the Green River formation contains 600 billion barrels of oil in place, with 80 billion barrels recoverable using present technology. With sufficient economic incentives, a U.S. industry producing 1-20 million barrels of oil per day is foreseeable. Such an industry would supply 1.3-26 million metric tons (MMT = 10^9 kg) of raw shale per day to surface retorts and would produce 1.1-22 MMT of spent shale. Modified *in situ* (MIS) retorting would probably reduce the amounts of shale handled on the surface by 70 to 80 percent with the remainder processed by underground retorts. Approximately 500-700 ha of land is expected to be required annually for spent shale disposal for a 1 million barrel per day industry, and a similar amount of land would be required for raw shale storage.

Slawson (1979) identified more than two dozen potential water quality impacts associated with a Western U.S. shale oil industry. Such sources include high-molecular weight organics, polycyclic aromatic hydrocarbons, heavy metals, other toxicants such as ammonia, arsenic, and fluoride, increases in salinity and turbidity, and alterations in pre-existing hydrologic regimes (Messer and Liff 1982). The potential impacts are of particular concern because the Colorado River, which drains the entire western oil shale region, serves as the virtual lifeline serving agriculture and the large metropolitan areas in the Pacific Southwest as well as providing the sole refugium of many rare and endangered species of fish (e.g., Adams and Lamarra 1983). The aquatic ecosystem of the river basin includes several important reservoirs with valuable recreational amenities, including Lake Powell (Utah-Arizona) and Lake Mead in Nevada.

Recent investigations have indicated that water soluble extracts from both raw and spent shales and from shale oils can be either phytotoxic or stimulatory to the growth of algae under bioassay conditions, depending on source, pretreatment, concentration and other poorly understood factors (Cleave et al. 1979, 1980; Griest et al. 1981; Giddings and Washington 1981). Although the effects of inorganic nutrients or toxicants could not be ruled out on the basis of these experiments, shifts from algal growth enhancement to toxicity with increasing organic concentration is characteristic behavior for both natural and synthetic organic ligands, both in cell culture and *in situ* (e.g., Huntsman and Sunda 1980).

Organic ligands are large molecules, usually with at least two functional groups that can become negatively charged, and so bind metal ions from solution, i.e.

$$M + L \rightarrow ML \quad . \quad . \quad . \quad . \quad (1.1)$$

The strength of the bond is reflected in the equilibrium constant for the reaction, K_f,

$$K_f = \frac{[ML]}{[M][L]} \quad . \quad . \quad . \quad . \quad (1.2)$$

with high values of K_f for a particular

metal-ligand complex being associated with a low free metal ion concentration in solution. Similarly, by mass action relationships, high ligand concentrations will also result in low free metal ion concentrations. Such organic functional groups capable of binding heavy metals have been found to be associated with oil shale process waters (e.g., Fish 1980), and metal-organic complexation also has been found to be associated with various process wastewaters by Stanley et al. (1982).

The findings reported above suggest that metal-organic complexation could affect both the transport and availability of heavy metals to phytoplankton in Colorado River Basin reservoirs if the oil shale industry develops and proper environmental precautions are not taken. The source of the organics would be leachate escaping piles of raw or spent shale or accidential spills or releases of process waters. In addition to these sources, heavy metals may also originate from deposits in river or reservoir sediments originating from historical mining operations in the basin (Fox 1977). The nature of the interactions between the organics and heavy metals is discussed more thoroughly below.

Research Goals

The approach taken here was to apply parallel developments in understanding heavy metal-humic acid interactions, a field that is presently young, but active (Christman and Gjessing 1983). The research goals were:

1. Evaluating different complexometric titration techniques that could potentially lead to a quick, low-cost, operationally defined method of determining the complexation capacity of a particular leachate.

2. Differentiating the effects of organic ligands, stripped of their associated salinity and inorganic nutrients and toxicants, from those of heavy metals on algal growth in laboratory bioassays.

3. Estimating metal detoxification by oil shale organic ligands from quasi-thermodynamic parameters determined using the complexometric titration techniques examined in 1.

However, several points about the goals of this study need emphasis at the outset.

The first is that oil shale and especially spent oil shale contain a broad range of compounds whose properties depend on the characteristics of the parent material but especially on retorting conditions. Retorting methods are still highly experimental, and retorting parameters are regarded as proprietary information. Most retort runs have been done in small batches, and spent shale that has not been contaminated by storage in association with pthalate-containing plastics is seldom easy to obtain. Consequently, the emphasis in this study was shifted to raw shale. The selected source was the Mahogany Zone, the richest of the oil-bearing zones in the Green River Formation. This raw material will have to be stored on the surface in large quantities in any scenario of an oil shale industry in the Upper Colorado River Basin.

The second point to be made is that both the physico-chemical and biological results obtained in a study such as this are operationally defined. Separation techniques based on membrane ultrafiltration are affected by surface charges and membrane interactions. There is also evidence that both analytical technique and sensitivity affect the observed values of conditional stability constants and complexation capacities, and in fact that these values have no thermodynamically rigorous meaning because of violations of the assumptions underlying the models used to define metal-ligand binding

(e.g., Perdue and Lytle 1983; Tuschall and Brezonik 1983b). Also, the sensitivity of different species of algae, as well as the chemistry of the algal growth medium are known to affect metal toxicity (Sakshaug 1980).

Knowing full well that these definitional and measurement problems exist, the goal of this study was to examine potential metal-organic interactions in a controlled setting, using the lowest cost and least sophisticated methods possible. Simplicity was desired in order to have a technique that could be used in field laboratories for monitoring of oil shale wastes and leachates.

Complexometric Titrations

A number of techniques were explored. Among the least expensive are physical separations based on membrane filtration rather than on more extensive separations based on acid or base solubility and charge (e.g., Leenheer 1981). The inexpensive pressure ultrafiltration could even be done in a bench-top centrifuge (Amicon 1977). Similarly, copper titration, using continuous ultrafiltration (Tuschall and Brezonik 1983a), coupled with an ion-selective electrode (ISE) finish, provides a simple, inexpensive method for determining the potential binding capacity for a given water. Direct potentiometric binding titrations using the copper ISE (Buffle et al. 1977) would also be simple and inexpensive.

On the expensive end of the scale are differential pulse anodic stripping voltammetric (DPASV) titrations (e.g., Tuschall and Brezonik 1981) and continuous ultrafiltration (CU) with a DPASV or carbon furnace atomic absorption (AA) finish. Although these techniques require more expensive equipment and expertise, they are necessary to obtain reliable information on water with low complexation capacities, and thus also were investigated.

Methods that were not investigated included equilibrium dialysis or fluorescence quenching techniques (e.g., Saar and Weber 1982) or competing ligand differential spectroscopy (Tuschall and Brezonik 1983a), which may prove useful in further investigations. Copper was used as the test metal in most experiments because it shows maximum binding reactivity and is extremely toxic to algae in its free ionic form.

Algal Bioassays

Bioassay experiments employed the standard EPA test alga, Selenastrum capricornutum Printz. Although this species has been criticized as being unrepresentative of hardwater habitats, it has the advantage of being well-characterized and highly studied, and the growth medium is well-defined (Miller et al. 1978, Leischman et al. 1979). Thus it was used rather than an endemic Colorado River Basin test species. Corrections for differences in ion activities between Colorado River Basin water and AAP medium can be made using an equilibrium model such as REDEQL.EPAK (Ingle et al. 1980). However, additional test species should be examined in future efforts.

Organization

Following a brief literature review, the experimental methods are detailed. The following chapter compares values for the metal-binding parameters estimated for the oil shale leachates by using the various chemical techniques investigated. These parameter values are also compared to those obtained for a well-defined ligand, EDTA (ethylene-diamine-tetra-acetic acid) as well as for a commercially available natural ligand, humic acid (Aldrich). The next chapter details the results of the algal bioassays, and the final chapter relates the bioassay results to the chemical parameters determined in Chapter IV, and some potential environmental impacts are discussed. In a

companion study, Selby et al. (1983) present the results of a study in which oil shale related ligands and an associated heavy metal (cadmium) are actually applied to environmental microcosms.

CHAPTER II

LITERATURE REVIEW

Relatively little research has been done on the effects of metal-ligand complexation in oil shale leachates specifically with respect to metal detoxification of algae. Previous studies of metal-ligand interactions associated with waste products from the oil shale industry have been largely limited to the organic analytical chemistry of shale oil or retort water extracts. Furthermore, the evidence collected for oil shale-related metal-ligand effects on phytoplankton growth has been evocative but largely circumstantial in that the data are insufficient to separate the effects of metal complexation from those of macronutrient enrichment. Fortunately, however, relatively young but expanding literatures on metal complexation by humic and fulvic acids and on the effects of such complexation on the availability and toxicity of metals to algae is available to provide some useful hypotheses regarding the probable role played by oil shale ligands, should they be transported to receiving water.

This review is divided into three parts: 1) a review of what little information is available on the organic ligand chemistry of shale oil and oil shale-related leachates and process waters; 2) a brief review of the theory and practice of determining complexing capacity and conditional stability constants; and 3) a review of the role played by organic ligands in heavy metal interactions with phytoplankton. The last section will also examine the previous studies on the effect of oil shale leachate and shale oil extracts on laboratory algal cultures. The latter two reviews are only to bring out highlights pertinent to predicting the environmental impacts of oil shale development owing to the existence of several thorough and recent reviews which summarize the earlier literature.

Organic Ligands in Oil Shale

The functional groups of organic molecules that may play an important role in metal complexation act as Lewis bases. They include the carboxyl, phenolic, aliphatic alcoholic, ketone and quinoid functional groups. Also included are the nitrogenous organic functional groups, such as the amino groups and "ring-N" present in aromatic compounds, that can act as a Lewis base. Complexation may involve inner or outer sphere binding, may be uni- or polydentate, and tends to follow the Irving-Williams series (Chaberek and Martell 1959). Shale oil has been found to contain many of the above functional groups.

Hertz et al. (1980) found a basic extract of Mahogany zone shale oil to contain phenol (334 ppm), o-cresol (322 ppm), and 2,4,6-trimethylpyridine (988 ppm). Riley et al. (1979) found a variety of aliphatic mono- and dicarboxylic acids to be present in Paraho direct process retort water ranging in size up to hendecanedioic acid and totaling 333 ppm. These authors suggest that the likely source of these acids was the parent kerogen material itself, rather than oxidation of precursors in the retorting process. Although concentrations were not reported, Fish (1980) found a wide range of aliphatic mono- and dicarboxylic acids, aliphatic and aromatic nitrogen heterocycles, and cyclic aliphatic ketones in a variety of oil shale process waters. Fish

(1980) found that the total metal binding capacity based on bound Zn (and hence probably an underestimate of the capacity based on Cu) in a batch of Geokinetics retort water was 1 ppm, which capacity he determined to be associated with aliphatic and aromatic nitrogen heterocycles.

Stanley et al. (1982) also reported a variety of compounds with metal-binding functional groups in Paraho, Occidental (OXY-6) and Omega-9 retort waters. Quantitatively, they found copper complexing capacities of 3-8, 39-42, and 570-750 mg/L respectively, for the Occidental, Omega-9, and Paraho process waters. The complexing capacity was found to be correlated only with the base-extractable organic carbon, which contains the nitrogenous functional groups described above. Gel chromatography indicated that copper was complexed both by large (>1800 amu) and smaller (hydrophilic base) solutes.

None of the three wastewaters, when applied to laboratory columns of Paraho spent shale, mobilized any metal except molybdenum, although the authors noted that the high retorting temperature of the spent shale studied (750°C) probably lowered the leachability of any metals present. Others (Leenheer et al. 1982) indicated some copper transfer to be associated with both hydrophilic and hydrophobic base solutes in Omega-9 retort water applied to soils. Thus far, no studies of metal-ligand interactions in unretorted shale appear to have been published.

These observations suggest two possible sources for the metal binding capacity of raw or spent oil shale: a high molecular weight organic component associated with the original kerogen and lower weight components dominated by ring nitrogen, produced in part from the retorting process. The high-molecular weight component may be similar to soil or aquatic humic and fulvic acids, while the lower molecular weight component may consist of phenol, 2,4,6-trimethylpyridine, and similar species. The former group of organic ligands in water has been characterized as polydisperse, highly heterogeneous mixtures of biopolymers (e.g., Langford et al. 1983). They are divided into fulvic and humic acids, the former being distinguished by their smaller average size, greater hydrophilicity, and solubility at both high and low pH. They contain carboxyl, phenolic, alcoholic, ketone, quinoid, and nitrogenous functional groups (e.g., Stevenson 1982, Tuschall and Brezonik 1980) and typically exhibit conditional stability constants for copper ion in the range of 10^5-10^8 in natural waters (Mantoura et al. 1978, Tuschall and Brezonik 1983b). Phenols and substituted pyridines generally exhibit lower formation constants in the range of $10^{2.5}$-$10^{3.5}$ (Sillen and Martell 1964).

Metal-Binding by Complex Organic Ligands

The literature on metal-ligand interactions as they apply to complex, poorly characterized organics in water has been summarized in the proceedings of a state-of-the-art symposium (Christman and Gjessing 1983). Additional reviews include those of Saar and Weber (1982) on fulvic acid-metal ion interactions and Neubecker and Allen (1983) on determination of complexation capacity and condition stability constants for metal-ligand interactions in natural waters. These sources should be consulted for a thorough compilation of earlier citations, and only the more recent work will be cited here.

Mathematical treatment

Binding sites on simple monomeric molecules (e.g., resorcinol) may be characterized by a conditional stability constant for a free metal ion such as copper according to the formula:

$$K_f^c = \frac{[ML]}{[M'][L']} \quad . \quad . \quad . \quad (2.1)$$

where [M'], [L'], and [ML] represent the molar concentrations of the metal ion, free ligand not associated with ML, and the concentration of the complex, respectively. The constant is conditional because its value depends on ionic strength, degree of protonation of the weakly acidic ligand binding sites (e.g., COOH) and the degree of complexation of the metal ions by competing ligands (e.g., OH^- or $CO_3^=$). K_f^c is usually treated as the product of the thermodynamic equilibrium constant, K_f, and a series of correction factors:

$$K_f^c = \frac{K_f \cdot \alpha_M \alpha_L \cdot \gamma_M \gamma_L}{\gamma_{ML}} \quad . \quad . \quad . \quad (2.2)$$

where the α values indicate the fractions of uncomplexed metal and deprotonated ligand, respectively, and the γ terms represent activity coefficients (e.g., Stumm and Morgan 1982). The conditional stability constant also may depend on the concentrations of metal ions competing for the binding site. For example consider a second metal M' with conditional stability constant $K_f'^c$

$$K_f'^c = \frac{[M'L]}{[M'][L]} \quad . \quad . \quad . \quad . \quad (2.3)$$

Such a competing reaction adds a second α_L term to the numerator of Equation 2.2. This term may be quite small in the event that either [M'] (e.g., $[Ca^{++}]$) or $K_f'^c$ (e.g., for Fe^{+3}) is large.

Thus far, only single-ligand models have been considered. For a mixture of i ligands, or a mixture of i binding sites on the same ligand, an average conditional stability constant ($\bar{K}_f^c$) can be presented by the weighed averages

$$\bar{K}_f^c = \frac{\sum_i ML_i}{[M] \sum_i [L_i]} \quad . \quad . \quad (2.4a)$$

$$= \frac{\sum_i K_{f,i}^c [L_i]}{\sum_i [L_i]} \quad . \quad . \quad (2.4b)$$

However, Perdue and Lytle (1983) summarize earlier work that indicates when the numerator and denominator of Equation 2.4b are divided by the concentration of a reference ligand, L_r,

$$\bar{K}_f^c = \frac{\sum_i K_{f,i}^c [L_i/L_r]}{\sum_i [L_i/L_r]} \quad . \quad . \quad (2.5)$$

unless L_r and L_i have identical affinities for M, $\bar{K}_f^c$ will not be a constant, but a function of the concentration of competing ligands in solution. This variability emphasizes the highly operational nature of a $\bar{K}_f^c$ value determined by titration of a complex water sample. That is to say, changes in concentrations of constituents other than the reactants alter the value of $\bar{K}_f^c$ for the same metal-ligand complex.

The value of K_f^c, together with the total complexing capacity of a test water sample for a given metal (CC), is usually determined by some type of titration (Rosotti and Rosotti 1961). In potentiometric titrations, free metal is added to the solution, and the activity of the free metal ion is detected using an ion selective electrode (ISE). The free metal ion activity increases slowly during the early stages of the titration, according to Equation 2.1, with a break in the slope occurring when titration of the ligand is complete, or

$$C_M = xC_L \quad . \quad . \quad . \quad . \quad . \quad (2.6)$$

where C_M and C_L are the total metal and ligand concentrations, respectively. A variety of equations have been used, as

alternatives to using the break in slope, to estimate complexation capacity and K_f^c, from titration data.

Shuman and Woodward (1973) rearranged Equation 2.1 to get

$$K_f^c = \frac{C_M-[M]}{[M](C_L-C_M+[M])} \quad . \quad . \quad (2.7)$$

in the early stages of a titration, when $[M]<<C_M$,

$$K_f^c \cong \frac{C_M}{[M](C_L-C_M)} \quad . \quad . \quad . \quad . \quad (2.8)$$

and a plot of [M] versus $C_M/(C_L-C_M)$ gives a slope of $1/K_f^c$. Such a plot shows a clean break for a 1:1 complex at the equivalence point, provided that $K_f^c \times C_L > 1.0$. These authors used differential pulse anodic stripping voltammetry (DPASV) to measure [M]. Its value is proportional to the peak current, i_p, observed during the stripping of the metal ion from the electrode:

$$i_p = \kappa[M] \quad . \quad . \quad . \quad . \quad . \quad (2.9)$$

with κ being a function of stripping current, plating time, cell and electrode geometry, and other factors. Therefore, Equation 2.8 can be plotted as ip versus $\kappa C_M/(C_L-C_M)$. Above the equivalence point, $C_M>>C_L$, i_p approaches κC_M, and κ can be obtained from the upper slope of the titration curve.

Shuman and Woodward (1977) determined the complexation capacity (CC) from the plot by dropping a vertical line from the breakpoint to the X axis. Chau et al. (1974), assuming the slope of the lower curve to be close to zero, instead extended the upper slope of the titration curve to the x-axis to determine CC. This practice underestimates CC significantly if $K_f^c \times C_L < 100$ (Shuman and Woodward 1977, Figure 2). The latter authors went on to show that Equation 2.8 could be extended to complexes with a:b stoichiometry using the equation

$$i_p = \left(\frac{\kappa}{K_f^c}\right)^{1/a} \frac{(C_M/a)^{1/a}}{(C_L-(b/a)C_M)^{b/a}} \quad . \quad (2.10)$$

thus enabling the stoichiometry of the binding sites to be determined for non-1:1 complexes.

Earlier, Scatchard (1949) had proposed another formula for determining K_f^c for binding sites on proteins, which can be modified to include multiple ligands or binding sites. Perdue and Lytle (1983) summarize this concept as

$$\nu_i \equiv \frac{[ML_i]}{C_{L,i}} = \frac{K_{f,i}^c[M]}{1 + K_{f,i}^c[M]} \quad . \quad . \quad (2.11)$$

For a mixture of i ligands, whose total concentration equals C_L,

$$\bar{\nu} = \frac{\sum_i \nu_i C_{L,i}}{\sum_i C_{L,i}} = \sum_i \left(\frac{K_{f,i}^c[M]}{1 + K_{f,i}^c[M]}\right)\left(\frac{C_{L,i}}{C_L}\right)$$

$$= \frac{C_M-[M]}{C_L} \quad . \quad . \quad . \quad . \quad (2.12)$$

The interior term in Equation 2.12 can be rearranged to give the Scatchard equation for a 1:1 complex:

$$\frac{\bar{\nu}}{[M]} = K_{f,i}^c\left(\frac{C_{L,i}}{C_L}\right) - K_{f,i}^c\,\bar{\nu} \quad (2.13a)$$

A plot of $\bar{\nu}/[M]$ versus $\bar{\nu}$ thus yields a line with a slope $-K_{f,i}^c$ and an x-intercept $C_{L,i}/C_L$ = CC for a single ligand or binding site. Buffle et al. (1977) used a rearrangement of Equation 2.13a:

$$\frac{1}{\bar{\nu}} = \frac{C_L}{C_{L,i}} + \frac{C_L}{C_{L,i}} \left(\frac{1}{K_{f,i}^c [M]} \right) \quad . \quad (2.13b)$$

For two ligands or binding sites, Equation 2.13a can be expanded to

$$\bar{\nu} = \left(\frac{K_{f,1}^c [M]}{1+K_{f,1}^c [M]} \right) \left(\frac{C_{L,1}}{C_L} \right) + \left(\frac{K_{f,2}^c [M]}{1+K_{f,2}^c [M]} \right) \left(\frac{C_{L,2}}{C_L} \right) \quad . \quad (2.14)$$

with each added term adding two new parameters and consequently improving the ability to fit to a titration curve. Perdue and Lytle (1983) demonstrated that, unless there are actually only two ligands or binding sites, K_f^c and C_L cannot be assumed to be constant outside the range of experimental determination.

Two recent contributions to the binding analysis literature are found in the graphical methods of Ruzic (1980) and Klotz (1982). Ruzic (1980) rearranged Equation 2.7 to give

$$\frac{[M]}{C_M - [M]} = \frac{1}{CC} \cdot [M] + \frac{1}{(K_f^c)(CC)} \quad . \quad (2.15)$$

which can be used for the entire range of a titration. Klotz (1982) criticized many published Scatchard plots on the basis that the titrations often failed to reach their true endpoints, usually because the presence of more than one binding site causes the slope of the graph to change near the apparent endpoint. He suggested that only by plotting log [M] versus [ML] can one be assured that CC is correct.

Titration techniques

Other methods (than DPASV) also exist for determining the metal ion concentrations [M], by far the most straightforward is the ion-selective electrode (ISE). In a typical application (e.g., Buffle et al. 1977), free metal is added to a water sample, and the ISE gives a Nernstian voltage response (ΔE) to the uncomplexed metal. The potential can be converted to [M] by using a suitable calibration curve, or a plot such as that recommended by Shuman and Woodward (1977) can be made, with 10 $\Delta E/S$ replacing i_p on the ordinate. E represents the potential and S represents the slope of the calibration curve. Alternatively, titrations in the presence and absence of the suspected ligand can be made, and the difference between the potentials (E_o-E) at corresponding points in the titrations is proportional to:

$$\frac{[M]}{C_M} = C_M \times 10^{(E_o - E)/2.3\ RT/zF} \quad . \quad (2.16)$$

where RT/zF are the parameters in the Nernst equation. Those who have used this ISE technique include Buffle et al. (1977), Giesy et al. (1977), and Tuschall and Brezonik (1983b).

Problems with ISE titrations include high detection limits, calibration drift, and uncertain responses to inorganic complexes. The copper ISE is the most frequently used, largely because of its high sensitivity, but it is limited to pCu < 8 (Orion 1977). ISE titrations are thus extremely difficult at pCC > 6.3, which is in the range of many natural waters (Giesy et al. 1978). Concentration of organics from water samples is not advisable, because K_f^c values may be dependent on ligand concentration, if multiple ligands can bind to the same metal ion in a manner similar to hydrogen bonding (Langford et al. 1983). Calibration drift, caused by light or temperature changes during a titration, may cause serious errors at low CC (Dempsey and O'Melia 1983). Finally, Cu^{++} released from an organic ligand may become complexed by weaker organic or inorganic ligands or may

precipitate as a colloid under high pH or alkalinity conditions (Leckie and Davis 1979). Although some inorganic species (such as $CuOH^+$, $Cu(OH)_2^0$, and $CuHCO_3^+$) appear to be measured by the copper ISE (Wagemann 1980), an incomplete response to other complexes or precipitates would cause CC to be overestimated. Similar problems exist for estimating other metal ISE's, and their effects are even more severe owing to higher detection limits or heteroion interferences.

DPASV, briefly described above, also has difficulties. The ability to detect lower concentrations for ions such as copper and cadmium (pM ≈ 10) allow low CC waters to be studied, but, in these ranges, contamination during sampling and analysis become a greater problem (e.g., Raspor 1980). To add to the problem, Tuschall and Brezonik (1981) found that many metal-organic complexes are reducible at the mercury dropping electrode during the plating step. The consequence is that i_p is a function not only of [M] but also of [ML], according to some constant that is a function of the dissociation kinetics under the experimental conditions. Bhat et al. (1981) described an equation designed to correct for the dissociation current:

$$i_p = \frac{Su}{2}\left\{C_M - C_L - \frac{1}{K_f^c} + \left[\left(C_L - C_M + \frac{1}{K_f^c}\right)^2 + \frac{4\,C_M}{K_f^c}\right]^{1/2}\right\} \quad . \quad (2.17)$$

The equation is fitted by a nonlinear regression computer program, and presumably works only if rate of dissociation is not too fast.

The final method for estimating metal ion concentrations investigated for use in this study was continuous ultrafiltration (UF). Tuschall and Brezonik (1980) used this technique to determine CC and K_f^c values for colored lake water. In this technique, a Cu titrant is added under N_2 pressure to a stirred cell containing 50 mL of the test water. Successive sample aliquots are taken and analyzed for C_M, using any sufficiently sensitive method. Metal-ligand complexes not retained by the membrane filter pass into the filtrate. C_M is analyzed in the filtrate, rather than [M], because only the K_f^c for the retained organics is of interest and some of the free metal in the filtrate is bound to smaller ligands. A series of filters with different nominal pore size and charge characteristics can be used to separate binding capacity into a set of operationally defined fractions. Because of the highly negative charges on many organic ligands, the range of sizes retained may bear little relationship to the distribution of nominal pore sizes on the filters (e.g., Dempsey and O'Melia 1983).

Treatment of the data from continuous ultrafiltration is based on a material balance in the UF cell:

$$M_{ML} = V_{EFF}([M]_{IN}) - V_{CELL}([M]_{EFF}) - M_{OUT} \quad . \quad . \quad . \quad (2.18)$$

where V_{EFF} and V_{CELL} are effluent and cell volumes, respectively, and M_{ML} and M_{OUT} are the masses of metal bound in the cell and lost from the cell, respectively, and $[M]_{IN}$ and $[M]_{EFF}$ represent the respective metal concentrations in the titrant and the cell effluent. The output data can be linearized by plotting log $([M]_{IN}/[M]_{IN} - [M]_{EFF})$ versus V_{EFF} (Tuschall and Brezonik 1983a).

Measurement by ultrafiltration is relatively inexpensive, provides some fractionation, and can be used for any metal. It can be combined with using carbon furnace atomic absorption spectroscopy for low-level metal detection. Principal problems include

membrane interactions and difficulty in preselecting a suitable titrant concentration.

In reviewing these techniques, one finds that they are all operationally defined. Both CC and K_f^c values have little meaning in a thermodynamically rigorous sense. However, Tuschall and Brezonik (1983b) have presented evidence that values obtained using different techniques were similar (except for DPASV uncorrected for complex dissociation). Also, the overwhelming sense of the papers presented in Christman and Gjessing (1983) was that these techniques, if properly applied, would give valuable insight into metal-organic interactions in natural waters. Some of the problems in making these applications will be considered further in the context of the research reported here.

Binding Bioassays

As alternatives to the chemical methods for estimating CC and K_f^c values for water samples, bioassays employ algae (as well as other microorganisms and invertebrates) as indicators in metal titrations. In an algal bioassay, inocula are grown in media containing a range of metal concentrations, and some indicator of biomass (e.g., chlorophyll a or cell counts) or metabolism (e.g., $H^{14}CO_3^-$ uptake) is plotted against the metal concentration. The extent to which metals (e.g., copper) are detoxified by chelation with natural or synthetic organic ligands can be determined either by comparing cultures spiked with the ligand against unspiked controls (Davey et al. 1973) or by comparing the response in natural water containing the ligand of interest with synthetic media containing an identical C_M, but without the ligand (Gachter et al. 1978). The latter authors, for example, determined that organic ligands in Lake Alpewach, Switzerland, contained two classes of biologically effective ligands, one with CC = 0.03-0.07 µM Cu/L and log K_f^c = 10.1-10.7, and the other with CC = 1.8-2.6 µM Cu/L and log K_f^c = 7.4.

Additonal studies of this type have been reviewed by Skulberg (1978), Leischman et al. (1979), and Maciorowski et al. (1981, 1982). Here, we will only present a brief rationale for the interactions among metals, organic ligands, and phytoplankton. Huntsman and Sunda (1980) have provided an excellent review of most of the relevant literature. Because the chemical analyses stressed copper interactions, the focus will be on this metal.

Toxicity of free metal ions. Ample evidence exists for the hypothesis that, for many heavy metals, it is the free ion (probably together with some of its inorganic complexes) that is toxic to algae. Sunda and Lewis (1978) showed that Monochrysis lutheri was sensitive only to copper measured by a copper ISE, and Allen et al. (1980) determined that Microcystis aeruginosa was sensitive only to free Zn^{++} plus $ZnOH^+$ in the presence of synthetic organic chelators. Similar studies abound. It would seem that free Cu^{++} concentrations as low as 1-3 x 10^{-11} M/L can be inhibitory to phytoplankton (Huntsman and Sunda 1980). This value is much larger than the 1-10 x 10^{-8} M/L found in typical river waters (Boyle 1979), indicating that much of the copper found in natural waters is in an unavailable and consequently nontoxic form.

Factors reducing free metal ion concentrations. Many factors inactivate and thus reduce the toxicity of heavy metal ion concentrations in water. These include:

1. Binding by organic ligands, as described above, including organics excreted by the cells, and the active sites on cell surfaces themselves (Jackson and Morgan 1978, Christ 1981).

2. Binding to particulate surfaces, including clays (Pickering

1979) or to cell surfaces, coatings, and the like (Bentley-Mowat and Reid 1977).

3. Coprecipitation with Fe or Mn hydroxides (Vuceta and Morgan 1978) (Fe hydroxides have a much higher affinity for Cu and precipitate more rapidly under typical environmental conditions).

4. Chemical transformations, including precipitation (e.g., as HgS) in the cell membrane of Dunaliella tertiolecta or change in oxidation state (e.g., reduction of Hg^{+2} to Hg^{+}) (Davies 1976).

5. Increasing the concentration of an antagonistic ion.

Petersen (1982) showed that subtoxic increases in $[Zn^{+2}]$ in a medium containing EDTA decreased the growth of Scenedesmus quadricaudata solely by displacing Cu^{++} from the EDTA. Antagonism can also result via reversible replacement of a toxic ion on a specific or nonspecific metal binding site on an enzyme by increasing the concentration of its nontoxic competitor (e.g., Mn vs Cu in the photosystems of Chaetocerus socialis (Huntsman and Sunda 1980)).

Effects on algal cells

The effects of metal toxicity may be expressed in many ways in phytoplankton. Some examples include:

1. Photosynthetic rates may be reduced (e.g., Steeman-Nielsen and Bruun-Laursen 1976).

2. Overall standing crops may be unaffected, but the length of the lag phase prolonged (Bartlett et al. 1974) or growth rates reduced (Payne and Hall 1978).

3. Cell division and membrane permeability may be affected (Anderson and Morel 1978).

4. Mobility of flagellate species can be affected, even at extremely low (10^{-11} M/L) Cu concentrations (Anderson and Morel 1978).

Effects on community structure

The concentrations of free metal ions, and their subsequent reductions by binding to organic ligands, may cause significant species shifts in both phytoplankton (Thomas and Seibert 1977, McKnight 1981) and periphyton (Rushforth et al. 1981) communities. Generally, cyanobacteria (blue-green algae) and dinoflagellates appear to be most sensitive to Cu, while diatoms generally exhibit more resistance, but there is undoubtedly much variation among individual species (Huntsman and Sunda 1980). At least part of the differential toxicity is probably caused by excretion of organic chelators by the phytoplankton themselves.

Among the strongest chelators known to exist are hydroxymates, which are released into the environment by procaryotic organisms in response to Fe-starvation. These compounds bind Fe strongly ($K_f^c \simeq 10^{32}$) and transfer Fe into the cell, either as the intact complex or through certain highly organism-specific alterations to the complex on cell membranes (Emery 1982). These compounds also have been found to have a high affinity for Cu ($K_f^c \simeq 10^8$-10^{12} at pH 6.2), and thus could detoxify significant quantities of Cu, if they were present in stoichiometric excess of Fe (McKnight and Morel 1978, 1980). These authors found nine of fourteen eucaryotic phytoplankton species also to produce nonhydroxymate chelators with K_f^c values ranging from $10^{6.5}$ to $10^{8.5}$ in the pH range from 6 to 8. It is not clear whether phytoplankton excrete such chelators in specific response to toxic metals or whether the chelators result from a leakage of organic compounds in response to a more general stress (Huntsman and Sunda 1980).

Summary of bioassay methods

Bioassay methods for determining CC and K_f^C have the advantage of integrating the effects of the various chemical parameters into the resulting effects on the test algae. They can be much more sensitive than chemical assays, especially those based on ISE techniques, although contamination from culture vessels and media can present severe problems when working at very low metal concentrations (Fitzwater et al. 1982). On the negative side, the interactions outlined above, together with time required to conduct growth bioassays and possible problems with species specificity, require that caution be used in interpreting and extrapolating bioassay results.

Bioassays with oil shale and shale oil materials

As described in the introduction, very few algal bioassays have been described in the literature for oil shale related materials. Cleave et al. (1980) studied the effects of aqueous leachates and elutriates from raw and spent shales (Paraho and Union B processes) on the growth of a strain of Scenedesmus bijuga isolated from Lake Powell Reservoir. The alga was grown in AAP medium (Miller et al. 1978) with major cation additions to simulate the 780 ppm salinity water in the reservoir. Water soluble fractions (WSF) obtained by leaching shales in an upflow column or elutriated in shaker flasks generally stimulated algal growth, relative to salt controls, at least when applied at low concentrations, and process shales were more stimulatory than raw shales. Increasing the WSF concentrations in the bioassays, however, tended to inhibit both growth rate and maximum standing crops, at least with Paraho processed shale. These results suggest that if a nutrient was being added in the leachates, its beneficial effects are overcome by accompanying toxicants at higher application rates. Metal ion toxicity also could have resulted from replacement on EDTA with increasing concentration of a nontoxic metal (e.g., Petersen 1982).

Giddings (1981) described an experiment in which WSF's of various shale oil products were applied to Selenastrum capricornutum cultures. WSF's were obtained by 1:8 organic:water extraction (18 hr, dark) of crude shale oil, hydrotreated shale oil, hydrotreated residue, JP-S jet fuel, and marine diesel fuel. JP-5 WSF was stimulatory to $H^{14}CO_3^-$ uptake rates, even at 10 percent concentration, and the WSF from the hydrotreated oil were stimulatory at 1 percent additions. Diesel fuel WSF was stimulatory at 10 percent, but not at 1 percent addition. Microcystis aeruginosa was not stimulated by either crude or hydrotreated oil WSF's, the only fractions tested. Although neither the Giddings (1981) nor Cleave et al. (1980) study indicated that metal binding was an important factor in their results, they both suggest that metal-ligand interactions have a role in determining the effects of shale oil WSF's on algal growth.

CHAPTER III

MATERIALS AND METHODS

Description of Oil Shales Used

Both raw and spent oil shales were examined. The raw oil shale used in this study was excavated from tract C-a of the federal prototype oil shale lease approximately 1.5 years before this study. It was mined from the oil-riched Mahogany Zone of the Green River formation, and had been stored in sealed 55 gallon drums during the interim. The exact source of the shale within the Mahogany Zone is unknown. Retorted (spent) oil shale was obtained from the Paraho pilot scale retorting operation in Anvil Points, Colorado. This shale was retorted at a higher than normal temperature. A full description of this shale is presented in Hinchee (1983).

Extraction Methods

Both raw and spent oil shales were extracted using the "Proposed Methods for Leaching of Waste Materials," Method A, developed by ASTM Committee D-19 on Water (Gulledge and Webster 1981). Both the raw and retorted shales were crushed mechanically, in order to maximize extraction efficiency. The retorted shale was then sieved through a standard 100-mesh sieve (0.147 mm) to leave only the smaller sizes. For the hard, raw shale, heat was generated during mechanical crushing, which may alter the chemical state of the hydrophilic organics, so no further attempt was made to reduce the size. More than 85 percent of the crushed shale passed through a standard 32-mesh sieve (0.5 mm). All glassware and polyethylene containers were leached free of trace metals and organics by soaking in 10 percent HNO_3 for two days, and then rinsed thoroughly with deionized water. The extraction method used (Method A) is a 48-hr shake test performed at room temperature using deionized water (MilleQ, Millipore Corp.) as the extracting medium, and a shale to water ratio of 1:4 (by weight), as outlined in Figure 3.1.

Other preliminary extractions were performed using the same technique, but with 1) other inorganic solvents (0.5 M HCl, 0.5 M NaOH, 0.5 M $NaHCO_3$), 2) hot deionized water, and 3) cold deionized water bubbled with CO_2 to reduce the pH. Different shale to water ratios (1:1, 1:2, and 1:4) also were tested in order to optimize extraction of the hydrophilic organics.

Little difference was found in the amount of DOC extracted by the various solvents, and thus deionized water was used for later extractions, because it was felt to be the closest, chemically, to precipitation in the oil shale development area (Messer 1983). These later extractions were performed using an oil shale to water ratio of 1:4 in 5-gallon borosilicate bottles for a period of 3 weeks in the dark, with frequent mixing.

Bulk leachates were centrifuged in one-liter polyethylene bottles at 2750 x G for 15 minutes in an IEC Model DPR-6000 centrifuge at room temperature. The resulting supernatant was filtered through a Millipore type HA sterilized 0.45 µm membrane filter immediately after centrifugation. The filtrate was then transferred to a polyethylene carboy and stored at 4°C in the dark for future use. Each batch of the oil shale leachate was analyzed for pH, EC

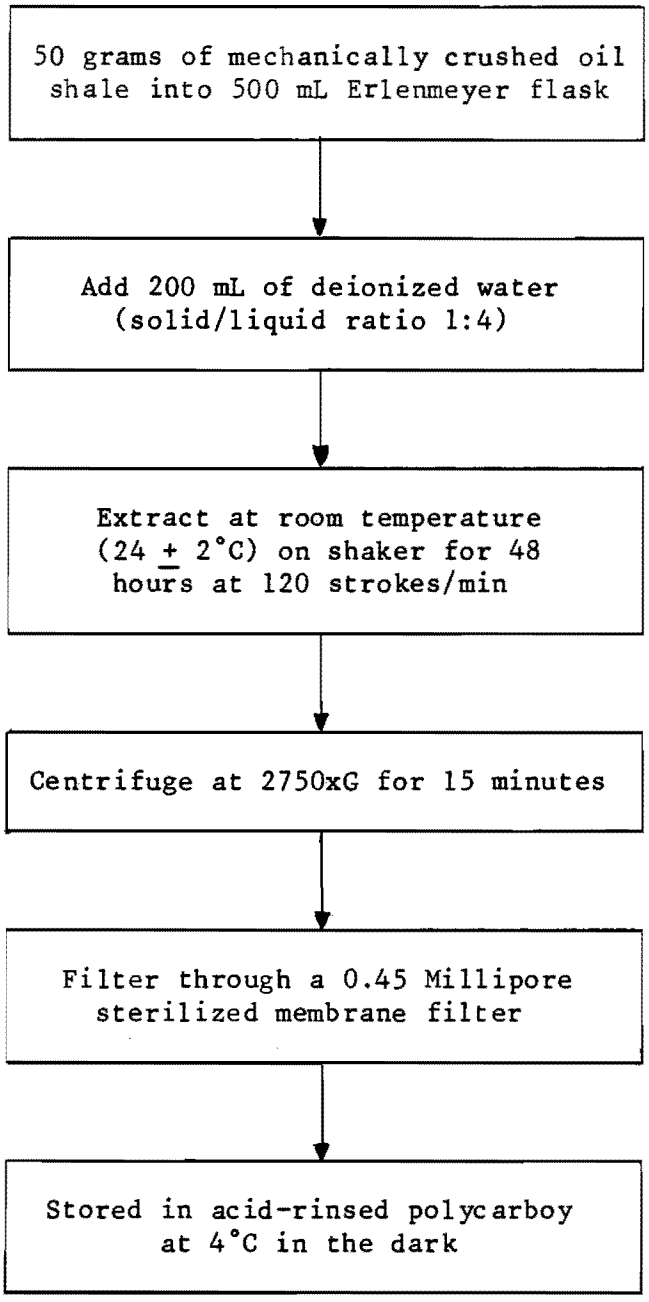

Figure 3.1. Oil shale extraction based on ASTM method A (Gulledge and Webster 1981).

(electrical conductivity), DOC (dissolved organic carbon), and major anions and cations following American Public Health Association Standard Methods (APHA 1980).

Desalting and Concentration of Leachates

Ultrafiltration (UF) membranes (Amicon Diaflo ®) were used for desalting the inorganic salts while concentrating the organic ligands in the oil shale leachates by retaining them within the UF cell. The filters were pre-cleaned by soaking for at least an hour in deionized water with frequent solution changes. Prior to each use, the whole UF system (UF cell, connecting tubings, and the UF reservoir) was sterilized with 5 percent formalin and rinsed with excess deionized water. The UF membrane then was placed inside the UF cell (Amicon Model 52) and flushed with at least another two cell volumes (>100 mL) of deionized water before being used to concentrate the leachate.

A known volume of stock oil shale leachate was introduced into the UF cell and the 800 mL UF reservoir, and the whole system was pressurized with nitrogen. The leachate first was ultrafiltered through a XM300 membrane filter with a molecular weight cutoff size (MWCS) of 300,000 amu in order to exclude colloidal materials. The filtrate from the XM300 filter was fed into the UF cell from the reservoir. The leachate then was desalted by continuous ultrafiltration (diafiltration) through a UM2 membrane filter (MWCS 1,000 amu) to remove microspecies, those smaller than the effective pore size, by convective transport while retaining the macrospecies in the UF cell.

The solutions in the UF cell and in the reservoir were stirred constantly to avoid creating a concentration gradient at the filter surface and in the reservoir. Pressures as high as 4.1-4.8 x 10^5 pascals were used to force the leachate through the filters during early experiments, but later the pressure was reduced to 6.9-13.8 x 10^4 pascals in order to avoid forcing the macromolecules through the membrane.

Because the solute concentration in the leachate was relatively low, extensive concentration could be accomplished before fouling the membrane. After a 10 to 25 fold concentration was reached, deionized water was added to the reservoir to further dialyze the retentate, thus purifying the retained macrospecies. Five cell volumes of deionized water were passed through the retentate to ensure 99 percent removal of the microspecies in the UF cell. Both the ultrafiltrate and the retentate were collected and stored in acid-washed polyethylene bottles for future use. If only desalting of a leachate was desired, the retentate then would be made up to its original volume with deionized water. If a concentrated desalted leachate was desired, the retentate was used directly. Leachates treated in this way are referred to as UM2 or nX UM2, where n represents the concentration factor.

Other leachates were size fractionated using a series of Amicon ultrafiltration membranes, following XM300 prefiltration: YM30 (MWCS 30,000 amu), YM10 (MWCS 10,000 amu), YM5 (MWCS 5,000 amu), and UM2 (MWCS 1,000 amu). The ultrafiltrate collected from each step was sequentially fractionated using membranes with the next lower pore size until the smallest pore size membrane filter was used, and the retentate and the ultrafiltrate for each fractionation step were preserved for further analysis. Volumes of both the retentate and the ultrafiltrate were recorded at each stage. The respective leachate fractions are referred to according to the ultrafilter designations delimiting their range of detention. That is, ligands passing through YM5, but not UM2, would be designated YM5-UM2.

Continuous Ultrafiltration

The continuous ultrafiltration (diafiltration) technique (Amicon 1977) was conducted at room temperature (24°C) to determine the binding capacities and conditional stability constants for the oil shale leachates. An Amicon UM2 ultrafiltration membrane (MWCS 1,000 amu) was used in conjunction with an Amicon Model 52 (50-mL) ultrafiltration cell. The cell was filled with the desalted leachate and buffered with enough $NaHCO_3$ to return the EC of the leachate to its original level. The reservoir was filled with a copper solution of known concentration as the titrant. The copper titrant was made by sequential dilutions of the Orion 0.1 M $Cu(NO_3)_2$ standard solution with deionized water until the working concentration of the titrant was reached. The titrant was not buffered with any pH or metal buffers in order to avoid precipitating the copper ion in the reservoir.

After the reservoir and cell were equally pressurized, pressure was directed solely to the reservoir. The volume of the titrant entering the UF cell was equal to the volume of the ultrafiltrate that left, thus maintaining a constant fluid volume (50 mL) in the UF cell. The pressure within the system was controlled to a level sufficient to deliver ultrafiltrate at a rate of 1 percent or less of the cell fluid volume per minute (<0.5 mL/min) as suggested by the manufacturer, in order to ensure that the filtrate was in binding equilibrium with the cell contents. Based on the flow characteristic of the UM2 ultrafiltration membrane, a pressure of 3.1×10^5 pascals was applied. More than 250 mL (5 cell volumes) of titrant were passed through the UF cell. It has been shown that the exchange of a freely permeable microsolute is more than 99 percent complete when five multiples of the retentate volume have passed through the system (Amicon 1977). Successive ultrafiltrate samples were taken throughout the diafiltration process at one hour intervals, with each sample representing a different equilibrium copper ion concentration. The copper content in each sample collected in polyethylene vial was acidified and measured on the following day using a copper ISE. CC

and K_f^c were determined by the method described by Tuschall and Brezonik (1983a).

Copper Ion-Selective Electrode

The complex-formation properties (CC and K_f^c) of the oil shale ligands were measured by potentiometric titrations using a copper(II) selective electrode of the type described below. Determinations of the binding capacities of EDTA, humic acids, and the oil shale leachates were conducted by titrating the sample solution (100 mL) with copper nitrate standard solutions. Small increments of the copper standard titrant were dispensed from a graduated 10 mL burette or from Eppendorf micropipets. The electrode was used to measure the fraction of copper in the uncomplexed state by monitoring the electrode potential during the course of the titration. The solution was allowed to mix completely following addition of an aliquot of titrant, until a relatively steady potential (<0.1 mV/30 sec) was observed before addition of the next increment of titrant.

Measurements of the free cupric ion were made with a Fisher Accumet ® Model 750 Specific-Ion Analyzer coupled to an Orion Model 94-29 solid state copper ion-selective electrode (ISE). The reference electrode was a single-junction reference electrode, Orion Model 90-01. The sensing surface of the ISE was polished with an abrasive strip, rinsed and soaked in 10^{-5} M/L copper nitrate solution for about 5 minutes, rinsed well with deionized water, and then blotted dry with a clean, dry tissue before each use. Measurements were performed at a constant temperature of 25 $\pm$0.5°C and with a constant light intensity. The titrate was stirred continuously with a Teflon stir bar on a magnetic stirrer at a constant rate, kept sufficiently low to avoid creating a vortex. A layer of styrofoam was placed between the magnetic stirrer and the titration flask to insulate the titrate from heat generated by the magnetic stirrer. Copper titrants were prepared fresh daily from Orion 0.100 M copper nitrate standard solution.

The electrode potentials corresponding to standard solutions were measured and plotted on semilogarithmic paper. The slope of the linear region of the curve was determined either graphically or by calculation to ensure a Nernstian electrode response of 29.5 mV per decade (tenfold change in concentration). A calibration curve was run prior to each determination of the binding capacity of a sample. CC and K_f^c were determined according to several of the methods described in the preceding chapter using the data obtained from the titrations.

Differential Pulse Anodic Stripping Voltammetry

Determinations of CC and K_f^c values for EDTA, humic acid, and the oil shale leachate with cupric ion were measured by differential pulse anodic stripping voltammetry (DPASV) using a Princeton Applied Research Polarographic Analyzer (Model 384) equipped with a static mercury drop electrode (Model 303) and a X-Y digital plotter (RE 0082). The Model 303 consists of a three-electrode cell with the hanging mercury drop electrode as the working electrode, an Ag/AgCl reference electrode and a platinum counter electrode supplied by the manufacturer. The instrument was set in the differential pulse stripping voltammetry mode, and pseudo-polarograms were constructed by the method of Figura and McDuffie (1979) to determine appropriate plating potentials for each metal, and the metal-complexes.

Two methods of electroplating were employed. In the first method, designated the "simultaneous" method, Zn, Cd, Pb, and Cu were reduced simultaneously at an E_d of -1.20 V. Subsequent stripping operations gave the respective metal peaks. In the second method,

designated the "individual" method, the concentration of each metal was determined separately by depositing at the least negative potential ($E_{d(min)}$) which gave maximum plating efficiency for that particular metal, based on the pseudo-polarograms obtained earlier.

Copper was plated onto a medium drop size hanging mercury droplet at -0.20 V vs. an Ag/AgCl electrode for 90 sec (60 sec under constant stirring, followed by a 30 sec equilibration period), before stripping by reversing the applied potential. Copper concentrations were determined by monitoring the current, while scanning the potential between -0.20 and +0.15 V at a scan rate of 2 $mV.s^{-1}$. A detailed description of the parameters used for the DPASV method appears in Table 3.1.

For the binding analysis, an aliquot of 10 mL of the sample to be titrated was placed in the three-electrode cell . This sample served as a blank, and blank subtraction was used to subtract the trace amounts of metal detected in the sample itself, so that only the "residual" binding capacity of the ligand would be determined. Small aliquots of standard copper nitrate solution were sequentially added to the cell using Eppendorf micropipets (5 µL or 100 µL) in order to minimize dilution. The solution was purged for 4 min with prepurified N_2 to remove oxygen before DPASV analysis following each addition of metal titrant.

Another binding titration was performed by adding different amounts of Cu(II) to a series of polyethylene bottles containing equal amounts of a given sample. The titrated samples were equilibrated at room temperature for at least 2 hr before transferring to the three-electrode cell for measurement. The measured peak currents were similar to that of the previous procedure, therefore further complexation titrations were performed with a 10 mL sample. Calibration curves for the free metal ion also were determined, and the

Table 3.1. Instrumental settings for the determination of copper using differential pulse anodic stripping voltammetry.

Settings	
Mode	:Differential pulse stripping (DPS)
Initial Potential	:-0.20 V for Cu(II)
Final Potential	:+0.15 V
Working Electrode	:Hanging drop mercury electrode (HDME)
Reference Electrode	:Ag/AgCl
Counter Electrode	:Platinum wire
Drop Size	:Medium
Purge Time	:240 seconds
Purge Gas	:Prepurified N_2/deoxygenated
Pulse Height	:50 mV
Deposit Time	:60 seconds
Equilibrate Time	:30 seconds
Drop Time	: 1 second
Scan Rate	: 2 mV/sec
Blank Subtraction	:Yes
Blank	:Acetate electrolyte (pH 6.3)
Tangent Fit	:Yes

binding capacity and the conditional stability constant of each sample were determined using the methods outlined by Scatchard (1949), Shuman and Woodward (1973 and 1977), and Ruzic (1980) outlined in the previous chapter.

Algal Bioassay

The algal bioassays bottle test (AB:BT) employed the standard AAP test alga Selenastrum capricornutum Printz (chlorophyceae, chlorococcales). This alga was used because its behavior and physiology in culture has been studied extensively (Leischman et al. 1979).

The standard technique described by Miller et al. (1978) was slightly modified in order to determine the effects produced by the additions of the oil shale leachate and metals. Variations made to the standard algal bioassay procedure included ensuring that the macronutrients (N and P) were in excess. Table 3.2 describes the basic nutrient medium used throughout this study. Trace metals and the artificial chelating agent (EDTA) were excluded so as to isolate the effects of metals and organic ligands associated with the leachates and metal solutions spiked into each set of bioassay flasks.

All media were autoclaved for 35 minutes at 13.8×10^4 pascals and equilibrated to room temperature before inoculation. Inoculations of 1000 cells/mL of the test alga were made into 100 mL of the media to which various leachates had been added. Sterile techniques were used for preparation of media and algal transfers, however, no tests were made for bacterial contamination. Glassware was rinsed with 50 percent HNO_3 and then rinsed with excess deionized water before sterilization. Metal additions to the bioassay medium were followed by an equilibrate period of at least half an hour. Cultures were incubated under standard light intensity (400 $\pm$10% ft-c) and temperature (24 $\pm$2°C) conditions. The algal bioassays were monitored at 1-2 day intervals for a period of 14 days or until algal growth was less than 5% of the previous sampling period for all

Table 3.2. The macronutrient concentrations used in the modified AAP medium.

Compound	Concentration (mg/L)	Element	Concentration (mg/L)
$NaNO_3$	25.500	N	4.200
K_2HPO_4	1.044	P	0.186
$MgCl_2 \cdot 6H_2O$	12.164	Mg	2.904
$MgSO_4 \cdot 7H_2O$	14.700	Ca	1.202
$CaCl_2 \cdot 2H_2O$	4.410	C	2.143
$NaHCO_3$	15.000	K	0.469
		S	1.911
		Na	11.001

cultures in the bioassay. The algal growth response during the assay period was monitored using chlorophyll a fluorescence, optical density, cell counts, and dry weight biomass determination:

1. Chlorophyll a: A Turner model 111 Fluorometer equipped with a #110-922 (430 nm) excitation and #110-021 (>650 nm) emission filters, #110-823L (10%) neutral density filter, a red-sensitive photomultiplier tube, and a high sensitivity door (APHA 1980) was used to measure the in-vivo fluorescence of a portion of the S. capricornutum cell suspension in a 1 cm cylindrical cuvette. The fluorometer was zeroed with a deionized water blank before each sample reading for each multiplier setting, and the samples were well-mixed by shaking the cuvette immediately before reading their fluorescence.

2. Optical density: the absorbance was measured with a Bausch & Lomb Spectronic 70 spectrophotometer at a wavelength of 750 nm using a cell path of 1 cm.

3. Cell counting: direct microscopic counting of S. capricornutum cells was made using an American Optical Bright-line hemacytometer.

4. Dry weight: a measured portion of algal suspension was filtered through a tared Whatman glass microfibre filter, rinsed with deionized water, dried at 103°C for 24 hours, cooled in a desiccator until a constant weight was reached, and weighed.

Data collected for each bioassay were transferred into data files set up on the university computer. The optical density biomass measurements, although collected, were not analyzed because of their insensitivity to toxicity. For all bioassays, fluorescence data were used in the analyses because of the greater sensitivity of this measurement compared to the optical density measurement.

Batch algal bioassays were conducted to study the effects of additions of the oil shale leachates and/or metals on the test alga (S. capricornutum). The initial experiment was conducted to ensure that adsorption would not occur on the wall of the bioassay flasks. Two sets of bioassay flasks containing the MAAP medium were spiked with copper ranging from pCu 4 to 7 and analyzed for total copper using Cu-ISE. One set of the Erlenmeyer flasks was conditioned with copper solution for 48 hours, then the medium was disgarded and fresh copper was added to the medium before the copper content was determined.

A bioassay was set up to determine if there were sufficient macronutrients in the MAAP medium for significant algal growth. The concentrations of the macronutrients used for the MAAP medium are listed in Table 3.2 and were the same as recommended by Miller et al. (1978). Algal growth was monitored for one week, and rapid growth was observed.

Three bioassays were conducted to determine the individual metal toxic levels for copper, cadmium, and nickel to the test alga. Copper nitrate, cadmium nitrate, and nickel sulfate standards were prepared from Orion 0.100 M standard solutions. At least six different metal concentrations, ranging from pM 5 to 10, were used. All test treatments were conducted in triplicate and a control (consisting of just the MAAP medium) was run for each bioassay.

In order to determine the effect of the organic ligands on the test alga, bioassays were set up using a model ligand, humic acid. First, concentrations of humic acid (Aldrich) at 5, 10, 25, and 50 mg/L were added to the MAAP medium. Then two more bioassays were conducted to determine the effect of addition of humic acid to different copper concentrations to the test alga. Two concentrations of humic acid (5 and 10 mg/L HA) were added to the

MAAP medium containing 10^{-5} to 10^{-8} M/L of copper nitrate. All treatments were allowed to equilibrate for half an hour before the test alga was added.

After completing the above preliminary bioassays, the remaining bioassays focused on examining the effects of the oil shale leachates. The oil shale leachates were size fractionated and desalted by the UF process (i.e. 0.45 μm-UM2). In the first test, spent (retorted) oil shale leachate (SSL) was introduced into the medium to study its effects on the test alga. Three different size fractions were used (stock, YM10-UM2, and <UM2). Five percent of the original stock SSL containing all sizes of ligands (inorganic and organic) was spiked into three levels of copper and cadmium concentrations (pM=7, 8, and 9). In another set of bioassays, 5 and 10 percent of SSL_1 (YM10-UM2) were spiked into three levels of Cu and Cd concentrations. The third set of bioassays was conducted by adding 5 percent of the SSL_2 (<UM2) into the same Cu and Cd concentrations. The three different SSL samples containing the different sizes of molecules were also added to the MAAP medium without the metals so as to compare the algal growth.

Due to the limited quantity of spent oil shale available, the later bioassays examined the effects of raw oil shale leachate (RSL). For the first bioassay with raw shale leachate, different concentrations of RSL (1:4) were added to the MAAP medium (5, 10, 25, and 50 percent of the RSL containing 10 mg/L TOC) to study the effect of RSL on the test alga. Then bioassays consisting of different size fractionated RSL samples (Table 3.3) were conducted to determine which size fraction present in the oil shale leachate had the greatest impact on the growth of the test alga.

Three bioassays were conducted to determine the effects of additions of RSL to the test alga in the presence of different concentrations of three different metals (Cu, Cd, and Ni) ranging from pM 5 to 10. The first two bioassays were performed with additions of different concentrations of Cu, Cd,

Table 3.3. Different ultrafiltration (UF) size-fractionated RSL samples used in the algal bioassay.

5% RSL	Size Range	Molecular Weight Cutoff Size (MWCS) in amu[a]
UF Retentate	0.45 μm - YM 30	0.45 μm - 30,000
	YM30 - YM10	30,000 - 10,000
	YM10 - YM5	10,000 - 5,000
	YM5 - UM2	5,000 - 1,000
UF Filtrate	<YM30	<30,000
	<YM10	<10,000
	<YM5	< 5,000
	<UM2	< 1,000

[a]amu = atomic mass unit.

and Ni individually to MAAP medium containing 10 and 50 percent of RSL (1:4). The final bioassay was performed with additions of different concentrations of copper to MAAP medium containing 5 percent of RSL (2:1).

Table 3.4 summarizes all the complexation analyses performed in this study using model ligands (EDTA and humic acid), raw shale leachates, and spent shale leachates as determined by UF, ISE, DPASV, and algal bioassay.

Table 3.4. Summary of complexation analyses performed in this study.

Ligands		Techniques			
		UF	ISE	DPASV	Algal Bioassay
EDTA	10^{-5} (M/L)	--	Cu (T4.2; F4.5-6)	--	--
	10^{-4}	--	--	Cu (T4.5-6; F4.14-15)	--
Humic Acid	5 (mg/L)	--	Cu (T4.3; F4.7)	--	Cu (T5.5; F5.8)
	10	--	Cu (T4.3; F4.8)	Cu (T4.7; F4.16-17)	Cu (T5.5; F5.8)
	50	Cu (F4.1-3)		--	--
Raw Shale Leachate					
RSL (1:4)	10%	--	--	--	Cu, Cd, Ni[a] (T5.6, 5.7, 5.8; F5.9, 5.10, 5.11)
	50%	--	Cu[a](T4.4; F4.10)	--	Cu, Cd, Ni[a] (T5.6, 5.7, 5.8; F5.9, 5.10, 5.11)
	100%	Cu (F4.4)	Cu (F4.9)	Cu (T4.9; F4.18-19&A.)	--
(2:1)	5%	--	--	--	Cu[a] (T5.6; F5.9)
RSL_1	100%	--	Cu (T4.4; F4.11)	--	--
RSL_3	100%	--	Cu (T4.4; F4.12)	--	--
Spent Shale Leachate					
SSL_1 (1:4)	5%	--	--	--	Cu, Cd[a] (T5.9, 5.10; F5.12, 5.13)
	10%	--	--	--	Cu, Cd[a] (T5.9, 5.10; F5.12, 5.13)
SSL_2 (1:4)	5%	--	--	--	Cu, Cd (T5.9, 5.10; F5.12, 5.13)
SSL_3 (1:4)	5%	--	--	--	Cu, Cd (T5.9, 5.10; F5.12, 5.13)

[a]Desalted RSL in MAAP medium.

CHAPTER IV

RESULTS

The results of the experimental work are presented in two parts: 1) chemical determinations of the complexation capacities and K_f^C values for oil shale ligands, and 2) bioassay results. The chemical results for the oil shale leachate are organized by the technique used (UF, ISE, and DPASV) and compared with results obtained from the model ligands, EDTA, and a more complex organic, Aldrich humic acid (HA). Ancillary data on shale leachate inorganic chemistry are presented in Appendix A. Also, only representative titration curves are presented for discussion in this chapter, and the remaining relevant curves are presented in Appendices B, C, and D.

The bioassay results are presented as they relate to apparent free ion concentrations. The interrelation between the bioassay results and the complexometric titrations, together with the implications of the metal-binding parameters for water quality in the Colorado River Basin as impacted by a fully-developed oil shale industry, are discussed in the following chapter.

Chemical Techniques

Ultrafiltration

Model ligand

Determinations were made of CC and K_f^C for a model ligand in order to ensure that this complexometric titration technique using continuous ultrafiltration would work for oil shale ligands as it previously had for proteins and macro-ligands in biochemical studies. EDTA could not be used because of its low molecular weight, which allowed it to pass the smallest pore size UF membrane available (e.g., UM2, MWCS = 1,000 amu). Therefore only a more complex model ligand, Aldrich humic acid, was tested. Although this commercial preparation is not a single chemical species (Langford et al. 1983), it has the advantage of being widely used in aqueous humus studies and has information available in literature on copper binding characteristics.

In the titration, a 50 mL aliquot of 50 mg/L HA was titrated using 10^{-4} M $Cu(NO_3)_2$. N_2 was applied to the system through the reservoir headspace at 3.1 x 10^5 Pascals, resulting in an average flowrate of less than 0.38 mL/min for the whole titration. A total of 221.5 mL of filtrate (V_{OUT}), equal to approximately 4.5 multiples of the cell volume, was collected suggesting that the exchange of copper ion in the sample was more than 95 percent completed. The titration curve (Figure 4.1a) shows that the last two aliquots collected were approaching the titrant concentration. The volume (49 mL) of the highly colored retentate remaining in the cell was held constant throughout the analysis.

The plot of the log $([M]_i/[M]_i-[M]_e)$ versus V_{OUT} (Figure 4.1b) was not linear. Because Cu^{++} has been shown not to bind to the ultrafilters themselves (Tuschall and Brezonik 1983a), the nonlinearity indicates that the copper binding by the high-molecular weight organics is in the humic acid. The mass-balance equation (Equation

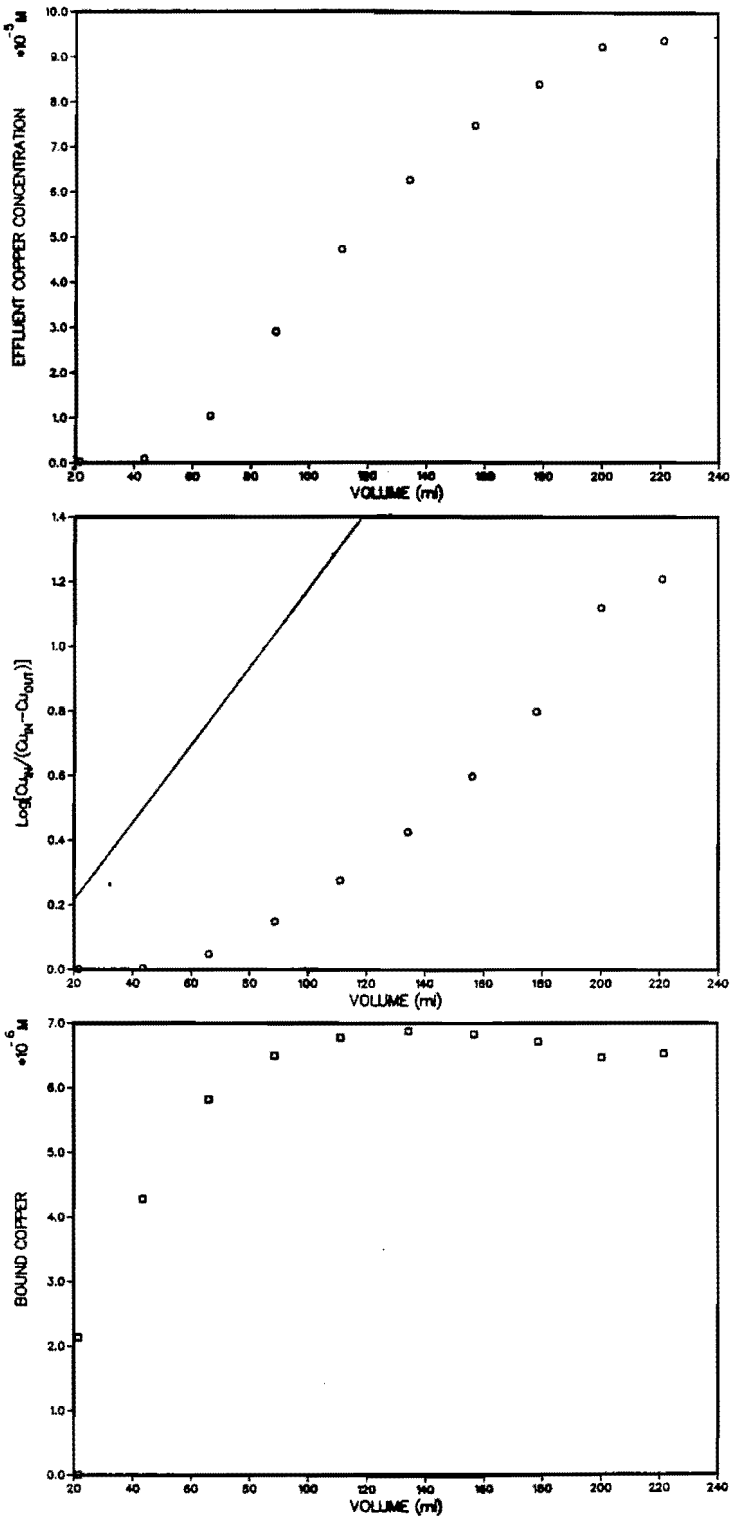

Figure 4.1. Ultrafiltration binding titration curve of 50 mg/L humic acid with 10^{-4} M copper using an Amicon UM2 (MWCS 1,000) membrane: a) effluent $[Cu^{++}]$, b) log $[Cu_{IN}/(Cu_{IN}-Cu_{OUT})]$ and c) Cu_{BOUND} versus titrant volume, respectively.

2.18) was used to determine the bound copper, M_b, and the calculated M_b values for each fraction collected plotted against V_{OUT} (Figure 4.1c) from the figure. The maximum CC was calculated to be 2.75 x 10^6 M Cu/mg HA, based on the amount of Cu bound following the addition of 134 mL of titrant. The reason for the slight decrease in the bound copper later in the titration is unknown, but it was characteristic of many of the UF titrations. Scatchard's (1949) analysis of the titration data (Figure 4.2) indicated a K_f^c of $10^{6.31}$. Although a break can be seen to occur in the

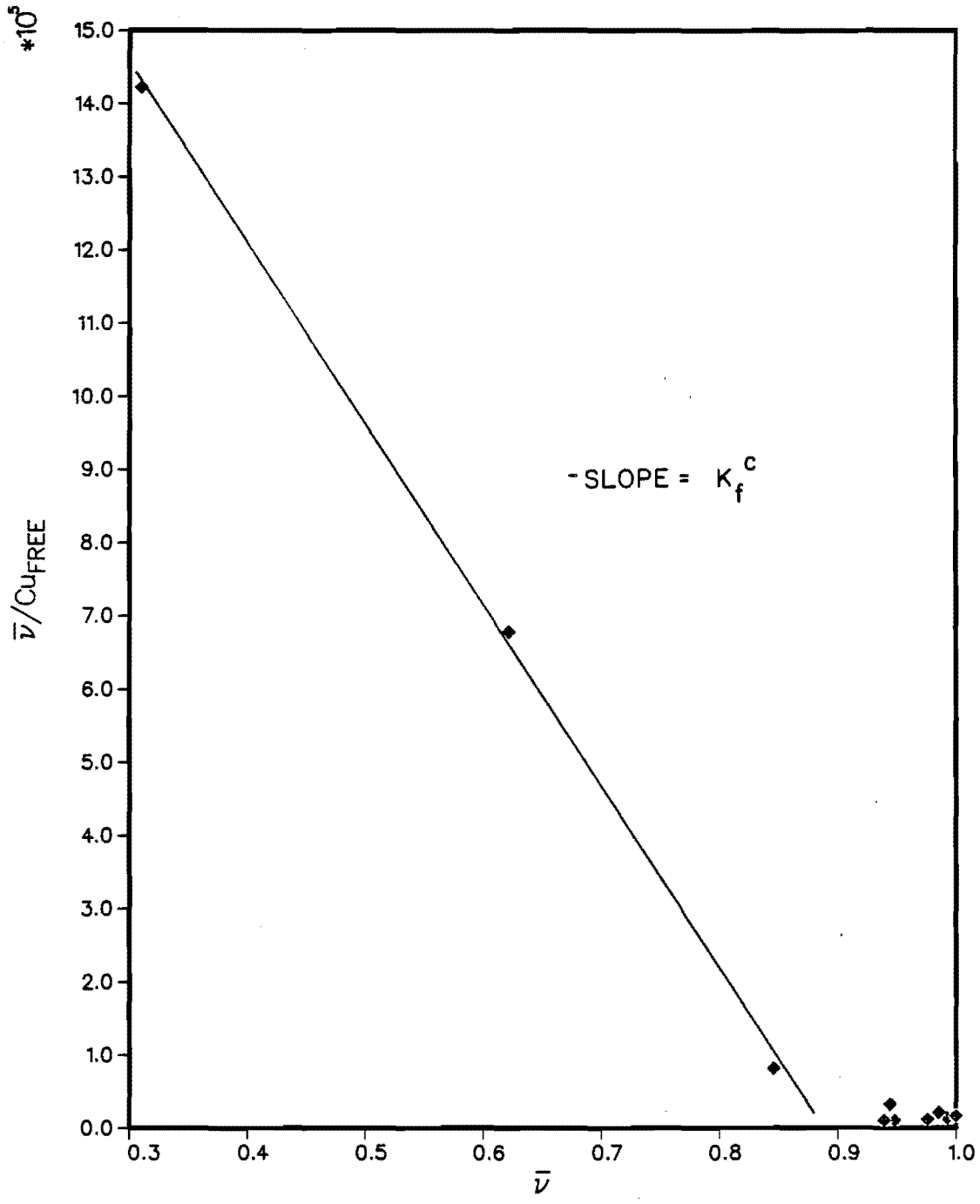

Figure 4.2. Scatchard plot of 50 mg/L humic acid with copper using continuous ultrafiltration.

plot for high values of $\bar{\nu}$, the calculated value for K_f^c is relatively unaffected by inclusion of the bottom data points ($10^{6.40}$). The number of binding sites (n=0.97) is close to the theoretical value of unity.

The data also were analyzed using the method of Ruzic (1980) (Figure 4.3). The CC calculated as the reciprocal slope, 2.70 x 10^6 M Cu/mg HA, is quite close to that calculated by mass balance. The Y-intercept is negative, however, producing a meaningless value for K_f^c. Although we are unaware of previous determinations of CC and K_f^c for Aldrich HA using UF, a CC of 2.7 x 10^{-6} M Cu/mg HA falls within the range of 1.5-5 meq Cu/g reported for various soil HA's by Stevenson (1982, p. 350). The K_f^c of $10^{6.31}$ is also reasonable for HA, as will be outlined below.

Finally, a slightly colored solution was observed in the first few aliquots of the filtrate collected. This suggests that the membrane employed (UM2) did not retain the smaller molecular size fractions of the HA. Thus CC for the total HA fraction may be somewhat underestimated. The effect would be important if the smaller size fractions contain much of the available binding capacity or if they have a higher K_{fc}.

Raw shale leachate (RSL)

An initial set of UF titrations was performed to assess the feasibility of using this technique, in conjunction with ISE detection of Cu in the filtrate fractions, for measuring the binding parameters of RSL. UF titration was desirable because it partitions the total binding capacity into a variety of operationally defined size fractions. Also UF fractionation was concomitantly being used in conjunction with algal bioassays. ISE analysis for copper was used because it was rapid and inexpensive, relative to atomic absorption (AA) analysis.

In this application, all of the filtrate aliquots were acidified to pH<2 on the day following the titration, in order to release any complexed Cu from organic ligands and to maintain the former in solution. The ISE then was recalibrated with fresh Cu standards, and all of the filtrates, as well as the acidified retentate and titrant, were analyzed for Cu within 15 min. This rapid analysis was desirable in order to prevent drifting of the potentiometric response of the ISE, which would almost certainly have occurred if the filtrate aliquots were analyzed over the 4-20 hr titration period.

The titrations were performed using RSL that had been pretreated using electrodialysis to remove macronutrients and salinity present in the RSL that would interfere with interpretation of the algal growth response to the action of the ligands alone. The pretreated RSL had an EC of only 65 µmho/cm and was poorly buffered against pH changes. Therefore, enough $NaHCO_3$ was added to bring the pH up to 8.2 (EC = 320 µmho/cm), the original pH of the leachate. The initial titrant chosen was 10^{-5} M $Cu(NO_3)_2$ in deionized water. The use of deionized water, rather than a bicarbonate buffer similar in composition to the RSL in the titration cell, would eventually decrease the pH of the retentate, and consequently reduce the apparent CC and K_f^c values. However, we wanted to avoid any unforeseen precipitation of Cu during the rather long titrations, especially at higher titrant Cu concentrations, and thus the aqueous titrants were judged to be reasonable for use in these preliminary titrations.

For the RSL titrations, a plot of Cu_B versus titrant volume using 10^{-5} M Cu titrant is shown in Figure 4.4a. In the initial 10^{-5} M titration, $[Cu]_e$ was much lower than the value predicted on the basis of simple dilution (no binding), and CC apparently was not even approached at α = 3 cell volumes,

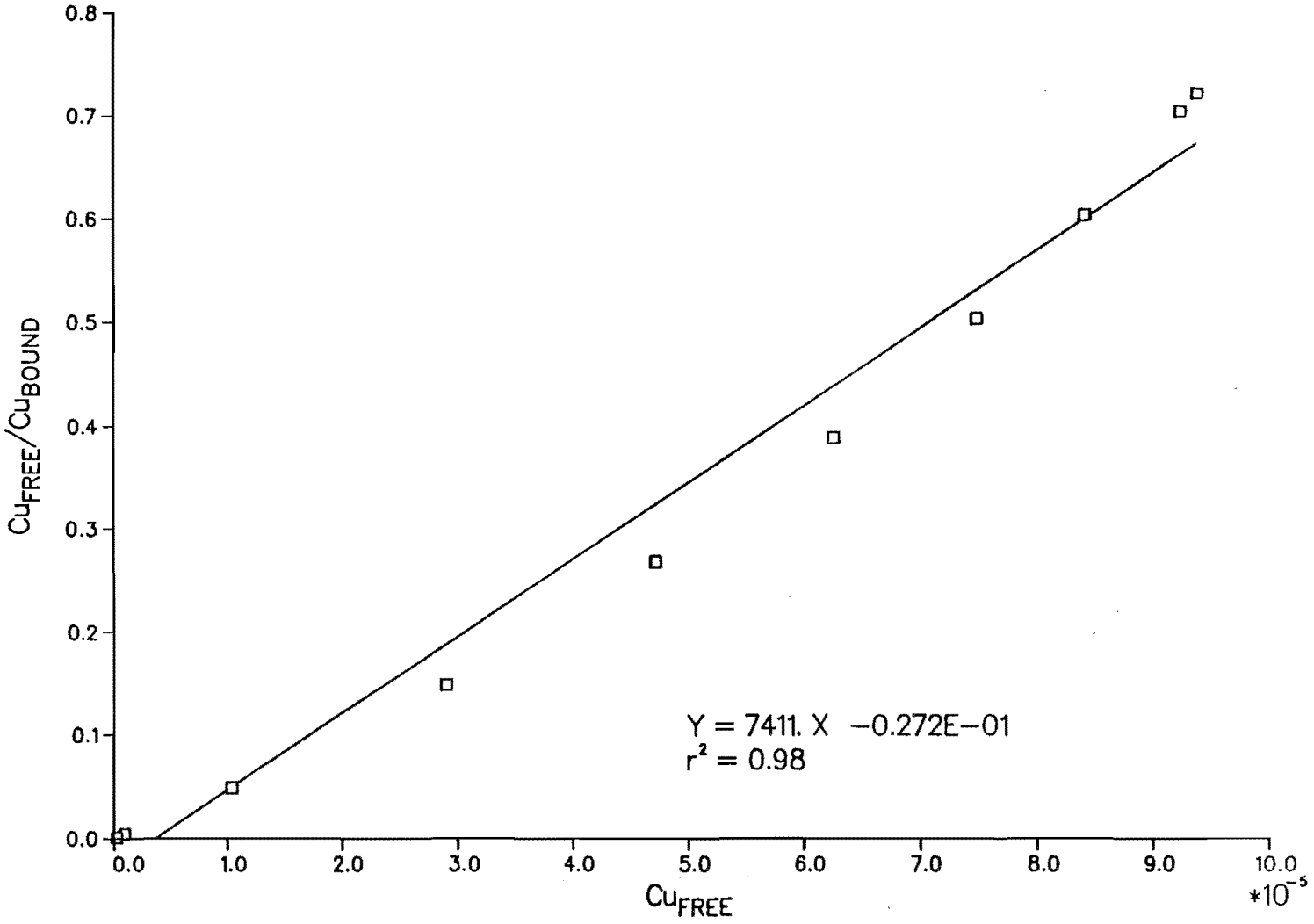

Figure 4.3. Ruzic plot of 50 mg/L humic acid with copper using continuous ultrafiltration.

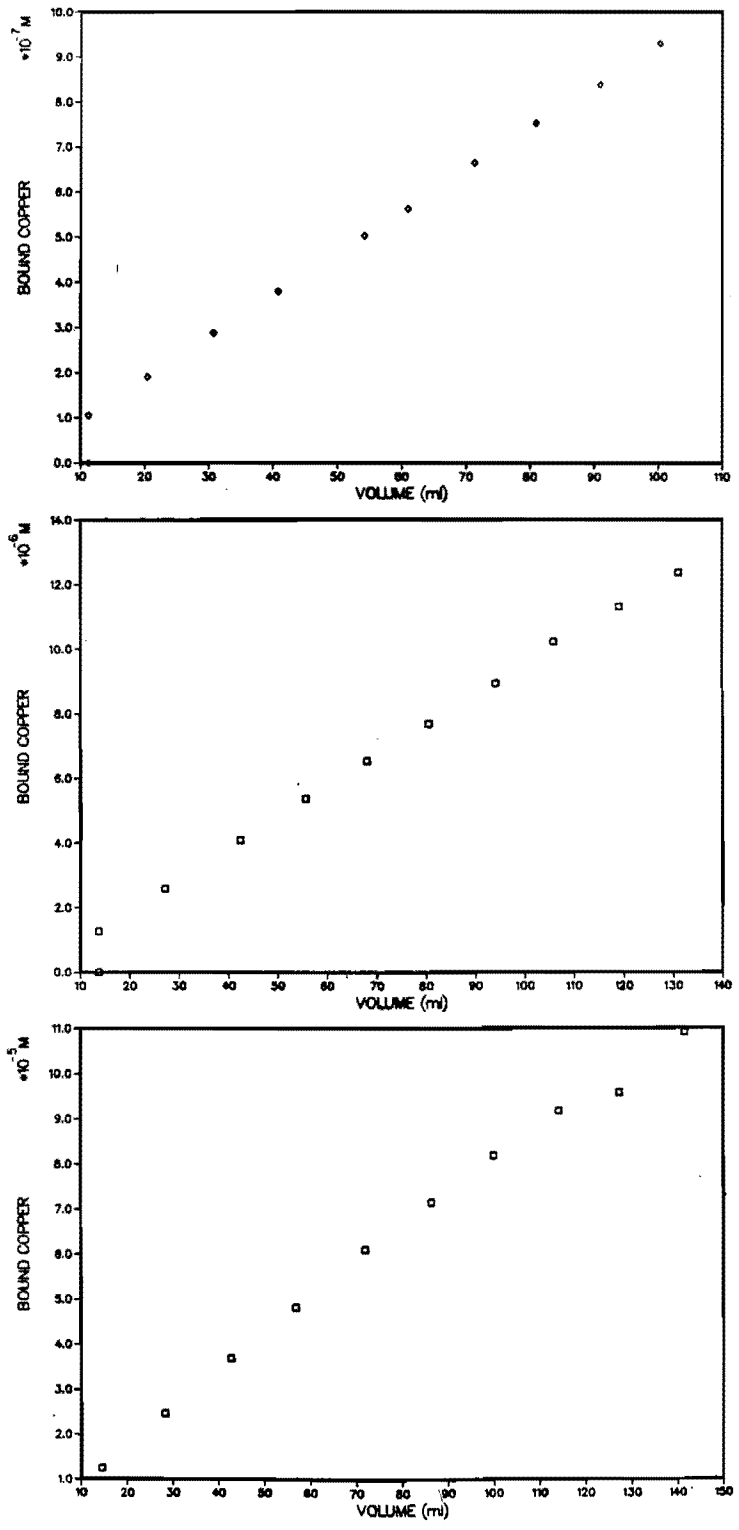

Figure 4.4. Cu_{BOUND} versus titrant volume for titrations of raw shale leachate (RSL) with a) 10^{-5} M Cu, b) 10^{-4} M Cu, and c) 10^{-3} M Cu.

at which point binding should be 95 percent complete. Subsequent titrations using 10^{-4} and 10^{-3} M Cu titrants (Figures 4.4b and c, respectively) showed similar results. Because simultaneous experiments using other techniques suggested that CC should have been far exceeded in the latter experiments, another explanation for the low $[Cu]_e$ values was sought.

The most likely explanation was felt to be that precipitation occurred either in the UF cell or in the titrant reservoir. The results of an examination of copper concentrations in the acidified UF cell retentate and in the remaining titrants for the three RSL titrations are given in Table 4.1. It can be seen that, in all cases, the analyzed Cu concentration in the reservoir is lower than the calculated nominal concentration and further concentration reductions are found in the reservoir in all but the first titrant. Quality control during standard solution preparation yielded reproducibility to within 5 percent as determined by AA and DPASV analyses, thus suggesting that the problem resulted from reactions occurring during the titrations rather than from analytical error.

The generally lower measured values suggest that losses of Cu occur, either in the reservoir or UF cell during titration or in the polyethylene bottles during the 12-14 hr storage period following titration. Binding of Cu to a UM-05 membrane at pH<6.5 has been reported by Leenheer et al. (1982), and the UM2 membrane used here has similar surface characteristics. Another alternative is that ISE response drifted, even during the short residence times, and that all of the values reported are low by some ratio equal to the nominal:analyzed titrant concentration. This explanation would still not account for loss of Cu in the UF cell, however. In any event, the need to use the UF apparatus for the other analyses and bioassays reported below prevented refinement of the UF titrations. Future research should pursue the possibilities of using higher ionic strength titrants, perhaps employing a metal buffer, to reduce polarization and Donnan exclusion effects at the membrane surface, and using membranes with different surface characteristics (Amicon YM, PM and XM series).

Ion selective electrode titrations

EDTA

In order to observe the behavior of copper in contact with a known concentration of a relatively well-defined organic ligand in dilute solution, an ISE titration of 10^{-5} M Na_2EDTA was performed using 10 µM $Cu(NO_3)_2$ as the titrant. The results of the titration are displayed, along with various graphical techniques recommended in

Table 4.1. Concentrations of Cu in acidified UF cell retentates and titrants for RSL UF titrations.

Analyate	Copper Concentration (M/L)		
Nominal titrant	1.00×10^{-3}	1.00×10^{-4}	1.00×10^{-5}
"Actual" titrant	0.75×10^{-3}	0.25×10^{-4}	0.23×10^{-5}
Retentate	1.02×10^{-3}	0.18×10^{-4}	0.13×10^{-5}

Chapter II for interpreting such data, in Figures 4.5 and 4.6. The resulting values of CC, expressed as M Cu/M EDTA, are presented in Table 4.2. The curve of potential vs. Cu_T (titrant) (Figure 4.5a) indicates a sharp break at an equivalence point of about 8.75 μM Cu, and the Klotz plot (Figure 4.5b) indicates a plateau corresponding to the theoretical single binding site, equivalent to a CC of 10 μM Cu. The plot of p[Cu] vs. pCu_T (Figure 4.6a) shows a break at 8.91 μM Cu. A plot of Cu_B vs Cu_T (Figure 4.6b) indicates a plateau corresponding to 10.3 μM Cu. The Ruzic plot (Figure 4.6c) indicated CC of 10.0 μM with an r^2=0.998. Finally, the Scatchard plot (Figure 4.6d) shows an anomalous rising limb, instead of the straight line with decreasing slope that should correspond to a 1:1 complex at a single binding site. This anomaly is caused by the fact that the ISE calibration curve is nonlinear below 10^{-7} M [Cu], which corresponds to virtually the entire titration range corresponding to a r^2<0.85. Regression of the remaining data points in the linear region of the calibration curve resulted in a CC of 9.53 μM.

Most of the CC values in Table 4.2 fall close to the theoretical value of 1 for the Cu-EDTA complex, and the Klotz and Ruzic plots also give values close to 1. Identical K_f^c values (pH=5.3) were calculated using the Scatchard and Ruzic plots, $10^{7.54}$. The latter value is considerably lower than the theoretical value of $10^{12.9}$ (based on Schwarzenbach 1957). We shall return to this anomalously low value in further discussions.

Humic acid

ISE titrations were performed on two concentrations of Aldrich humic acid (HA) in deionized water, 5 mg/L and 10 mg/L. In both cases, plots of pCu versus pCu_T indicated that Cu binding had occurred during the early stages of

Table 4.2. Copper complexation capacities (CC) for EDTA as determined by six procedures based on Cu-ISE complexometric titration data.

Method of Analysis	CC[a]
Plot of Cu_T vs. POTENTIAL	0.875
Plot of Cu_{TOTAL} vs. Cu_{BOUND}	1.034
Plot of pCu_T vs. POTENTIAL	0.891
Klotz (1982)	1
Ruzic (1980)	1.003
Scatchard (1949)	0.953
Theoretical value	1

[a] M Cu/M EDTA.

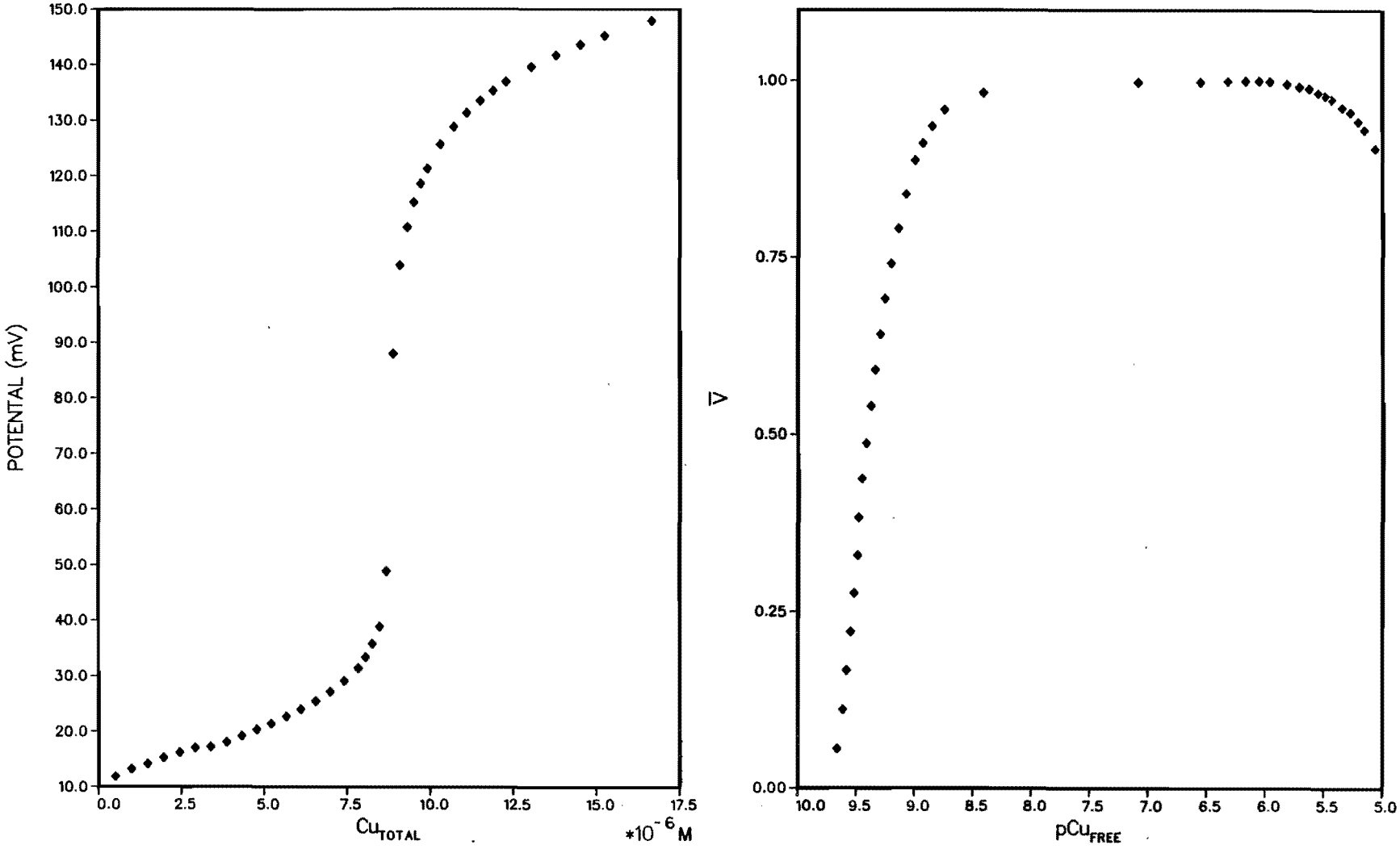

Figure 4.5. Cu-ISE complexometric titration of EDTA with 10^{-5} M copper: a) Cu_T vs. potential and b) Klotz plot.

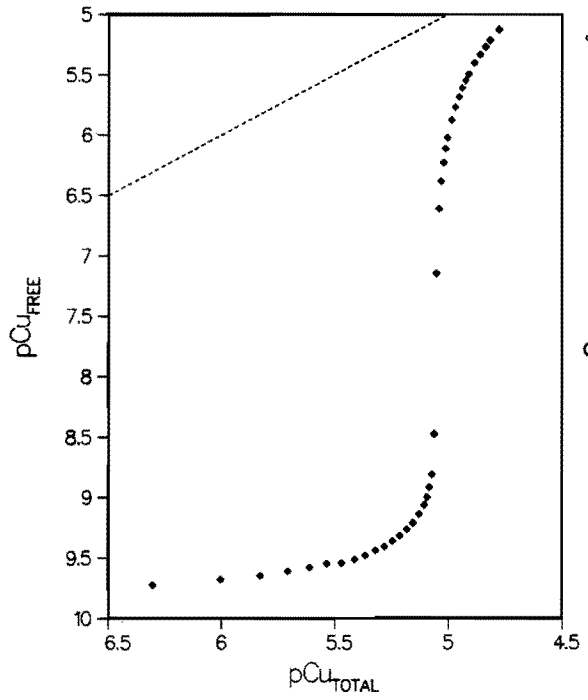

a) pCu_T vs. p[Cu] (dashed line represents Nernstian response for free [Cu])

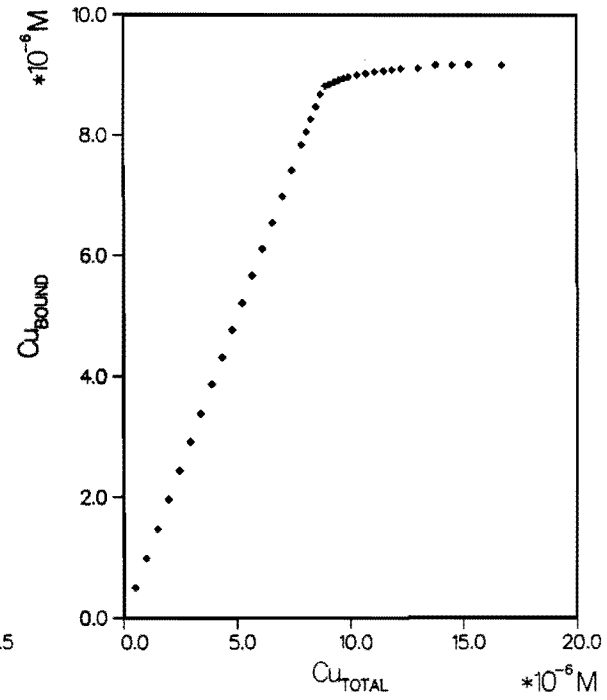

b) Cu_T vs. Cu_{BOUND}

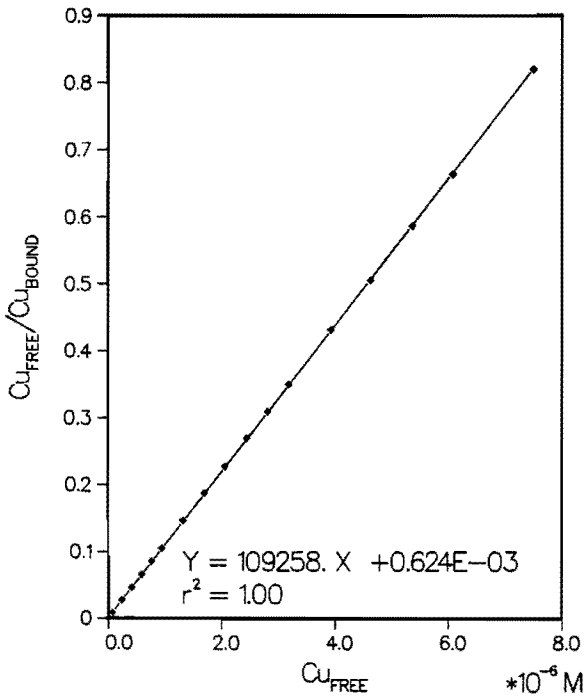

c) Ruzic plot

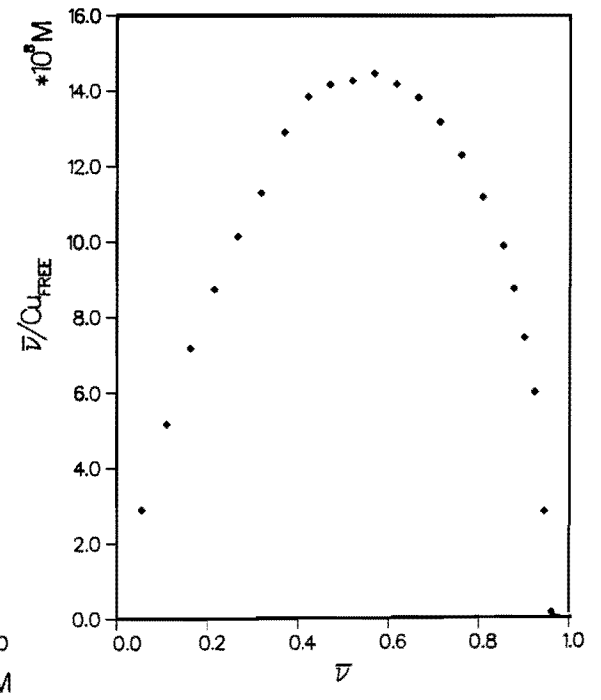

d) Scatchard plot

Figure 4.6. Cu-ISE complexometric titration of EDTA with 10^{-5} M copper.

the titration, but the upper region of the Cu_{BOUND} versus Cu_T curve failed to show a plateau, even at quite high Cu_T values. Instead, the slope became highly linear, suggesting that a constant fraction of the Cu titrant was being bound or otherwise becoming unavailable for detection by the ISE. This same pattern also was observed for the shale leachate fractions described below.

It was subsequently assumed that Cu_{FREE} was being underestimated by a constant factor over the entire range of the titration. The factor $(1 - (Cu_{BOUND}/Cu_T))$ was used over the linear portion of the Cu_{BOUND}/Cu_T curve. All Cu_{FREE} data were adjusted upward by this factor, and the corresponding corrected titration curves were used to calculate the mass action parameters, CC and K_f^c. The uncorrected Cu_{FREE} data were tabulated along with the adjusted data for each Cu-ISE titration as presented in Appendix C. The causes of overestimation of Cu are unclear, but one explanation would be reduction of the potentiometric ISE response through poisoning of the electrode surface by adsorption of the organic being tested. At least five calibration curves run in the absence of an organic ligand showed a Nernstian potentiometric response, which rules out ISE malfunction and inorganic precipitation in deionized water in the pH range and Cu_T concentration used here. Since the temperature was held within $\pm 1.5°C$ during a titration, temperature differences could not have resulted in the lower Cu_{BOUND}/Cu_T slopes observed ($\simeq 0.5$) in some of the titrations.

Although adjustment was not attractive from an analytical standpoint, it was necessary for further interpretation of the data. The most serious potential errors in the interpretations below would result if the assumption was incorrect that the reduction in ISE response was exerted early in the titration and was constant throughout. Such an error would affect the K_f^c values to a greater extent than it would CC. Further work should be done to clarify the reasons for this phenomenon.

Various transformations of the data from the titration with 5 mg/L of HA are plotted in Figure 4.7. Corresponding data from the 10 mg/L HA titration are shown in Figure 4.8 and the resulting CC and K_f^c values for both concentrations are given in Table 4.3. At the 5 mg/L concentration all three data transformations showed a CC of 1.2×10^{-6} M Cu/mg HA. This value corresponds reasonably well with the value determined by the UF titration in the previous section. The Ruzic plot shows good linearity and results in a log K_f^c of 6.23, which is again in reasonably good agreement with the UF titration. The Scatchard plot yields a "strong" site (of high K_f^c) from the straight line at low values of $\bar{\nu}$ with log K_f^c = 7.73 (n = 0.425) and a "weak" site (of lower K_f^c) from the linear region at high values of $\bar{\nu}$ with log K_f^c = 5.89 (n = 0.994). The pH of the solution at the beginning of the titration was 5.7. The corresponding 10 mg/L HA titration showed a higher CC, 1.3×10^{-6} M Cu/mg HA, which suggests that some intermolecular bridging (e.g. Langford et al. 1983) by Cu may occur at the higher concentration thus leading to additional binding sites. The log K_f^c based on the Ruzic plot decreases relative to that found for 5 mg/L HA of 6.04. Scatchard analysis indicated a shift in the strong site log K_f^c upward to 8.65 (n = 0.21) but a similar weak site log K_f^c of 5.74 (n = 1.03). The pH at the beginning of the titration was 6.0.

Raw shale leachate (RSL)

Two raw shale leachate samples obtained from batch, static 1:4 48 hr extraction were titrated using the ISE technique and several concentrations of Cu titrant. Initially, the RSL was not diafiltered to remove the preexisting salts, because it was reasoned that the inorganic copper complexes

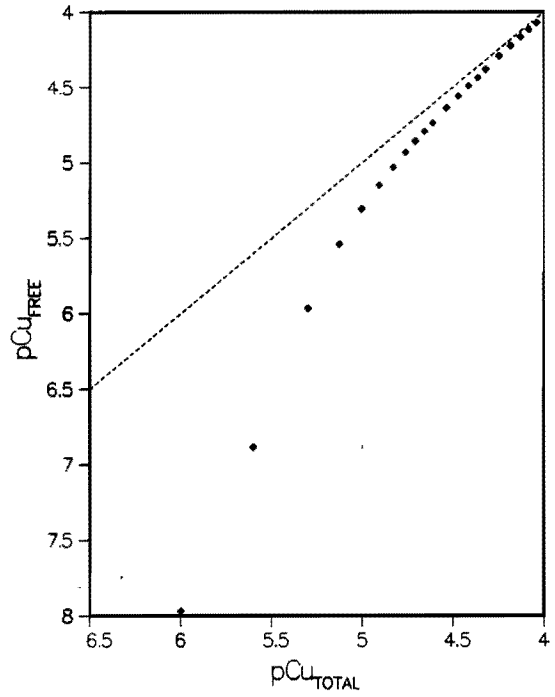

a) pCu_T vs. p[Cu] (dashed line represents Nernstian response for free [Cu])

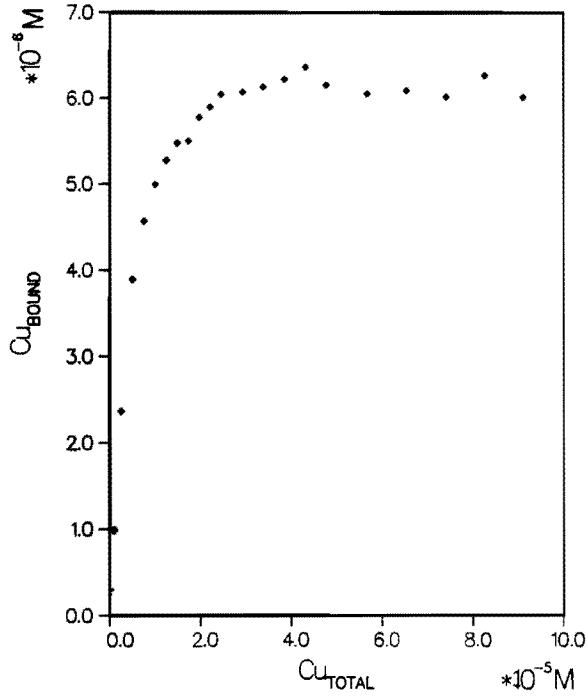

b) Cu_T vs. Cu_{BOUND}

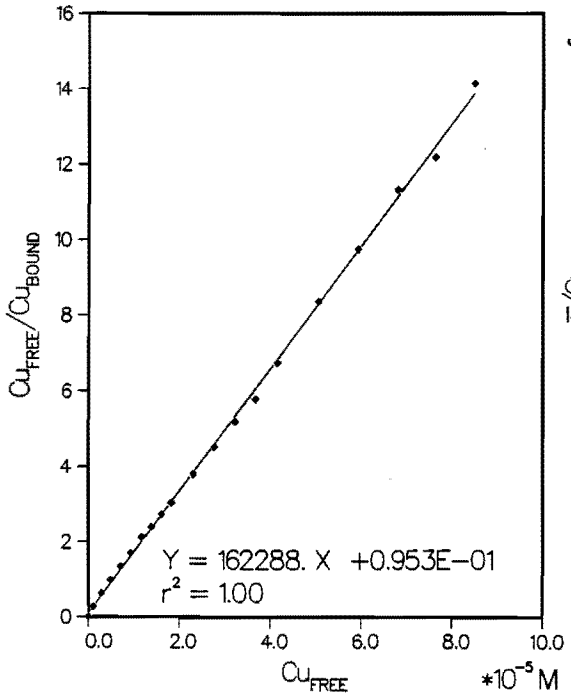

c) Ruzic plot

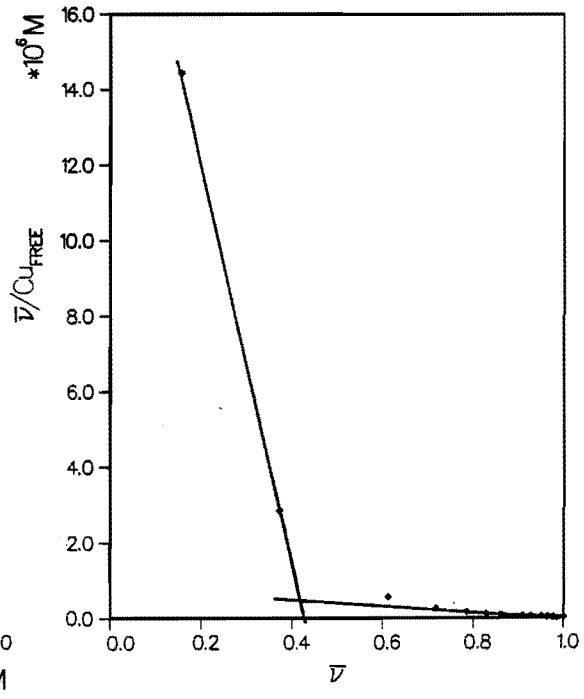

d) Scatchard plot

Figure 4.7. Cu-ISE titration of 5 mg/L humic acid with copper.

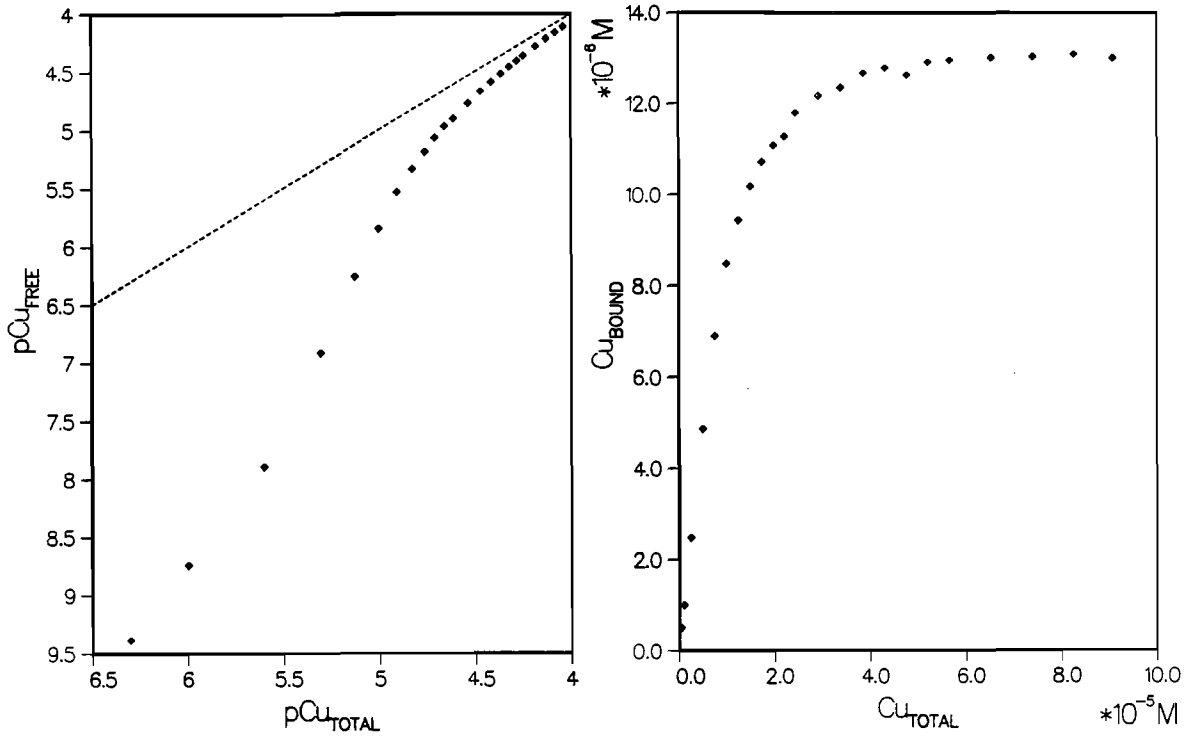

a) pCu_T vs. p[Cu] (dashed line represents Nernstian response for free [Cu])

b) Cu_T vs. Cu_{BOUND}

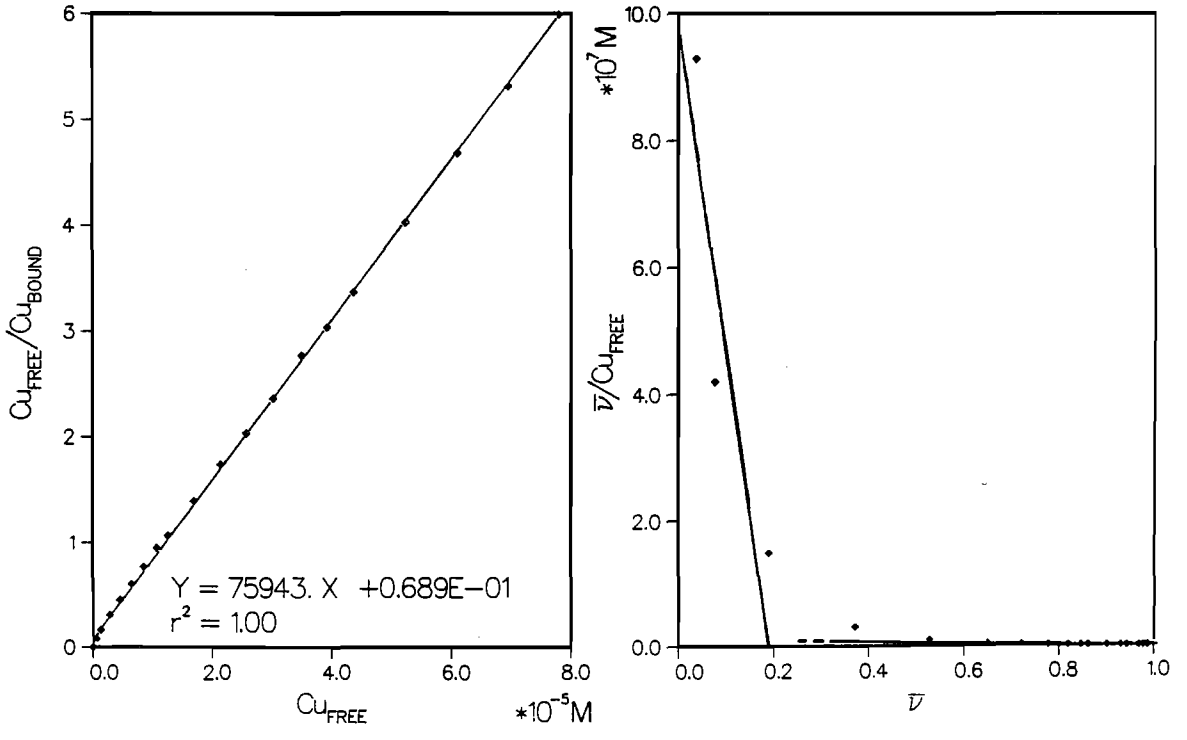

c) Ruzic plot

d) Scatchard plot

Figure 4.8. Cu-ISE titration of 10 mg/L humic acid with copper.

Table 4.3. Copper complexation capacities (CC) and log conditional stability constants (log K_f^c) for humic acid as determined based on Cu-ISE complexometric titrations.

	Concentration of Humic Acid			
	5 mg/L		10 mg/L	
Method of Analysis	CC[a]	log K_f^c	CC	log K_f^c
Cu_{TOTAL} vs. Cu_{BOUND}	1.24×10^{-6}	--	1.30×10^{-6}	--
Klotz (1982)	1.24×10^{-6}	--	1.30×10^{-6}	--
Ruzic (1980)	1.23×10^{-6}	6.23	1.32×10^{-6}	6.04
Scatchard (1949)				
(Stronger site)		7.73		8.65
(Weaker site)		5.89		5.74

[a]M Cu/mg HA.

would be detected by the ISE as free cupric ion and thus would not interfere with the measurement of the organic complexation. Titration data of this 100 percent RSL sample (DOC = 10 mg/L), which include two separate, overlapping titrations at different Cu_T ranges, are displayed in Figure 4.9.

The calculated CC for this RSL sample ranged from 4.60-4.73 x 10^{-4} M/L, which corresponds to 4.60-4.73 x 10^{-5} M Cu/mg DOC. The Ruzic plot yields a log K_f^c value of 4.91. The Scatchard analysis suggests a strong binding site with a log K_f^c of 6.96 (n = 0.19) and a weak binding site with a log K_f^c of 4.52 (n = 1.12). The high CC value and the low K_f^c for the weaker site suggested that metal complexation in the RSL sample may not be solely contributed by the organic ligands. The CC of the RSL batch extract would result in a Cu:TOC ratio of 0.57:1, which is clearly too high for an organic chelate. Alternatively, such a ratio could result from some combination of complexation by acetate ($K_f = 10^{1.87}$), glycine ($K_f = 10^{8.1}$), and/or NH_3 ($K_f = 10^{5.8}$) (Leckie and Davis 1979). Our experiments have shown that copper acetate complexes are not sensed by the Cu-ISE, but that Cu-NH_3 complexes, like many of the hydroxy- and carbonato-complexes (Wagemann 1980) are. These results suggested that precipitation of Cu may have been occurring in the titration cell.

A subsequent titration was carried out using a second RSL extract that subsequently was diafiltered through a UM2 ultrafiltration membrane to remove the pre-existing inorganic salts. MAAP medium made up in a 50 percent solution of this RSL in order to duplicate the conditions in the algal bioassay are described below. Titration data of this 50 percent diafiltered RSL (DOC = 6.2 mg/L) in MAAP medium are displayed in Figure 4.10 and the corresponding CC and K_f^c values can be found in Table 4.4. The calculated CC for this RSL sample ranged from 6.72-8.25 x 10^{-6}

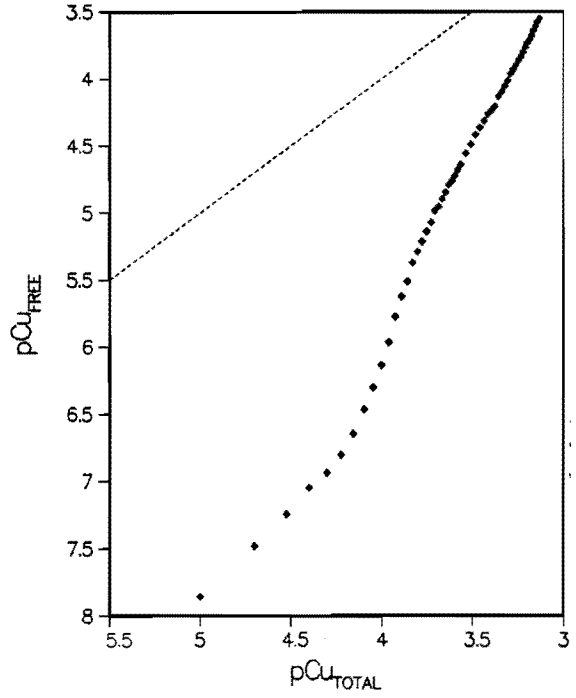

a) pCu_T vs. p[Cu] (dashed line represents Nernstian response for free [Cu])

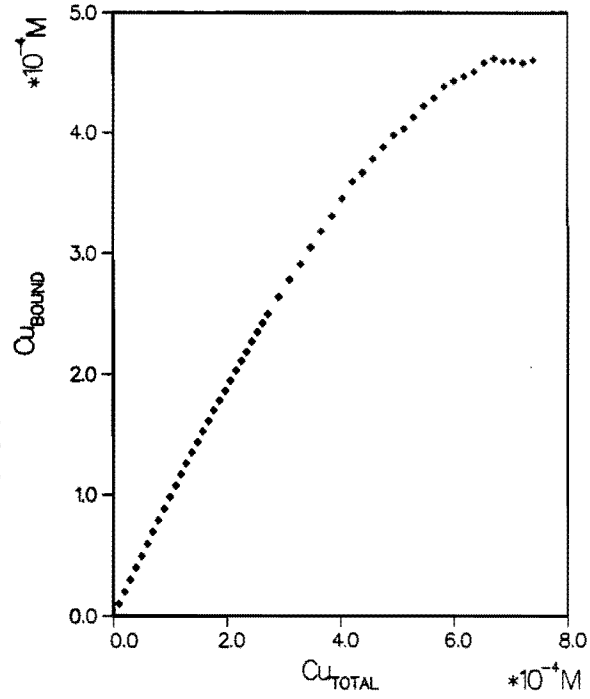

b) Cu_T vs. Cu_{BOUND}

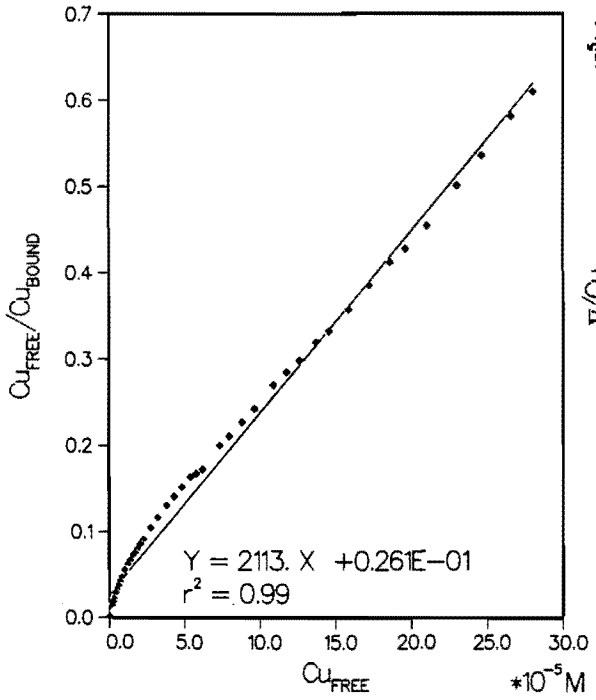

c) Ruzic plot

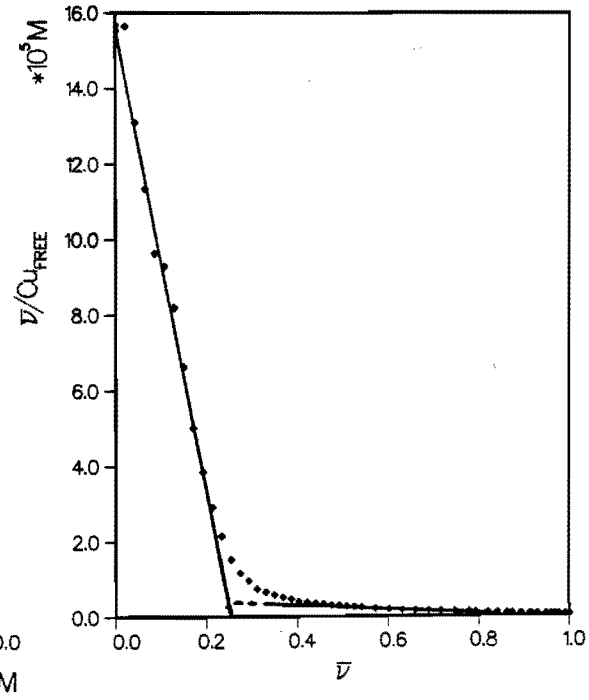

d) Scatchard plot

Figure 4.9. Cu-ISE titration of copper with 100 percent diafiltered raw shale leachate (RSL) obtained from batch, static 48 hrs extraction.

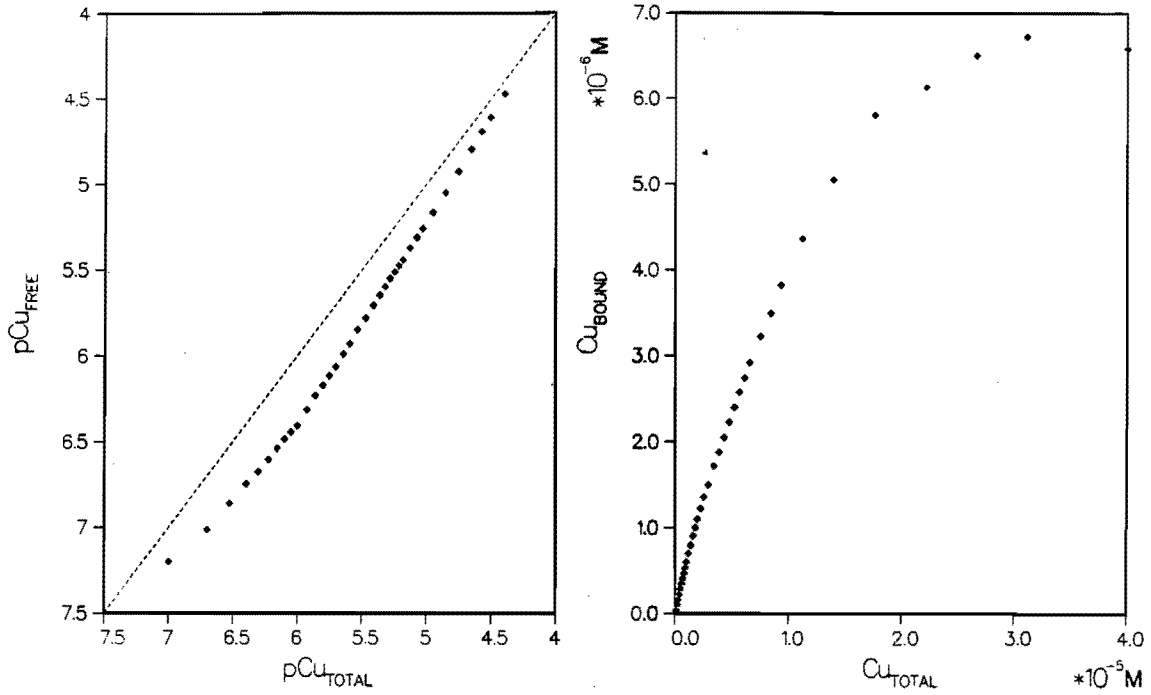

a) pCu_T vs. p[Cu] (dashed line represents Nernstian response for free [Cu])

b) Cu_T vs. Cu_{BOUND}

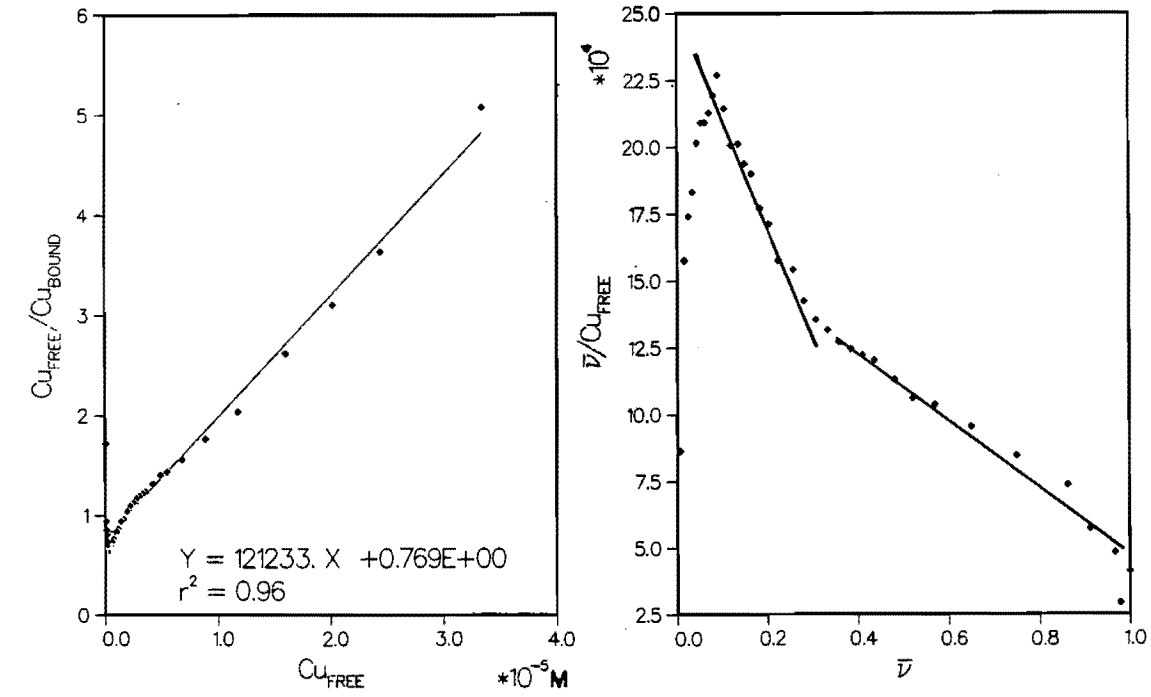

c) Ruzic plot

d) Scatchard plot

Figure 4.10. Cu-ISE titration of copper with 50 percent diafiltered raw shale leachate (RSL) in MAAP medium.

Table 4.4. Copper complexation capacities (CC) and log conditional stability constants (log K_f^c) for raw oil shale leachates as obtained from Cu-ISE complexometric titrations.

	Raw Shale Leachate					
	Batch, Static 1:4 48 hr Extracted RSL[a]		Pore Volumes Collected from an Upflow Column			
			RSL_1[b]		RSL_3[c]	
Method of Analysis	CC[d]	log K_f^c	CC	log K_f^c	CC	log K_f^c
Cu_{TOTAL} vs Cu_{BOUND}	2.17×10^{-6}	--	3.42×10^{-8}	--	3.00×10^{-7}	--
Klotz (1982)	2.17×10^{-6}	--	3.42×10^{-8}	--	3.00×10^{-7}	--
Ruzic (1980)	2.66×10^{-6}	5.20	3.33×10^{-8}	5.97	3.46×10^{-7}	4.92
Scatchard (1949) (Stronger site)		5.96		ND[e]		6.38
(Weaker site)		5.10		5.63		4.77

[a]RSL = 50 percent diafiltered raw shale leachate obtained from batch, static 48 hr extracted in MAAP medium (DOC = 6.2 mg/L).
[b]RSL_1 = first pore volume of raw shale leachate collected from an upflow column (TOC = 95 mg/L).
[c]RSL_3 = third pore volume of raw shale leachate collected (TOC = 18.5 mg/L).
[d]M Cu/mg TOC.
[e]ND = Not determinable.

M/L, which corresponds to 2.17-2.66 x 10^{-6} M Cu/mg DOC. The corresponding Cu:C ratio, 0.023:1, appears to be more in line with values reported for HA than does the ratio for the previous sample, and indicates that the former value was incorrect due to interfering reactions brought about by the dissolved salts (or organics able to pass the UM2 ultrafilter) associated with the undiafiltered sample. The Ruzic plot (Figure 4.10c) yields a log K_f^c value of 5.20. The Scatchard analysis (Figure 4.10d) suggests two binding sites, with the stronger site having a log K_f^c of 5.96 (n = 0.34), and a weak binding site with a log K_f^c of 5.10 (n = 1.36).

Another set of RSL samples were collected from an upflow column by Hinchee (1983), who collected five successive pore volumes of leachate using deionized water as the elutent. The first three pore volumes were analyzed for binding capacity by ISE titration, but only the first and third volumes RSL_1 and RSL_3 showed sufficient binding capacity to be measured. The corresponding titration data values are shown in Figures 4.11 and 4.12, and the data are summarized in Table 4.4. RSL_1 showed a CC of 3.3 x 10^{-6} M/L, corresponding to 3.4 x 10^{-8} M Cu/mg TOC. A Ruzic plot indicated a log K_f^c of 5.97. Only one binding site could be detected using Scatchard analysis, with a K_f^c of 5.63 (n = 1.03) corresponding reasonably well with the Ruzic values. The CC of RSL_3 was 5.5 x 10^{-6} M/L or 3.0 x 10^{-7} M Cu/mg TOC. The log K_f^c of this fraction was somewhat weaker than RSL_1, 4.92, and could be partitioned into strong (log K_f^c = 6.38, n = 0.23) and weak (log K_f^c = 4.77, n = 1.24) binding sites by using a Scatchard plot.

Differential pulse anodic stripping voltammetry (DPASV) studies

DPASV pseudo-polarograms

The DPASV characteristics of free Cu(II), Cu(II)-EDTA, Cu(II)-HA solutions were examined by constructing pseudo-polarograms in order to determine the least negative deposition potential ($E_{d(min)}$) that would result in the maximum plating efficiency for measuring free copper concentration during the complexation titrations. Pseudo-polarograms of free Cu(II), Cu(II)-EDTA, and Cu(II)-HA in 0.1 M acetate medium at pH values of 4.5 and 6.3 are shown in Figures 4.13a and 4.13b, respectively. Free Cu(II) required an E_p of -0.5 and -0.3 V at pH 4.5 and 6.3, respectively, for 100 percent yield. The stripping peaks occurred at -0.01 and -0.05 V, respectively. At these E_p, almost 100 percent of the Cu(II)-EDTA complex was reduced at pH 4.5, and 40 percent at pH 6.3. In the presence of EDTA, the Cu pseudopolarograms shifted -0.23 V and -0.15 V in the acetate medium at pH values of 4.5 and 6.3, respectively. The effect of a complexing agent, according to Figura and McDuffie (1979), is to shift the reduction potential of the free metal in the cathodic direction. For the Cu(II)-EDTA complex, maximum dissociation occurred at -0.5 V and -0.7 V at pH 4.5 and 6.3, respectively, and no Cu(II)-EDTA was reduced below an applied plating potential of -0.25 V at either pH level. At pH 4.5, a plating potential below -0.6 V caused the Cu(II)-EDTA complex to be hydrolyzed. This implied that the simultaneous determinations of Zn, Cd, Pb, and Cu could underestimate the Cu concentration in the sample, due to this counteracting hydrolysis reaction occurring at a more negative plating potential.

A pseudo-polarogram for Cu(II)-HA at pH 6.3 (Figure 4.13b) indicated that more than 70 percent of the copper was from the Cu(II)-HA complex and reduced at the plating potentials applied (-0.20 to -1.00 V). This is in accord with the arguments of Tuschall and Brezonik (1981) and others, that the DPASV technique might not be suitable for binding determination of complex heterogeneous organic ligands present in natural waters.

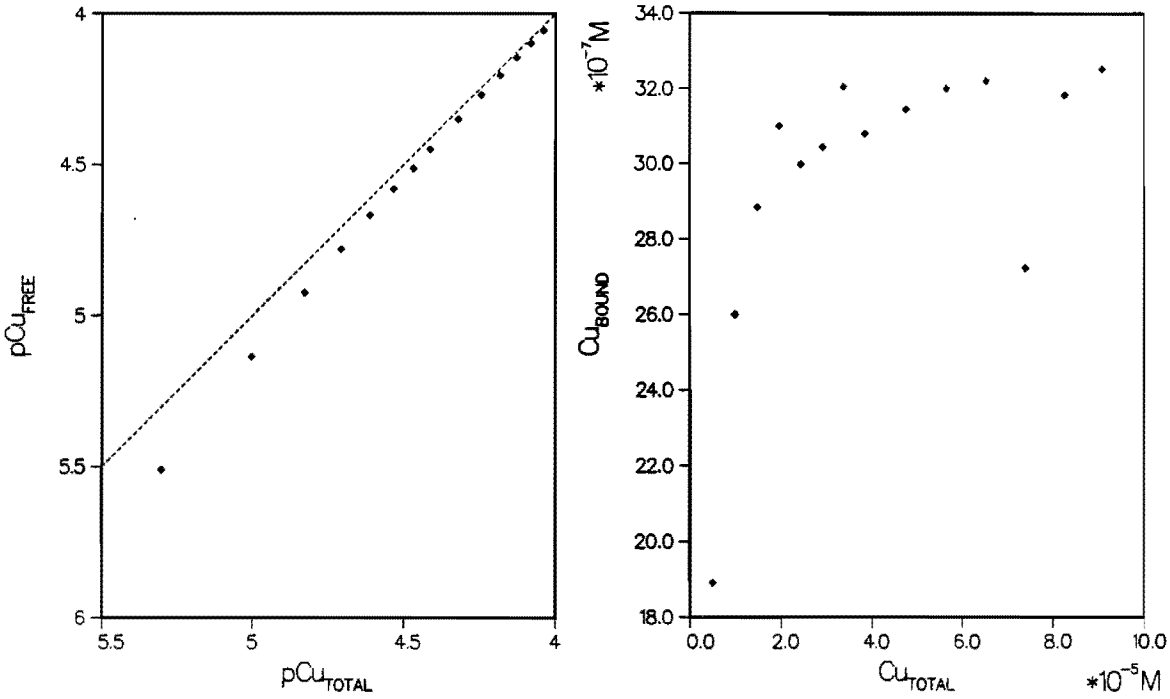

a) pCu_T vs. p[Cu] (dashed line represents Nernstian response for free [Cu])

b) Cu_T vs. Cu_{BOUND}

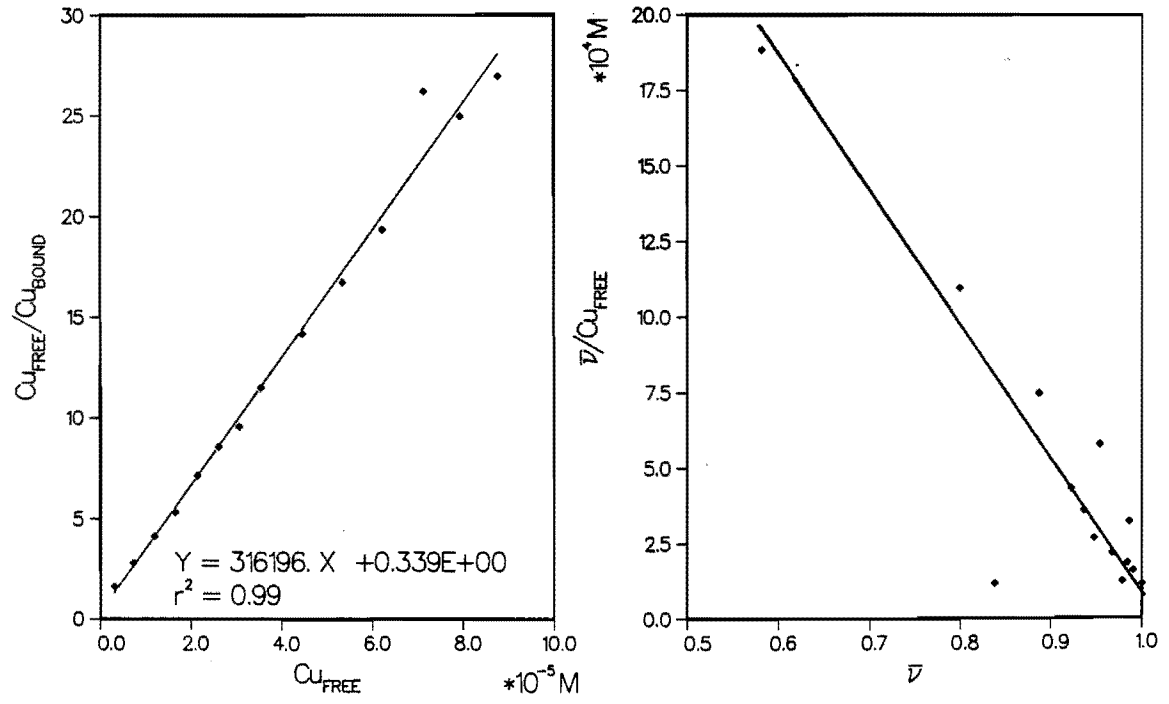

c) Ruzic plot

d) Scatchard plot

Figure 4.11. Cu-ISE titration of the first pore volume of raw shale leachate (RSL_1) collected from an upflow column with copper.

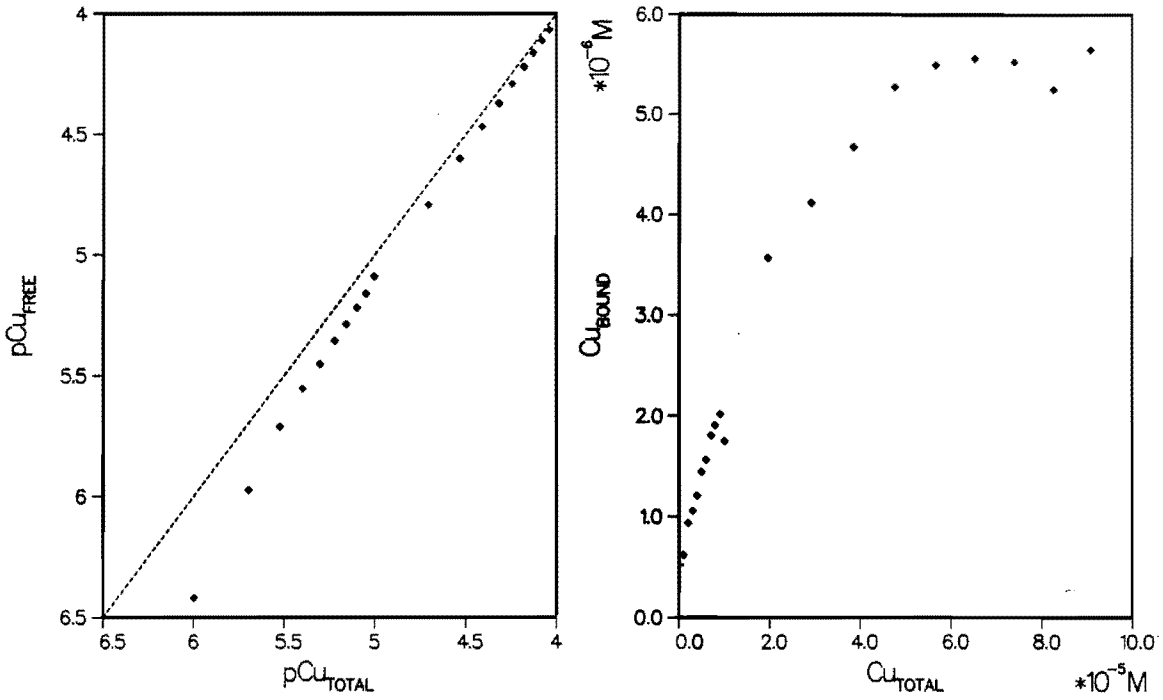

a) pCu_T vs. p[Cu] (dashed line represents Nernstian response for free [Cu])

b) Cu_T vs. Cu_{BOUND}

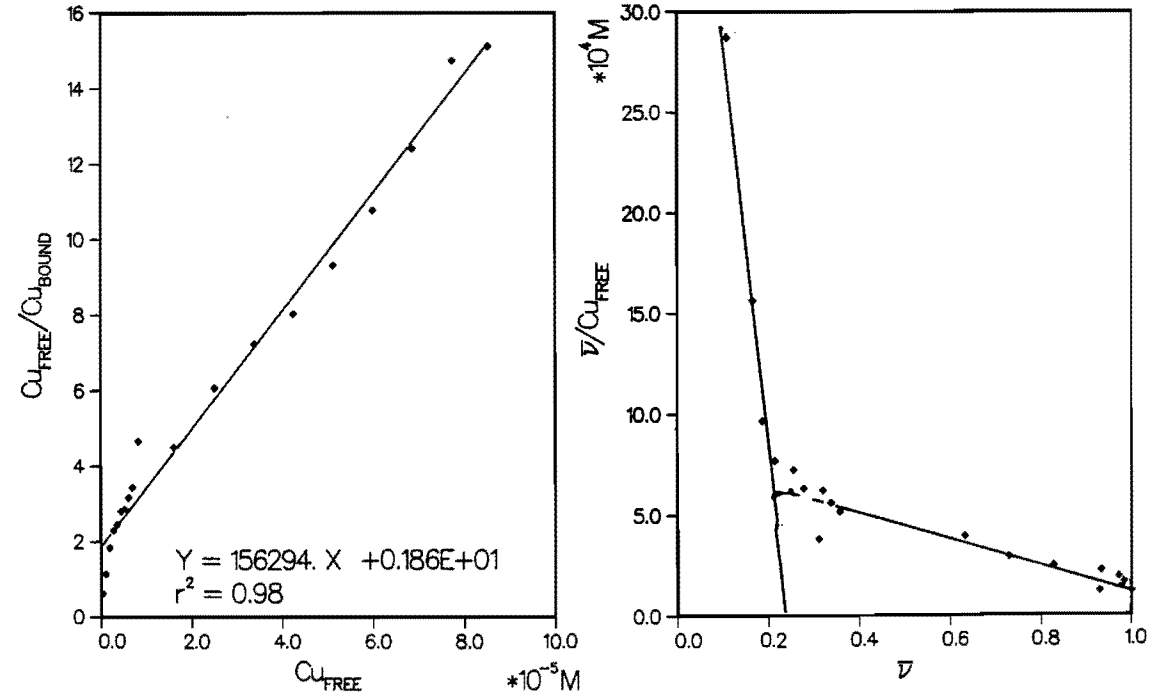

c) Ruzic plot

d) Scatchard plot

Figure 4.12. Cu-ISE titration of the third pore volume of raw shale leachate (RSL_3) collected from an upflow column with copper.

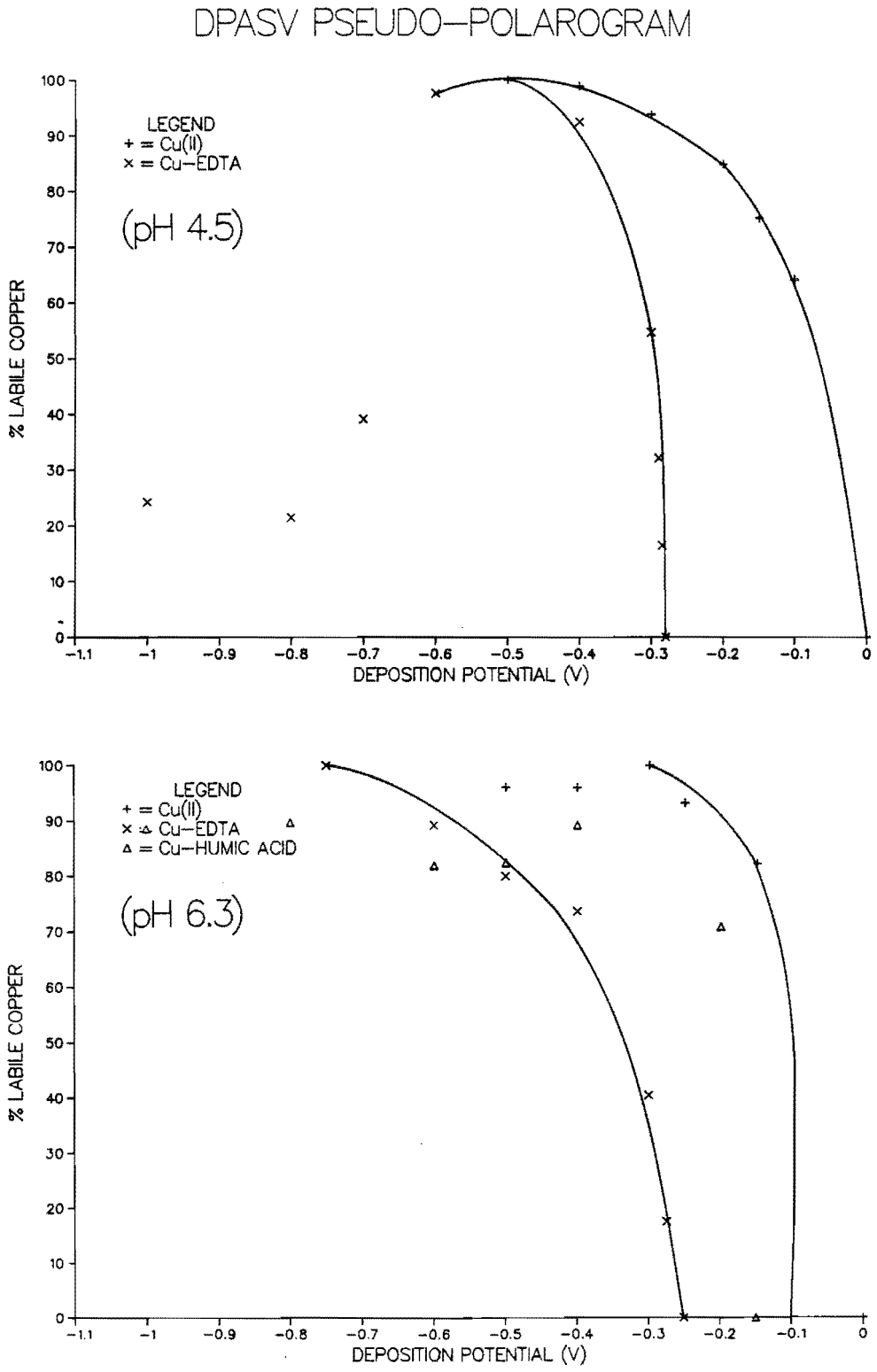

Figure 4.13. DPASV pseudo-polarograms of free Cu(II), Cu-EDTA, and Cu-HA in 0.1 M acetate medium at a) pH 4.5 and b) pH 6.3.

Based on these pseudo-polarograms, if too high an E_p is used in the DPASV binding experiments, direct reduction of the nonlabile complexes may occur, thus giving rise to the possibility of including nonlabile complexes in the DPASV-labile fraction and thus underestimating their binding capacities. Therefore, an E_p of -0.20 V was used for all further binding experiments and measurements of free copper concentrations. A change in the deposition time to 90 seconds (60 seconds of deposition followed by a 30 seconds of equilibration period) was used to reduce the possibility of dissociating any nonlabile complexes.

Complexometric titration using DPASV

EDTA. Titrations of EDTA and commerical (Aldrich) humic acid with copper were performed before using DPASV on the oil shale leachates. The DPASV complexometric titration curve for EDTA with copper is shown in Figure 4.14a. The upper slope $(S_U)=10^{5.30}$ corresponds well with the slope obtained for copper standards containing only the acetate electrolyte, thus indicating that the EDTA had no effect on the stripping current, other than that caused by complexation of the free metal.

Analysis of the DPASV data for the Cu-EDTA titration using different a:b molar stoichiometries for the complex, as recommended by Shuman and Woodward (1977), is shown in Figure 4.14b and Table 4.5. Although the data showed a reasonably good fit to a a 1:1 stoichiometry, all but one of the other stoichiometries tested (95:100) showed higher correlation coefficients. There is little reason to expect the stoichio-

Table 4.5. DPASV stripping current as a function of $(C_M/a)^{1/a}/(C_L - b/a\ C_M)^{b/a}$ for EDTA with copper using different a and b integers.

	$(C_M/a)^{1/a}/(C_L - b/a\ C_M)^{b/a}$					
Peak Current, i_p (A)	1:1[a]	2:1	3:1	2:2	3:2	95:100
4.590×10^{-2}	0.2294[b]	0.3208	0.4047	36.24	9.112	1.646×10^{4}
1.756×10^{-1}	0.3886	0.4033	0.4685	50.16	10.95	1.861×10^{4}
2.868×10^{-1}	0.5952	0.4789	0.5217	66.54	12.71	2.186×10^{4}
3.930×10^{-1}	0.8741	0.5515	0.5688	87.41	14.51	2.638×10^{4}
4.330×10^{-1}	1.271	0.6234	0.6120	116.03	16.42	3.312×10^{4}
r^2 (based on first 4 data points)	0.971	1.000	0.9995	0.9815	0.998	0.9586
S_L (Lower slope)	0.527	1.502	2.110	6.699×10^{-3}	6.42×10^{-2}	3.379×10^{-5}
K_f^c (= S_U/S_L^a)	5.58[c]	4.94	4.32	9.64	8.88	$+\infty$[d]

[a] a:b molar complexation stoichiometry as in $aM + bL = M_aL_b$.
[b] Values are based on $C_L = 1.072\times10^{-4}$ M.
[c] Values are log K_f^c, where $S_U = 10^{5.30}$.
[d] Value of K_f^c is + due to a slope of zero for the S_L^a term.

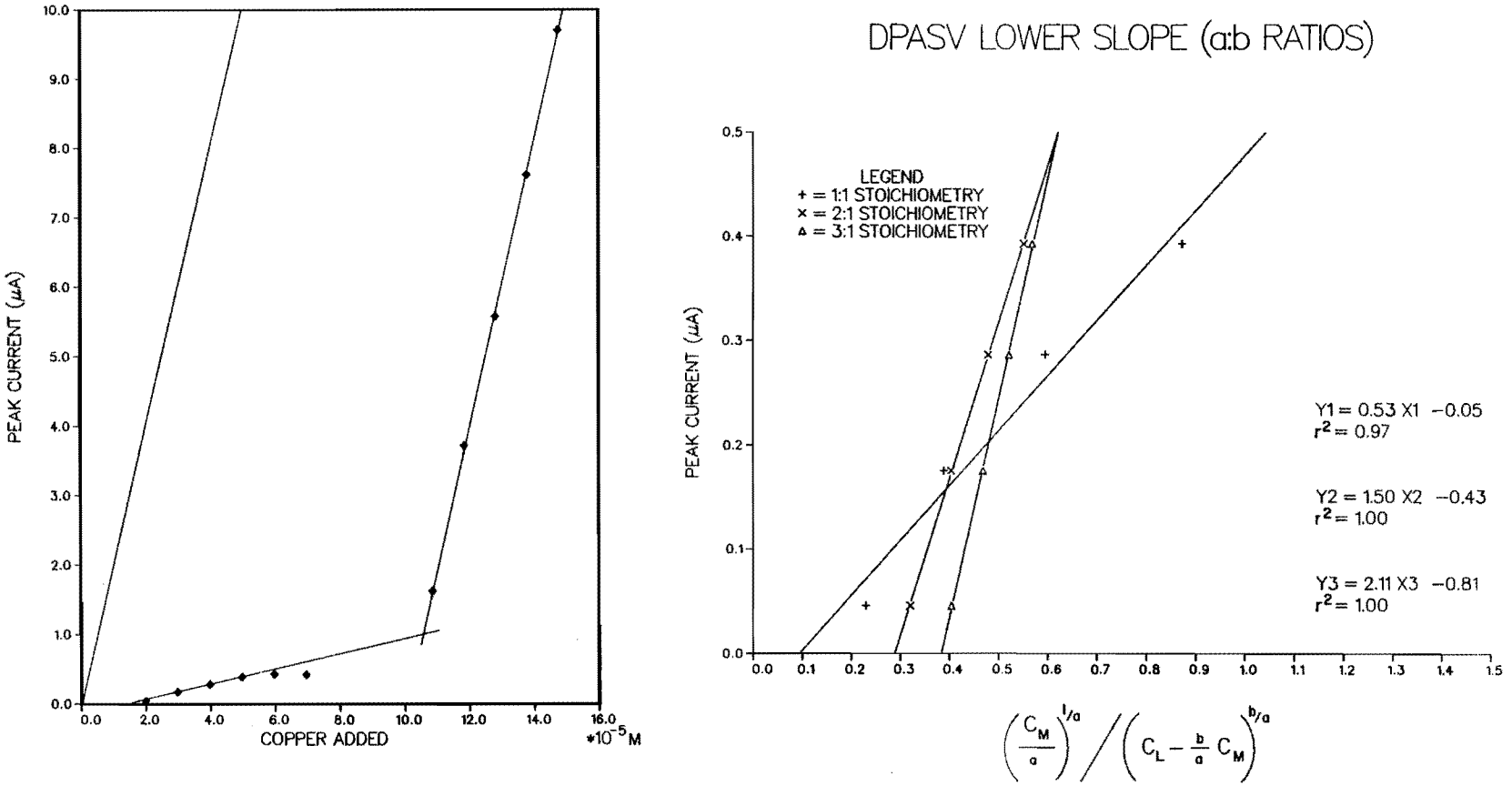

Figure 4.14. DPASV complexometric titration curve for EDTA with copper: a) peak current vs. copper added and b) peak current vs. $[(C_M/a)^{1/a}/(C_L - b/a\ C_M)^{b/a}]$.

metry of the Cu:EDTA complex to be much different than 1:1. Therefore, it is difficult to predicate a decision on the stoichiometry of an unknown complex on such DPASV data. The importance of determining the appropriate stoichiometry lies in the "a" term used to determine K_f^c (Shuman and Woodward 1977), $K_f^c = S_U/(S_L)^a$. The large effect of the term on K_f^c can be observed in Table 4.5.

The K_f^c values determined by DPASV for the Cu(II)-EDTA complex ranged from $10^{5.58}$ to $10^{6.19}$. All the values were well below the value cited by Schwarzenbach (1957) of $10^{12.8}$. However, Tuschall and Brezonik (1981) also found a lower value for the Cu-EDTA complex ($10^{7.7}$) when using a DPASV technique. Various plots used to interpret the CC and K_f^c values are shown in Figure 4.15. For 9.95×10^{-5} M/L of EDTA the complexation capacities (CC) determined are tabulated in Table 4.6, along with the K_f^c values. The CC values agree well among the procedures, and well with the 1:1 theoretical binding stoichiometry of EDTA with copper. This agreement implies that the DPASV complexometric titration is a reasonable method for determination of the complexation capacity of a simple ligand which only has one binding site, but does not necessarily distinguish the correct reaction stoichiometry between the metal and the ligand.

Humic acid. Commerical (Aldrich) humic acid (HA) was used as another model ligand. A DPASV complexometric titration curve of HA with copper is shown in Figure 4.16. CC and K_f^c results from this titration, based on different methods of data analysis, are

Table 4.6. Copper complexation capacities (CC) and log conditional stability constants (K_f^c) for EDTA as determined by different procedures using data from the DPASV complexometric titration.

Method of Analysis	CC[a]	Log K_f^c
Plot of Cu_{TOTAL} vs. Cu_{BOUND}	1.01	-[b]
Chau et al. (1974)	1.00	-
Klotz (1982)	1	-
Ruzic (1980)	1.04	5.74
Scatchard (1949)	1.14	5.61
Shuman and Woodward (1973) (1:1 stoichiometry)	1.03	5.58
Theoretical value	1	12.8

[a]M Cu/M EDTA.
[b]Method not applicable for K_f^c determination.

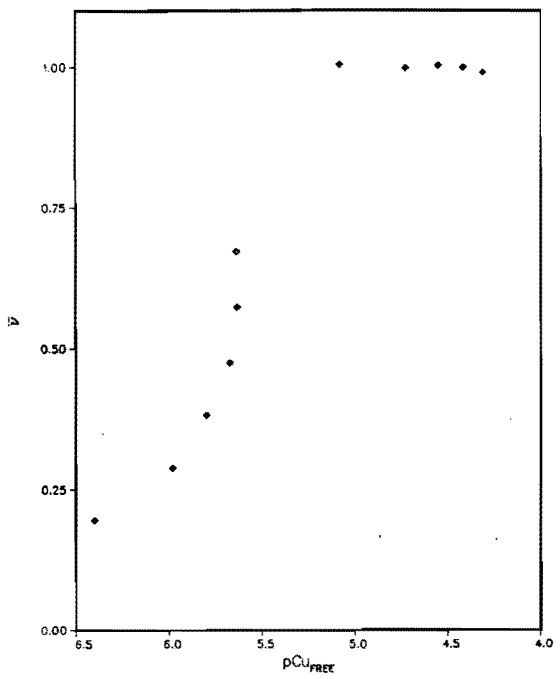

a) Klotz plot

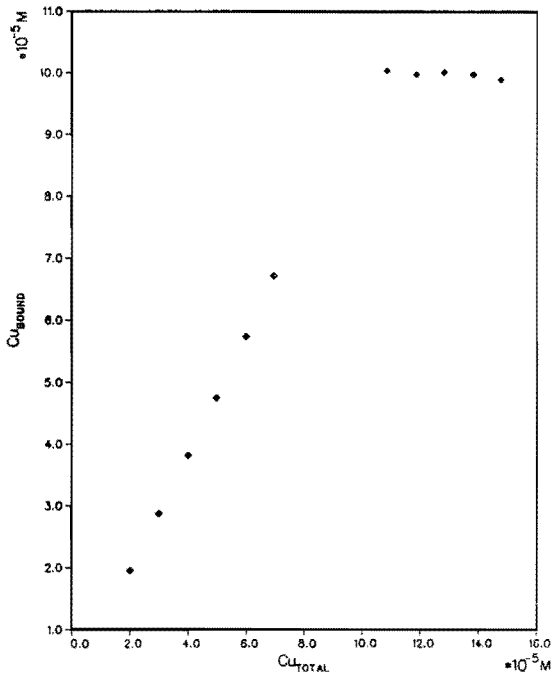

b) Cu_T vs. Cu_{BOUND}

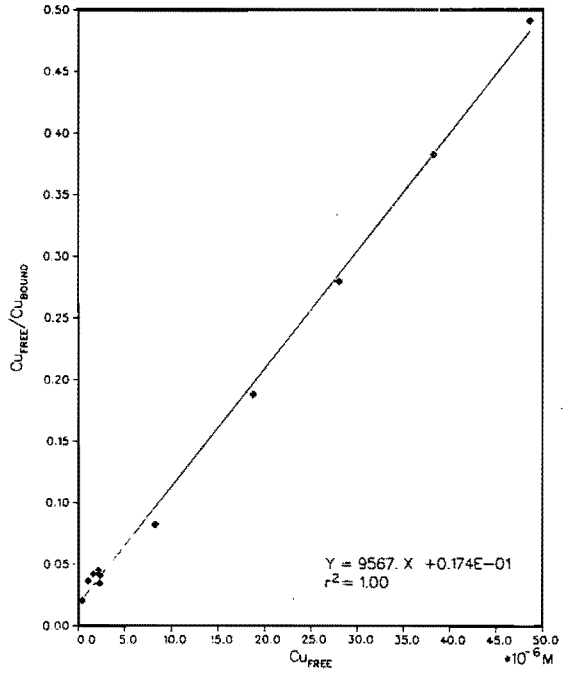

c) Ruzic plot

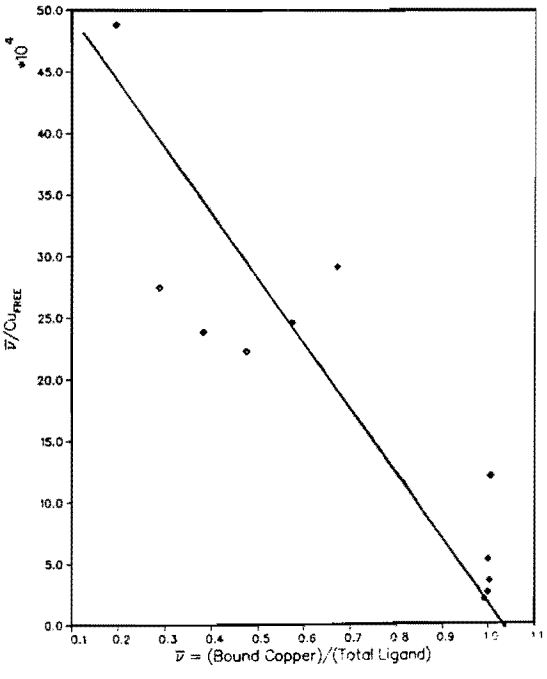

d) Scatchard plot

Figure 4.15. DPASV titration of EDTA with copper.

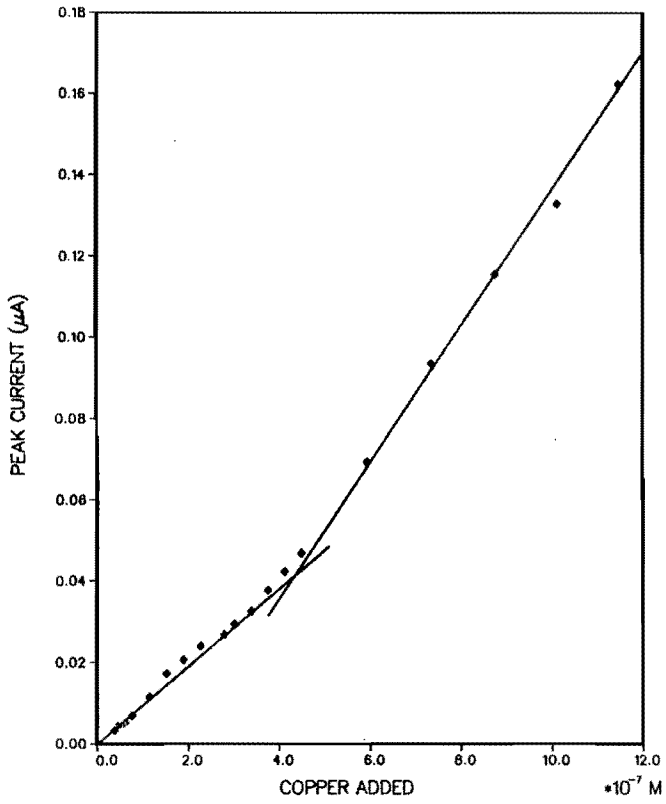

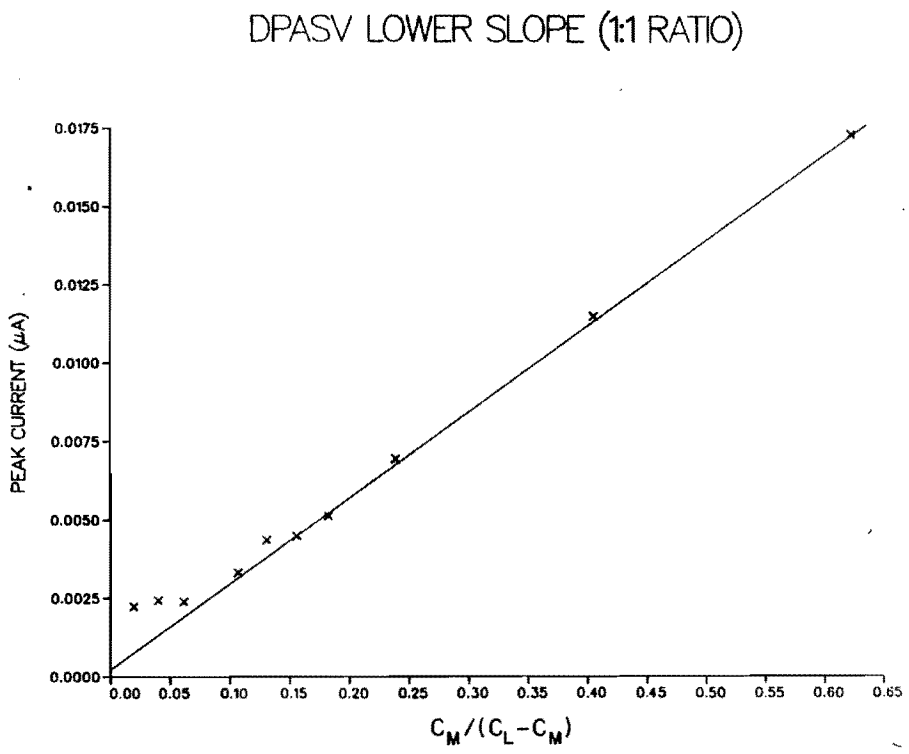

Figure 4.16. DPASV complexometric titration curve for 10 mg/L humic acid with copper: a) peak current vs. copper added and b) peak current vs. $[(C_M)/(C_L - C_M)]$ based on a 1:1 stoichiometry.

presented in Table 4.7 and plotted on Figure 4.17. Copper complexation capacities (CC) for humic acid ranged from 1.86×10^{-8} to 1.02×10^{-7} M Cu/mg HA. These CC values are lower than the values determined by either continuous ultrafiltration or Cu-ISE techniques, and they are much lower than the range of 1.5-5 meq Cu/g HA reported by Stevenson (1982).

Determination of the complexation capacity using the assumptions made by Chau et al. (1974) resulted in a lower CC, 1.86×10^{-8} M Cu/mg HA, than determining CC at the break point of the two different slopes on the titration curve. The formula of Chau et al. (1974), CC = -A/B (where A = the abscissa, and B = the slope of the upper slope), underestimates CC because the lower slope of the titration curves for the model ligands EDTA and humic acid failed to show an initial slope as close to the x-axis as expected. This error in determination of CC would be more pronounced with weak, more labile complexes, for which the initial slope would be steeper.

The K_f^c of the Aldrich humic acid, as determined by three different techniques, ranged from $10^{6.78}$ to $10^{8.78}$. These K_f^c values agree well with those determined by the continuous ultrafiltration and Cu-ISE techniques, and also agree with the values reported by other workers (Table 4.8) employing different techniques in different testing conditions (pH, electrolyte, and type of humic acid extracts).

The Scatchard plot (Figure 4.17c) for humic acid indicated that two distinct classes of binding ligands are present in HA with the stronger site (occurring at lower $\bar{\nu}$ value) having a K_f^c of $10^{8.78}$ and the weaker $10^{6.78}$. In contrast, there is only one K_f^c value (based on the Scatchard plot)

Table 4.7. Copper complexation capacities and conditional stability constant for 10 mg/L humic acid (HA) as determined by different procedures using data from the DPASV complexometric titration.

Method of Analysis	CC[a]	Log K_f^c
Plot of Cu_{TOTAL} vs Cu_{BOUND}	ND[b]	-[c]
Chau et al. (1974)	1.86×10^{-8}	-
Ruzic (1980)	1.02×10^{-7}	7.53
Scatchard (1949) (Stronger site)	-	8.78
(Weaker site)	-	6.83
Shuman and Woodward (1973) (1:1 stoichiometry)	4.07×10^{-8}	6.78

[a] M Cu/mg HA
[b] ND = not detected.
[c] Method not applicable.

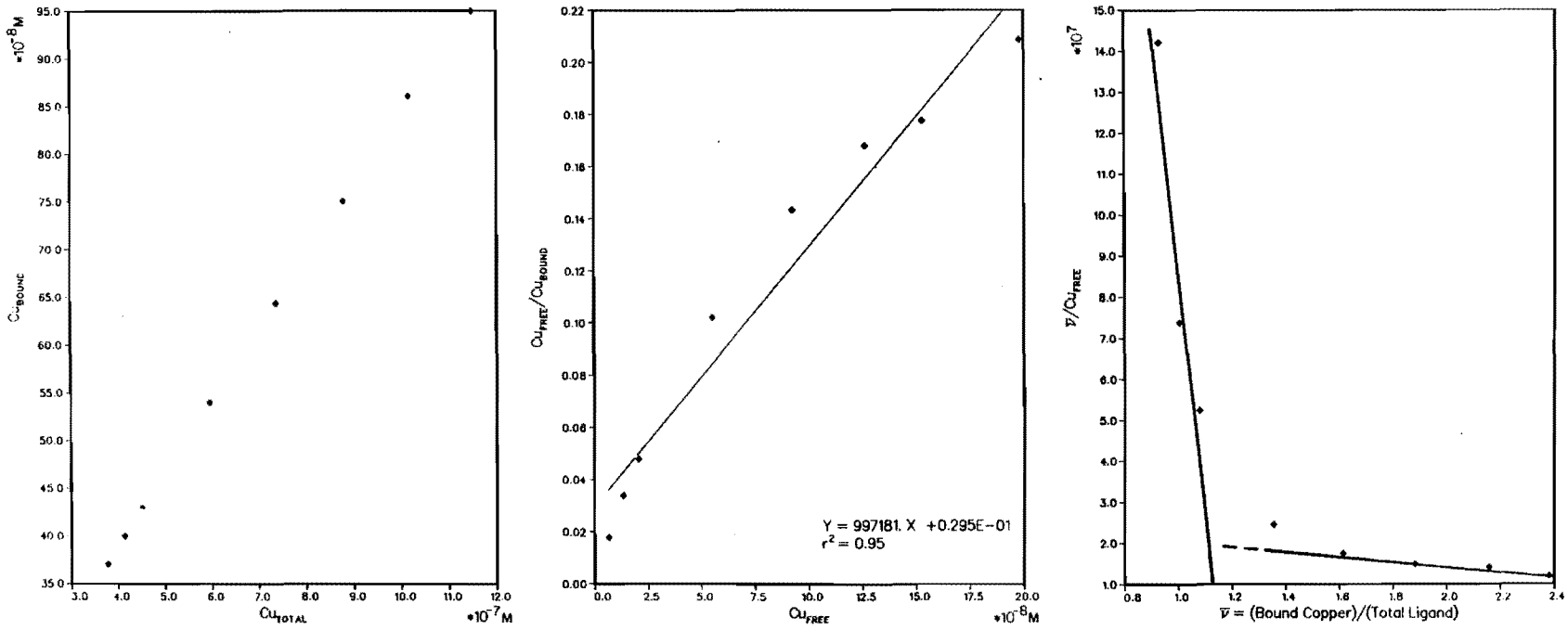

a) Cu_T vs. Cu_{BOUND}

b) Ruzic plot

c) Scatchard plot

Figure 4.17. DPASV titration of 10 mg/L humic acid with copper.

Table 4.8. Comparison of log stability constants (log K) for Cu^{2+} complexes with humic acid obtained in this study with values obtained by other workers using various methods.

Ligand (HA)	Method	pH	Electrolyte	Log K	Reference
HA-soil	Ion-exchange equilibrium	4.0	Not given	2.78	Adhikari et al. (1977)
HA-soil	Ion-exchange equilibrium	5.0	Not given	8.10-9.10	Rosell et al. (1977)
HA-soil	Base titration	4.0	0.1 M $KClO_4$	8.4	Ernst et al. (1975)
HA-soil	Base titration	5.0	0.1 M KCl	7.2	Stevenson (1977)
HA-soil	Base titration	5.0	0.1 M $NaClO_4$	8.7	Takamatsu and Yoshida (1978)
HA-sediment	Using Scatchard plot approach	8.0	0.01 M NaCl	9.91-11.37	Mantoura et al. (1975)
HA-sediment	Using Scatchard plot approach	8.0	0.01 M NaCl	8.29	Mantoura et al. (1975)
HA-Aldrich	Continuous ultrafiltration[a]	7.0	Not used	6.31	This study
HA-Aldrich	Cu-ISE[b]	6.0	Not used	5.75-8.65	This study
HA-Aldrich	DPASV[c]	6.3	0.1 M NaOAc	6.78-8.78	This study
Overall Range				2.78-11.37	

[a]Using Scatchard plot approach for a 50 mg/L HA sample.
[b],[c]Using Scatchard plot approach for a 10 mg/L HA sample.

for Cu(II)-EDTA DPASV complexometric titration, because there is only one dominant binding site for Cu on EDTA. Based on the Ruzic plot (Figure 4.17b), the K_f^c is $10^{7.53}$, and based on the Shuman and Woodward (1973) approach using a stoichiometry of 1:1, the K_f^c is $10^{6.78}$.

The values of K_f^c determined using the two latter techniques are often held to represent an "average" conditional stability constant for humic acid. However, humic material is heterogeneous and contains a variety of binding sites, possibly with a continuum of K_f^c values, and the "average" K_f^c therefore represents a greatly oversimplified and possibly incorrect approach, as suggested by Perdue and Lytle (1983). The stoichiometry of the complexation of these heterogeneous ligands with metal (e.g. Cu(II)) is usually assumed to be 1:1, which also oversimplifies the apparent complexation mechanism. These simplifications should be kept in mind while evaluating titrations of complex organic ligands.

Raw shale leachate. The DPASV complexometric titration curve for the raw oil shale leachate (RSL) with copper is presented in Figure 4.18. No DPASV response was observed below a Cu_T of 1.5×10^{-6} M. It might therefore be assumed that RSL consists of some strong DPASV-nonlabile complexing site or sites, which would pose a serious limitation for determination of the stronger available complexation ligands in RSL by this DPASV technique.

Shuman and Woodward (1977) indicated that considerable dissociation of a complex may occur if the term $K_f^c(CC)$ is small. They indicated that for a "break" in the titration to be easily observed, the term $K_f^c(CC)$ must be greater than unity. For the Cu(II)-RSL titration, $K_f^c(CC)$ is 15.3, which can be compared to 2.4 and 39.2 for HA and EDTA, respectively. Even though the $K_f^c(CC)$ value for the leachate would predict the occurrence of a better "break" in the titration curve than would be observed for HA, the intermediate value still may pose problems relative to DPASV titrations involving low concentration of the complexing ligands. For example, if the observed CC for RSL were ten times higher than the observed value, the $K_f^c(CC)$ term would be ten times higher, and the break in the titration curve would increase enormously, based on the same K_f^c value.

A summary of the results obtained using a variety of procedures to interpret the titration data is tabulated in Table 4.9. The complexation capacities of RSL range from 2.04×10^{-7} to 3.25×10^{-7} M Cu/mg DOC. The conditional stability constants (K_f^c) also are tabulated and, based on three different data interpretation procedures, range from $10^{6.20}$ to $10^{6.84}$.

The Scatchard plot obtained for the DPASV titration of the leachate with copper (Figure 4.19c) indicated only one major binding site (n=0.96), and thus only one K_f^c value ($10^{6.20}$). The results of a Scatchard analysis of data from a replicate RSL DPASV titration had an n value of 1.17 and an overall K_f^c of $10^{6.30}$ (see Appendix D). The K_f^c obtained following the procedure of Shuman and Woodward (1973, 1977) was $10^{6.84}$, assuming a 1:1 complex stoichiometry. From the plot of i_p vs. $[C_M/(C_L-C_M)]$ using the data obtained from the first few increments of titrant, a slope (S_L) of $10^{-1.36}$ was obtained, which corresponds to (κ/K_f^c). κ can be determined as the slope (S_U) of the upper region of the complexometric titration curve, which in Figure 4.19a is $10^{5.26}$. This upper slope agrees well with the result obtained by Shuman and Cromer (1979), who determined S_U to be $1.65 \pm 0.05 \times 10^5$ μA/M Cu ($10^{5.22}$) for various carbonate solutions containing no organics.

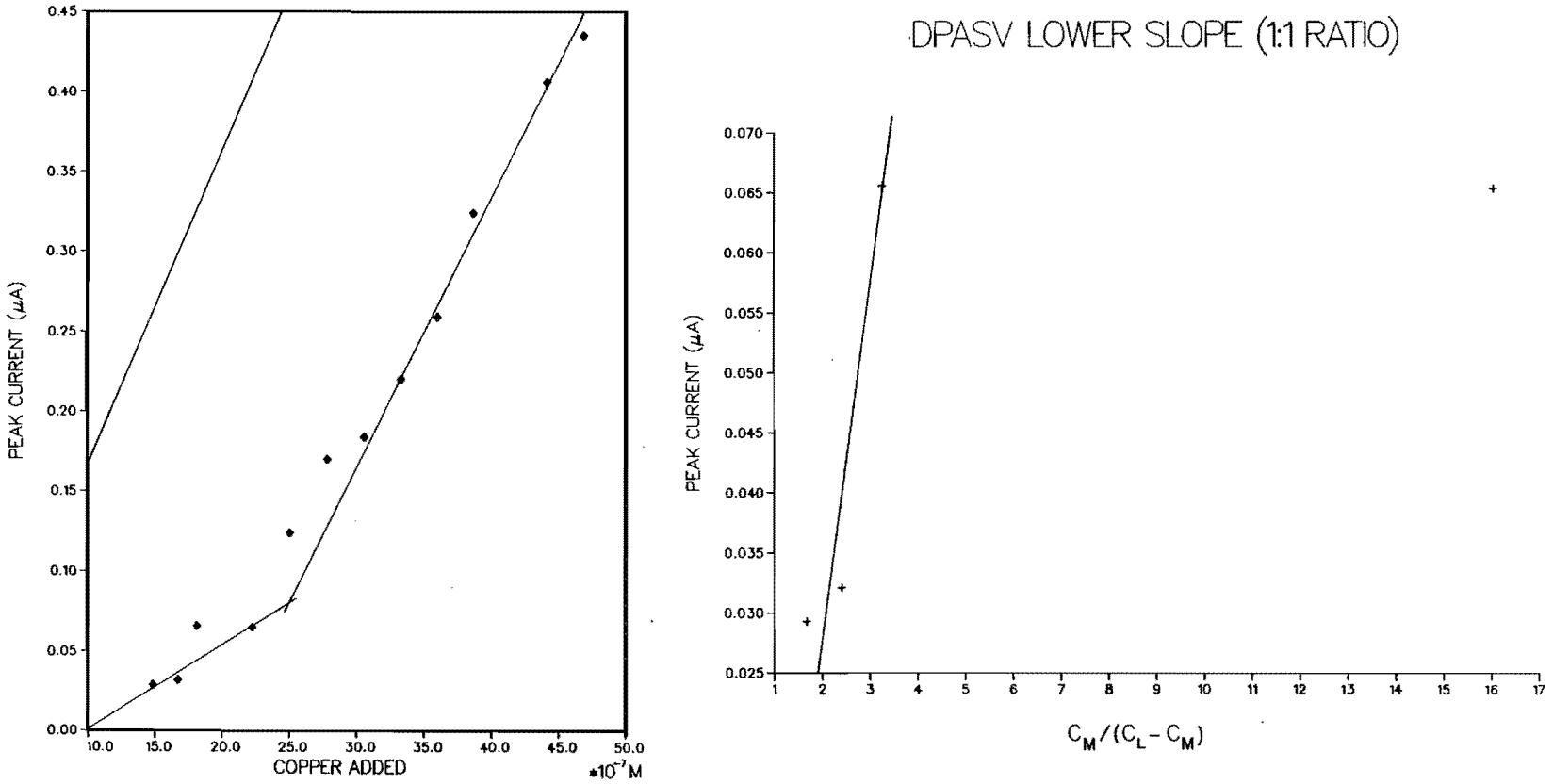

Figure 4.18. DPASV complexometric titration curve for raw shale leachate (RSL) with copper.

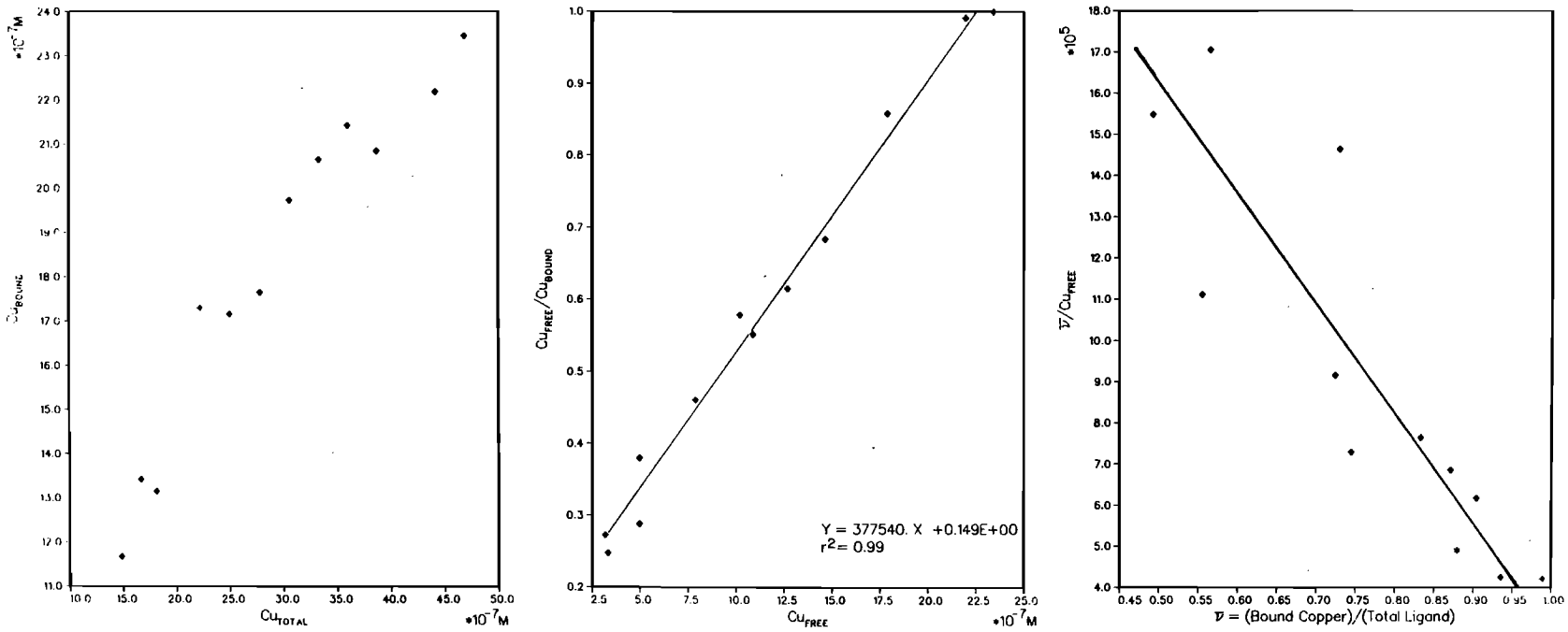

a) Cu_T vs. Cu_{BOUND} b) Ruzic plot c) Scatchard plot

Figure 4.19. DPASV titration of the raw oil shale leachate (RSL) with copper.

Table 4.9. Copper complexation capacities and conditional stability constants for raw oil shale leachate (RSL) as determined by different procedures based on the DPASV complexometric titration data.

Method of Analysis	CC[a]	Log K_f[c]
Plot of Cu_{TOTAL} vs. Cu_{BOUND}	2.8×10^{-7}	-[b]
Chau et al. (1974)	$2.04 \times 10^{-7}/2.30 \times 10^{-7}$	-
Ruzic (1980)	$2.65 \times 10^{-7}/2.88 \times 10^{-7}$	6.40/6.26
Scatchard (1949)	-	6.20/6.30
Shuman and Woodward (1973) (1:1 stoichiometry)	$2.50 \times 10^{-7}/3.25 \times 10^{-7}$	6.84/6.62

[a]Complexation capacity = unit M Cu/mg DOC
[b]Method not applicable.

Summary of binding analyses

The results of the various binding analyses, expressed as M Cu/mg TOC, are summarized in Table 4.10. For HA, CC is in the range of 2.5×10^{-6} to 5.4×10^{-6} for the UF and ISE techniques. A possible trend of increasing CC, on a mg TOC basis, with increasing HA concentration could well result from the formation of Cu bridges between adjacent HA colloids as their mean distance decreases in solution (Langford et al. 1983). Based on the increase between 5 and 10 mg/L HA, the 50 mg/L value of CC would be predicted to be 3.92×10^{-6} if this relationship were linear. However, a nonlinear increase, which would correspond more closely to the observed 50 mg/L CC, would be expected due to surface/volume relationships. The low CC based on DPASV analysis would suggest systematic underestimation of CC by an order of magnitude. Reasons for the underestimation in all likelihood center around the reduction of the Cu-HA complex at the mercury electrode reported by other workers.

Excluding the incorrect CC for the undiafiltered RSL sample, CC values range over approximately two orders of magnitude, which overlap HA at the high end of the range. Factors which could affect differences in the binding capacities of the RSL samples include origin, past history, and extraction procedures. The oil shale sample studied in batch extraction was composed of material recently excavated from the Mahogany Zone at tract C-a in the Piceance Basin and stored in steel drums. The shale extracted in the upflow columns was taken from a shale pile at the Anvil Points Naval Oil Shale Reserve Facility, more than 100 km from the C-a site, and had been exposed to the elements for a long (but unknown) time. The lower CC may represent the effects of weathering on the kerogen in the shale, which may have a higher binding capacity than HA that has been exposed to oxidizing conditions in the soil or surface water. Effects of

contact time on ligand leaching may also play a role in determining CC. The contact time was 7 days in the upflow columns, compared to 2 days for the batch extractions. As in the HA binding analyses, CC based on DPASV was considerably lower than that obtained from the ISE titrations, and it is again suspected that this may be due to reducibility of the complex at the electrode.

Based on the ISE titrations, which seem more reliable than the DPASV titrations, RSL appears to be characterized by having both fewer and weaker binding sites than HA (cf. Tables 4.4 and 4.10).

Table 4.10. Comparison of the complexation capacities, CC[a] for Cu-humic acid and Cu-raw shale leachates determined by continuous ultrafiltration (UF), Cu-ISE, and DPASV.

Ligand	Method of Analysis		
	UF	ISE	DPASV
HA			
5 mg/L	--	2.5×10^{-6}	--
10 mg/L	--	2.6×10^{-6}	2.0×10^{-7}
50 mg/L	5.4×10^{-6}	--	--
RSL (1:4) 50%[b]	--	2.66×10^{-6}	--
RSL (1:4) 100%	ND[c]	4.73×10^{-5}	2.65×10^{-7}
RSL_1	--	3.33×10^{-8}	--
RSL_3	--	3.46×10^{-7}	--

[a] M Cu/mg TOC.
[b] UF diafiltered raw shale leachate in MAAP medium (DOC = 6.2 mg/L).
[c] Not determinable.

CHAPTER V

BIOASSAY RESULTS

Algal bioassays were conducted to determine whether oil shale organic ligands could in their own right promote or inhibit phytoplankton growth (i.e., irrespective of any associated macronutrients or salinity) in a nutrient deficient modified algal assay medium (MAAP), and, if promotion were found, whether it could be attributed to the detoxification of heavy metals. If detoxification were found to be important, the goal was to construct a rational model, based on values for K_f^C and CC obtained in laboratory experiments, that would quantitatively explain the metal detoxification in a way that could be extended to conditions found in the field.

The discussion begins with the results of a set of bioassays designed to test the toxicity or stimulatory characteristics of metals alone, various shale leachates alone, and a model ligand (humic acid) alone, all tests in the MAAP medium. These results are then compared with the results of various combinations of humic acid, oil shale organics, and metals on algal growth. Finally the results of the bioassays are compared to those predicted with an equilibrium model using the CC and K_f^C values determined in the previous chapter.

Effects of Metals and Organics Alone

Metals

Algal growth responses in the MAAP bioassays in response to different concentrations of Cu, Cd, and Ni are displayed in Figure 5.1. Statistically significant concentration groupings are presented in Table 5.1. The groupings are based on three measures of effect: fluorescence at maximum standing crop (MSC), the day at which one-half of the maximum standing crop was reached, and the growth rate at 1/2 MSC. These different measures allow comparisons to be made between metal concentrations that limit the amount of growth possible, and concentrations that can eventually be compensated for by the test algae, resulting only in an increased lag period preceding the onset of logarithmic growth or in reduced maximum growth rate. The latter parameters may be important to the survival of a particular algal species under conditions of competition, or under conditions of limited residence time for growth, as in a turbid reservoir (e.g., Mayer and Gloss 1980, Messer et al. 1983). Fluorescence was chosen as the only practicable measure of biomass for use in these large bioassay experiments. Although the term "growth" is used below synonymously with chlorophyll a fluorescence, the results might better be interpreted in terms of physiological response, in the event that any of the treatments had a differential effect on fluorescence and biomass increase.

Copper can clearly be seen (Figure 5.1a) to be quite toxic to the test alga, with growth being effectively halted when pCu ($-\log [Cu_T]$) drops below 6.0. The results of the Duncan Multiple Range Test (DMRT) on Table 5.1 indicate growth rate was significantly reduced for pCu below 7.3 and that the lag time was similarly affected.

Low Cd additions (pCd>7.3) appear to have stimulated growth, relative to

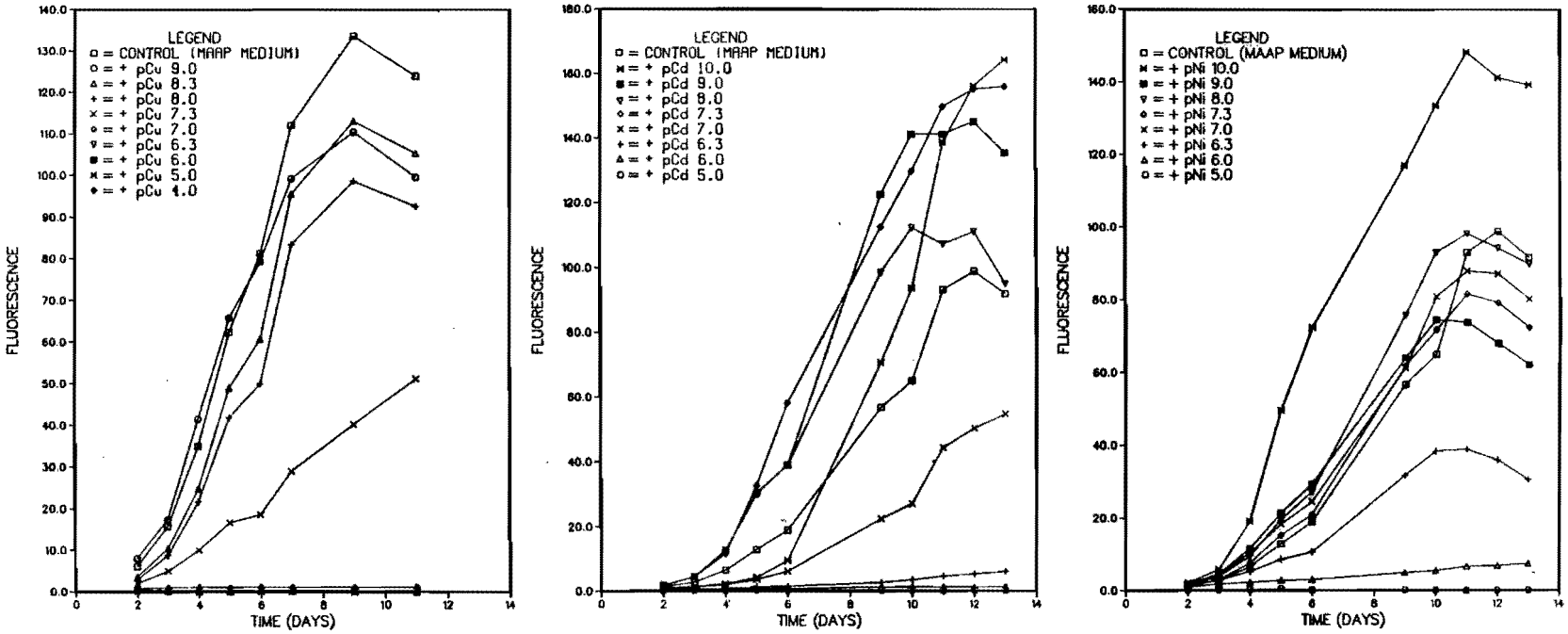

Figure 5.1. Growth responses of S. capricornutum to: a) Cu(II), b) Cd(II), and c) Ni(II) in modified algal assay procedure (MAAP) medium.

the control, but higher concentrations (pCd<7.0) reduced the maximum fluorescence below the control value. Of the three growth parameters, however, only maximum growth rate was affected at a statistically significant level of pCd<6.3.

Nickel appears to have stimulated growth at its lowest level of addition (pNi=10.0) and to have been inhibitory at pNi=7.0. The only significant response was the decrease in growth rate of pNi<7.0.

The absence of statistical significance in the difference among responses of the intermediate metal concentrations, despite an apparent difference in the dose/fluorescence curves, was frequently associated with one of the three test cultures showing an unusually

Table 5.1. Responses of S. capricornutum to different concentrations of Cu (II), Cd (II), and Ni (II) in terms of maximum standing crop (MSC), day on which 1/2 MSC occurred, and growth rate at 1/2 MSC.

Treatments	Fluorescence at Maximum Standing Crop (MSC)	Day on which 1/2 MSC occurred	Growth Rate at 1/2 MSC (Fluorescence/day)
Control[b]	133.5 C	5.6 B	12.6 D
+pCu 9.0	110.4 B C	5.3 B	11.2 C D
+pCu 8.3	113.0 B C	5.8 B	9.8 C D
+pCu 8.0	98.6 B C	6.0 B	8.6 C
+pCu 7.3	51.1 A B	7.3 B	4.5 B
+pCu 7.0	1.2 A	1.6 A	0.4 A
+pCu 6.3	0.4 A	1.0 A	0.2 A
+pCu 6.0	0.2 A	1.0 A	0.1 A
+pCu 5.0	0.2 A	1.0 A	0.1 A
+pCu 4.0	0.4 A	1.0 A	0.2 A
Control	98.8 A B	8.4 B C	6.0 C
+pCd 10.0	164.3 B	9.8 C	8.6 D
+pCd 9.0	145.0 B	7.2 B C	10.1 D
+pCd 8.0	112.2 A B	6.8 B	8.4 D
+pCd 7.3	41.5 B	5.2 A B	15.1 E
+pCd 7.0	54.6 A B	8.6 B C	3.2 B
+pCd 6.3	6.1 A	8.5 B C	0.4 A
+pCd 6.0	1.3 A	4.0 A	0.2 A
+pCd 5.0	0.4 A	1.6 A	0.1 A
Control	98.8 A B	8.4 B	6.0 B
+pNi 10.0	148.2 B	7.1 B	12.0 C
+pNi 9.0	74.4 A B	6.7 B	5.6 B
+pNi 8.0	98.2 A B	7.5 B	6.6 B
+pNi 7.3	81.6 A B	6.5 A B	6.6 B
+pNi 7.0	87.9 A B	7.5 B	5.9 B
+pNi 6.3	38.9 A	6.5 A B	3.0 A B
+pNi 6.0	7.4 A	6.8 B	0.7 A
+pNi 5.0	0.4 A	2.5 A	0.1 A

[a]Within each metal treatment, responses labeled with the same letter (e.g. A, B, or C) are not significantly different based on the Duncan Multiple Range Test (DMRT).

[b]Control = modified algal assay procedure (MAAP) medium.

high or low growth, relative to the corresponding replicates. This phenomenon may result from random inclusion of resistant individuals in some of the replicates. Once a culture attains exponential growth, detoxification occurs rapidly through immobilization of the toxic metal on to cell walls (Huntsman and Sunda 1980), and some of the effect of the metal on further growth is lost or reduced. This effect can often be avoided by using a metal buffer (e.g. Morel et al. 1979), although in this case a buffer could not be used because it would have interfered with the effect of the ligands of interest.

The effects of the various metals tested in the bioassay can be objectively compared using probit analysis (Hewlett and Plackett 1979). This technique assumes that the response of a test population to different dose levels can be approximated by a normal or lognormal distribution. In probit analysis normalized equivalent deviates (NED's) are calculated from the percentage of the population responding to a particular dose at each level tested, and incremented by 5.0 to avoid negative numbers. The resulting value is called a probit, the population of which is characterized by a mean of 5.0 and a standard deviation of 1.0. A plot of the probit values versus log dose gives a linear model from which the EC_{50} (the dose that would theoretically affect 50 percent of the population) can be determined.

An example of a probit plot generated using the SAS computer package (version 79.5, 1979) for copper versus reduction in fluorescence is shown in Figure 5.2. In all cases, zero response was set at the maximum MSC corresponding to a given experiment. In the case of Cu, the highest MSC occurred in the control, for which the pCu was not determinable, but assumed to be 10. The results fit the model well yielding an EC_{50} of 7.56. In the Cd and Ni bioassays, the zero response doses were set at pCd=9.0 and pNi=10.0, respectively. The corresponding EC_{50} for pCd was 7.35 and pNi was 6.35, indicating relative toxicities in the order Cu>Cd>Ni in the MAAP medium.

The EC_{50} values found in this experiment were higher than those reported by Chiaudani and Vighi (1978) for Selenastrum bioassays in AAP medium without EDTA but with the normal complement of metal ions except for reduced levels of Zn and Co. They reported EC_{50} values of pCu=8.66, pCd=8.42, and pNi=8.60 at day 7. Because their MSC was observed at zero dose, their probit curve would be expected to show a lower EC_{50}. This comparison strongly suggests that the trace metals (not necessarily the metals being added) supplied by low dilutions of the Cd and Ni spikes in our bioassays enhanced growth relative to that in controls receiving no metals. The effect ceases when the metals are being added in toxic concentrations, which points to the highly complex nature of bioassay results. Nonetheless, the EC_{50} values reported here for bioassays spiked with known metal concentration provide a necessary control against the EC_{50} values reported below for metals added in conjunction with various organic ligands.

Raw shale leachate

In order to determine whether oil shale leachates alone (in the absence of added metals) were phytotoxic or enhanced algal growth, bioassays were run using both fractionated and unfractionated raw shale leachates. Results of bioassays run on diafiltered, unfractionated raw shale leachate (RSL) are shown in Figure 5.3 and Table 5.2. Increasing concentrations of RSL can be seen to enhance MSC, with the MAAP using 50 percent RSL showing the greatest MSC. These results indicate that either RSL is supplying some trace nutrient absent in the MAAP medium or that it is detoxifying some extremely low background concentration of toxicant in the MAAP medium, perhaps Cu. Diafiltration

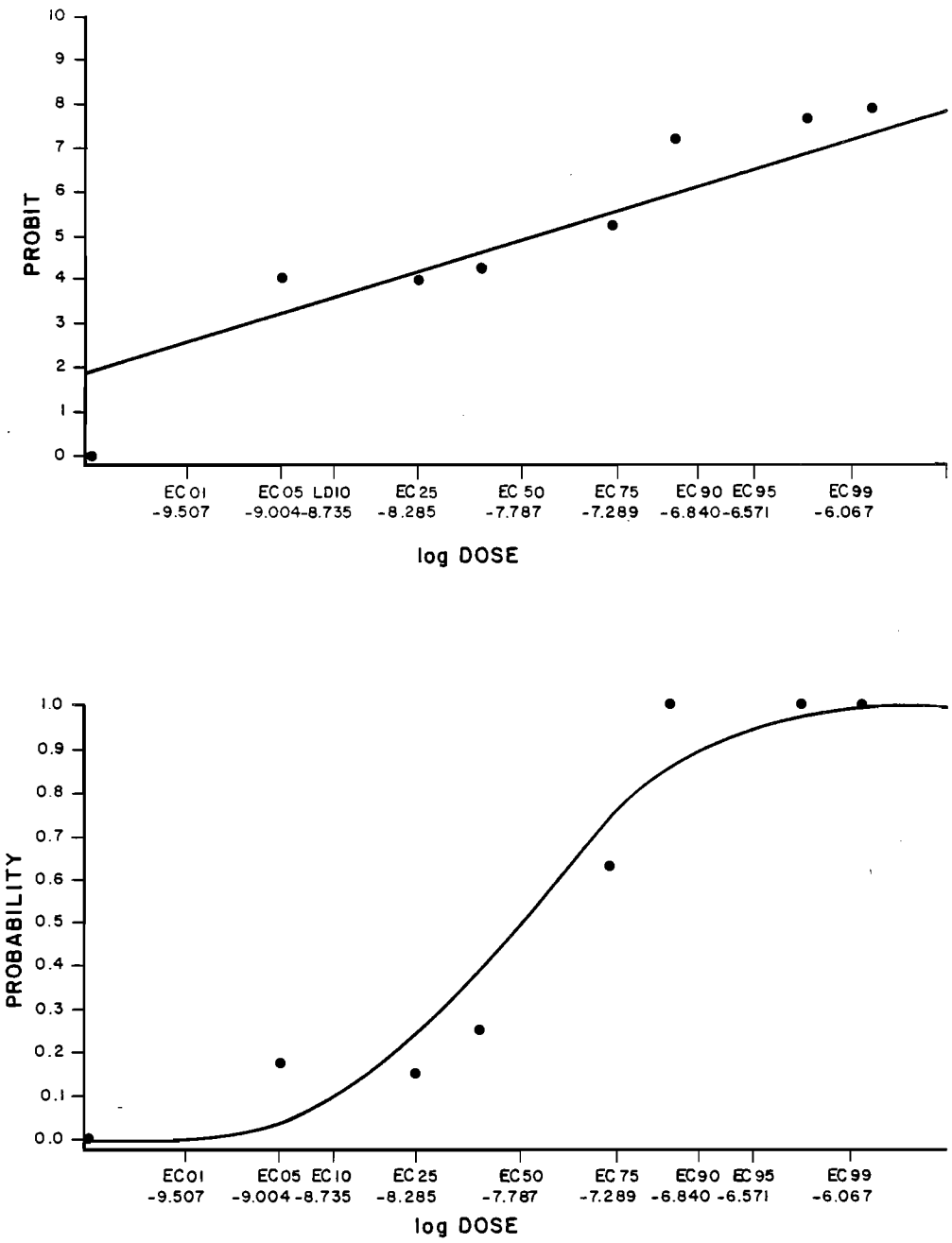

Figure 5.2. Probit analysis of copper (II): a) probit vs. log Cu dose and b) probability vs. log Cu dose.

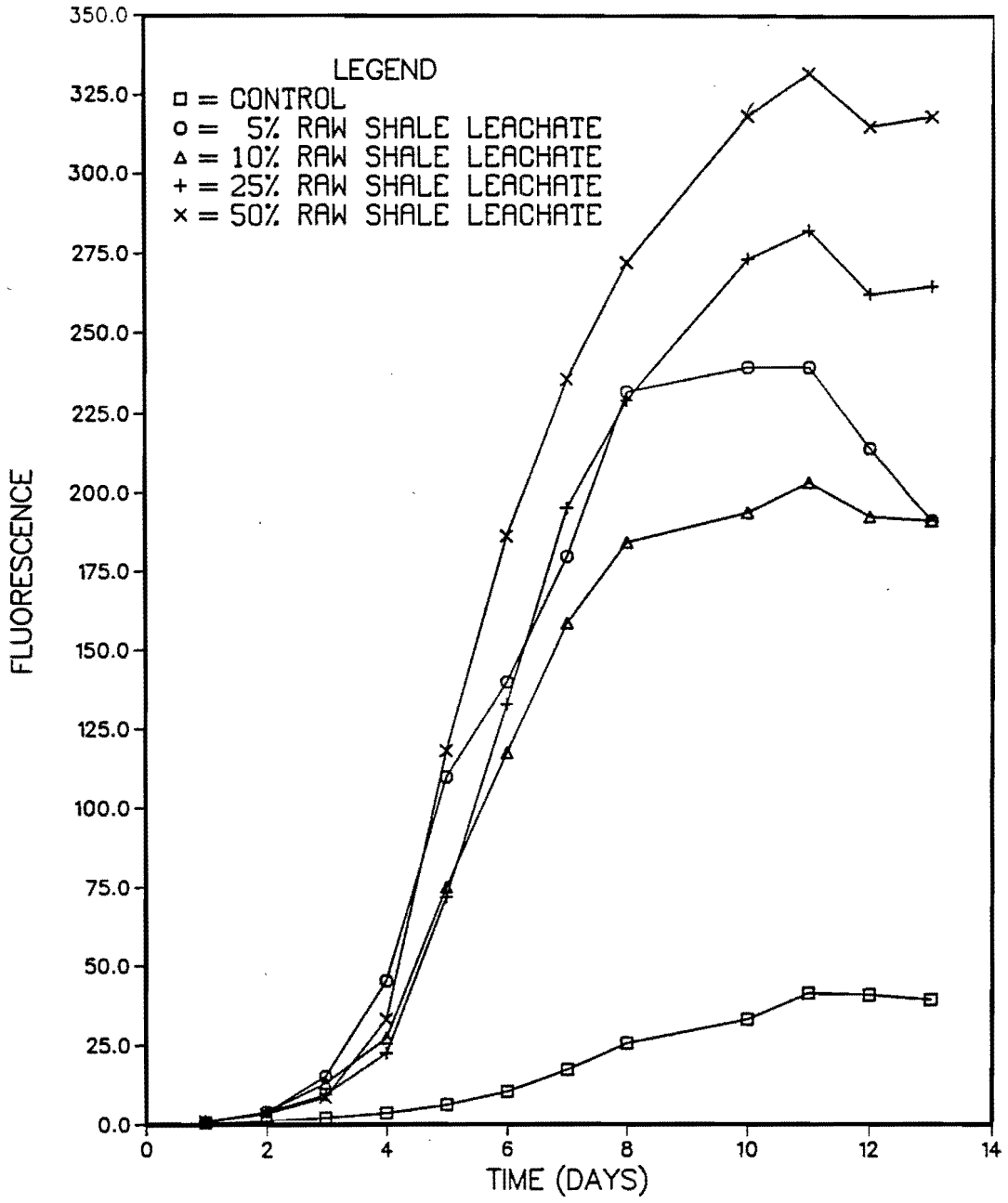

Figure 5.3. Growth responses of S. capricornutum to different concentrations of raw shale leachate in MAAP medium.

Table 5.2. Responses of S. capricornutum to different concentrations of raw shale leachate (RSL) in terms of maximum standing crop (MSC), day on which 1/2 MSC occurred, and growth rate at 1/2 MSC.[a]

Treatments	Fluorescence at Maximum Standing Crop (MSC)		Day on which 1/2 MSC occurred		Growth Rate at 1/2 MSC (Fluorescence/day)	
Control[b]	41.5	A	7.6	A	2.7	A
+ 5% RSL[c]	239.4	B C	6.4	A	20.4	B
+10% RSL	203.4	B	5.6	A	18.1	B
+25% RSL	282.3	B C	6.1	A	23.0	B C
+50% RSL	331.7	B C	5.7	A	29.1	C

[a]Algal responses labeled with the same letter (e.g. A, B, or C) are not significantly different based on the Duncan Multiple Range Test (DMRT).

[b]Control = modified algal assay procedure (MAAP) medium.

[c]RSL = raw shale leachate extracted with 1 part of shale and 4 parts of deionized water.

of the RSL with 5 cell volumes of deionized water through a UM2 ultrafilter should have removed the majority of inorganic salts associated with the extracted RSL. The possibility that the RSL retentate is providing an organic nutrient (e.g., a vitamin) seems unlikely but cannot be ruled out.

The effects of various 5 percent undiafiltered, UF-fractionated RSL retentates are shown in Figure 5.4, and the effects of the corresponding filtrates are in Figure 5.5. Results of the DMRT are presented in Table 5.3. The retentates all depressed MSC, relative to both the control and unfractionated RSL, with the "smallest" UF retentate, YM5-UM2, showing the most inhibition. This retentate fraction significantly increased the lag period and the growth rate at 1/2 MSC, relative to the other treatments. The UF filtrates all depressed growth, relative to the RSL or unamended controls, with the "soluble" component, <UM2, showing virtually no growth. This filtrate depressed MSC and the growth rate at 1/2 MSC, and increased the lag period, significantly more than any of the other treatments (Table 5.3).

Taken together, the bioassays indicate that inorganic salts or very small organic molecules associated with RSL have a net inhibitory effect on the growth of the test alga. In the unfractionated RSL bioassay, removal of these inhibitors allowed the otherwise beneficial effects of the UF retentate to be exerted. Without diafiltration, however, the inhibitors remained in the UF cell where the retentate prevented any of the retentate fractions from exerting their enhancing effects on algal growth, although the larger retentate fractions proved less inhibitory (or more ameliorative) than the smaller UF retentates. The generally low salinity of the RSL (320 μmho/cm) would suggest that the inhibitory effect of the UM2 filtrate was caused by some toxic species, rather than by osmotic stress, as suggested by Cleave et al. (1980). However, the salinity of the leachates used in the latter study was considerably higher than used here.

One would expect spent shale to have a considerably different effect on algal growth than would raw shale because of: 1) the chemical alteration of the organic fraction at the high retorting temperature and 2) the partitioning of mineral elements into various process streams during the retorting process (e.g., Fruchter and Wilkerson 1981). Results of an algal bioassay employing various fractions of leachate from a spent shale retorted using the Paraho process are shown in Figure 5.6 and Table 5.4. The spent shale was extracted for 48 hr in deionized water at a ratio of one part shale to four parts of water. Fraction SSL_1 represents the unfractionated leachate, diafiltered with five cell volumes of deionized water to remove associated salts and small organics that would pass through a UM2 ultrafilter. SSL_2 represents the undiafiltered leachate fraction, and SSL_3 represents the leachate passing through the UM2 filter. All treatments were tested at 5 percent of the MAAP medium, and SSL_1 was also tested at the 10 percent application level. In all cases, the leachates enhanced MSC and growth rate at 1/2 MSC and decreased the length of the lag phase relative to the control that did not receive SSL. The 10 percent application of SSL_1 gave the highest MSC, and produced a significantly greater growth rate at 1/2 MSC than did the 5 percent application. The smallest size fraction of the SSL produced the largest apparent stimulatory effect, in contrast with the results for the raw shale leachate. Retorting apparently removes whatever inhibitory substance was present in the raw oil shale, assuming that the raw shale from which the spent shale originated was similar in composition to that used here. Among the inorganic toxicants that partition into phases other than the spent shale in the Paraho process

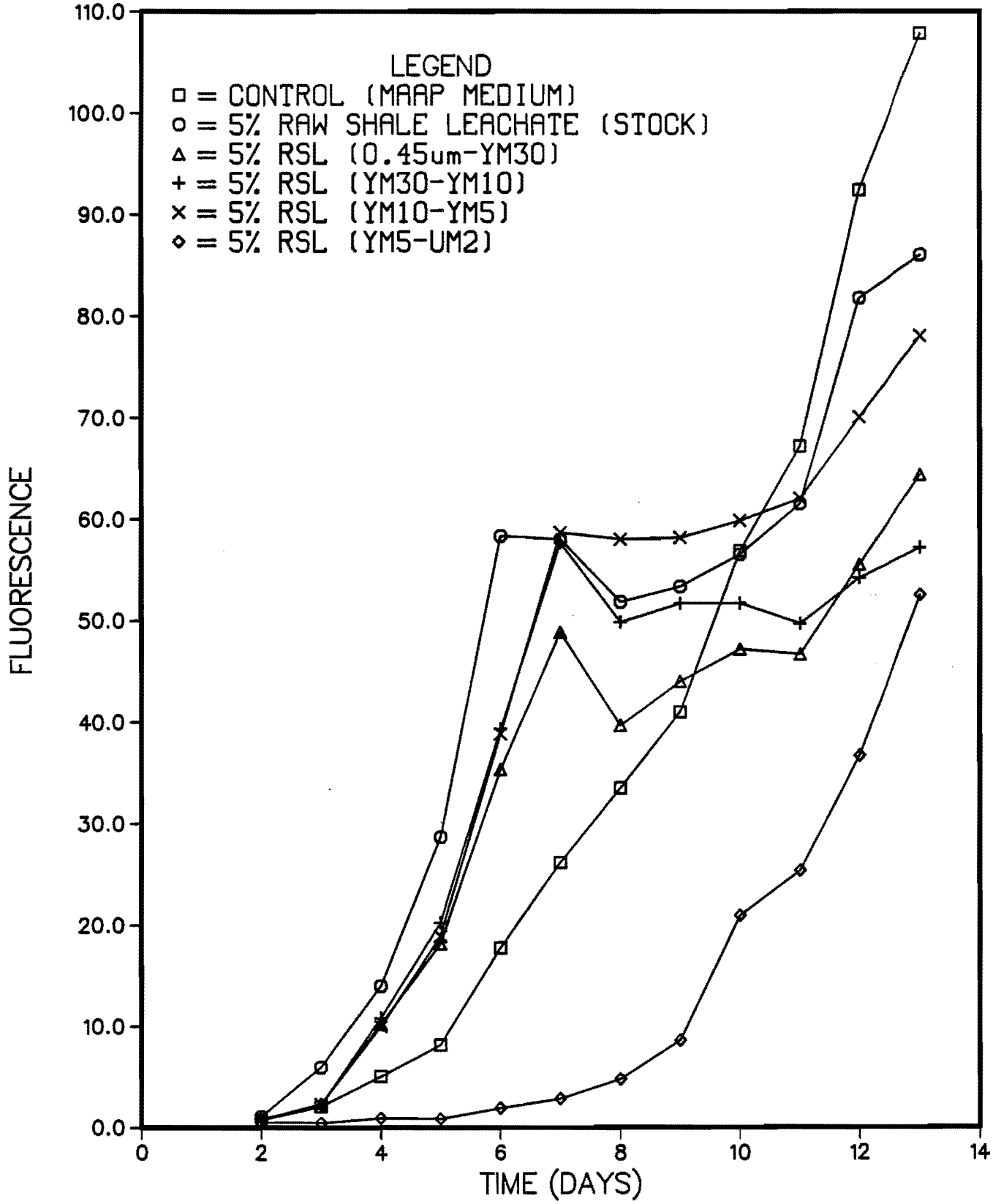

Figure 5.4. Growth responses of S. capricornutum to different UF size-fractionated RSL retentates in MAAP medium.

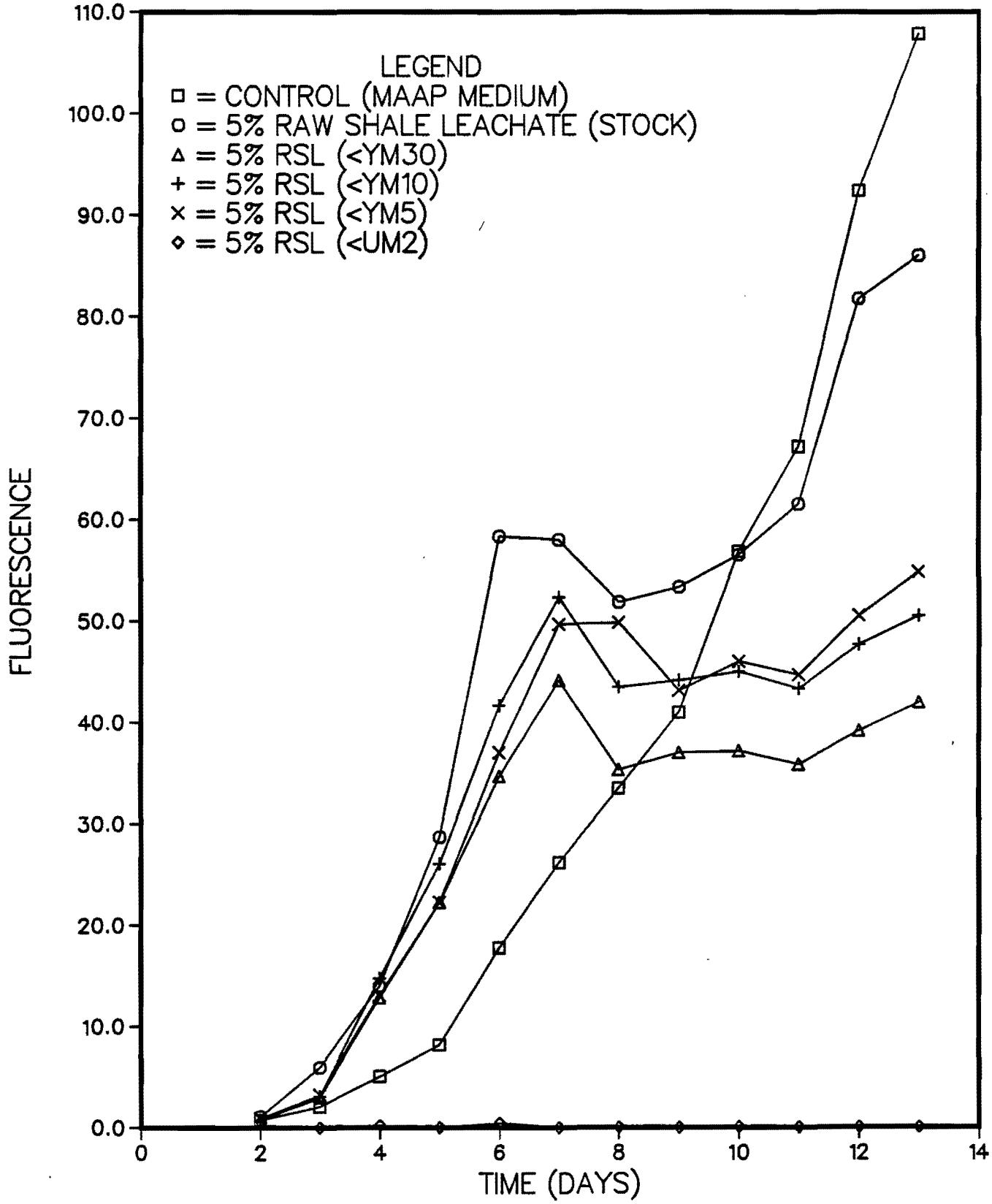

Figure 5.5. Growth responses of S. capricornutum to different UF-fractionated RSL filtrates in MAAP medium.

Table 5.3. Responses of S. capricornutum to different ultrafiltration (UF) size fractionated raw shale leachates in terms of maximum standing crop (MSC), day on which 1/2 MSC occurred, and growth rate at 1/2 MSC.

Treatments	Fluorescence at Maximum Standing Crop (MSC)	Day on which 1/2 MSC occurred	Growth Rate at 1/2 MSC (Fluorescence/day)
Control[b]	107.8 E	9.9 C	5.4 D
Stock RSL[c]	86.0 D E	5.5 B	7.8 F
0.45 m - YM30[d]	64.3 B C D	5.8 B	5.5 D
YM30 - UM 10	57.6 B C D	5.5 B	5.2 D
UM10 - YM5	78.0 C D	6.0 B	6.5 E
YM5 - UM2	52.5 B C	10.6 C	2.5 B
< YM30	44.2 B	5.1 B	4.4 C
< UM10	52.3 B C	5.1 B	5.2 D
< YM5	54.8 B C	5.4 B	5.1 D
< UM2	0.4 A	3.4 A	0.1 A

[a]Algal responses labeled with the same letter (e.g. A, B, or C) are not significantly different based on the Duncan Multiple Range Test (DMRT).

[b]Control = modified algal assay procedure (MAAP) medium.

[c]Stock RSL = stock raw shale leachate without size fractionation.

[d]Ligands passing through a 0.45 m membrane filter, but not YM30 ultrafiltration membrane filter.

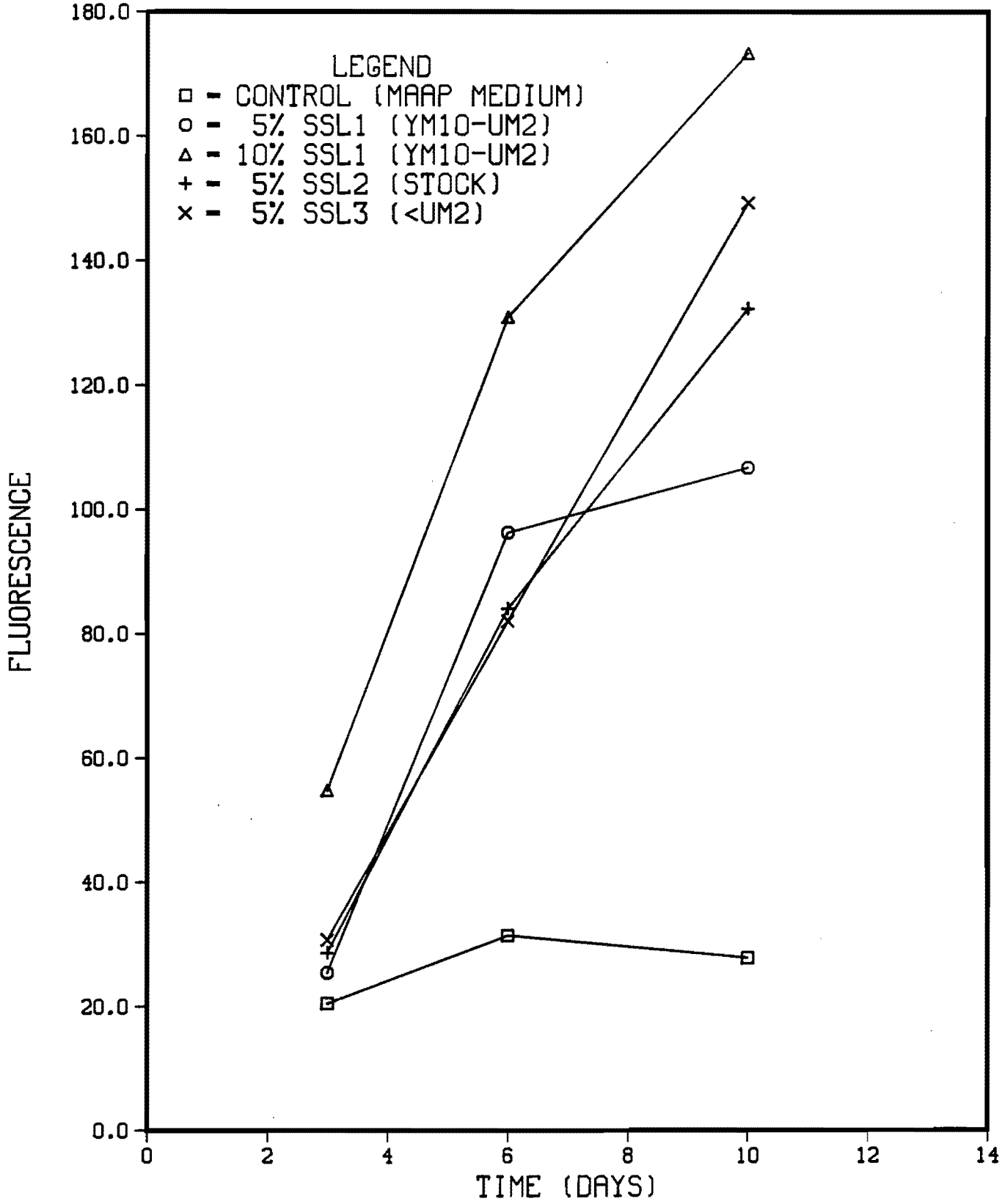

Figure 5.6. Growth responses of S. capricornutum to different UF-size fractionated spent (retorted) shale leachates (SSL) in MAAP medium.

Table 5.4. Responses of S. capricornutum to different size fractionated Paraho spent shale leachates (SSL) in terms of maximum standing crop (MSC), day on which 1/2 MSC occurred, and growth rate at 1/2 MSC.

Treatments	Fluorescence at Maximum Standing Crop (MSC)		Day on which 1/2 MSC occurred		Growth Rate at 1/2 MSC (Fluorescence/day)	
Control[b]	31.4	A	2.4	A	6.8	A
5% SSL1[c] (1:4)	122.6	B	4.7	B	13.2	B
10% SSL1 (1:4)	173.2	D	4.4	B	20.2	C
5% SSL2[d] (1:4)	132.2	B C	5.2	B	13.0	B
5% SSL3[e] (1:4)	160.8	C D	5.9	B	13.6	B

[a]Algal responses labeled with the same letter (e.g. A, B, or C) are not significantly different based on the Duncan Multiple Range Test (DMRT).

[b]Control = modified algal assay procedure (MAAP) medium.

[c]SSL1 = Paraho spent shale leachate between YM10-UM2.

[d]SSL2 = Paraho spent shale leachate without size fractionation.

[e]SSL3 = Paraho spent shale leachate with size fractionation < UM2.

are As, B, Co, Ni, Se, and Hg (Fruchter and Wilkerson 1981). Again, however, it is not known whether the retentate is acting to provide a trace nutrient or detoxifying a heavy metal in the medium.

Metal-ligand Interactions

In order to determine whether the growth-enhancing effects of the various shale leachates were due, at least in part, to heavy metal detoxification, bioassays were run using metal spikes in the presence of various concentrations of shale leachates. First, however, an experiment was conducted with a model ligand, Aldrich humic acid (HA), in order to determine how Selenastrum would respond to complexation by Cu in the MAAP medium.

Humic acid (HA)

HA was tested alone at four concentrations (Figure 5.7) to determine whether it had any intrinsic effect on algal growth in the absence of added Cu. The 5 mg/L addition enhanced MSC and the growth rate at 1/2 MSC. Ten mg/L provided even more enhancement, although the difference in enhancement between the 5 and 10 mg/L concentrations was not statistically significant (Table 5.5). Higher HA concentrations, 25 and 50 mg/L, produced significantly less stimulation, although the growth still exceeded the rate in the control. This reduction could be caused either by some toxic effect of the HA itself or by reduction of the concentration of some necessary metal (e.g., Ca) to an unacceptably low concentration through complexation. It is unlikely that Fe or some other trace metal was present in sufficiently high concentration to be incompletely bound by HA at the lower concentrations tested.

HA/Cu

Figures 5.8a and 5.8b show the effects of HA at two concentrations, 5 and 10 mg/L respectively, on algal growth over Cu concentrations ranging from pCu=8 to pCu=5. It can be seen from Table 5.5 that statistically significant reductions in MSC and growth rate, and increases in the lag phase, are not encountered until pCu drops below 7.0. Growth is not halted until pCu drops below 6.0. This is in contrast to the metal bioassay depicted in Figure 5.1, in which growth was significantly lowered at half of the Cu concentration in the presence of HA, and growth was virtually stopped at 1 percent of the Cu concentration in the presence of HA. At 10 mg/L of HA, results were similar to those obtained at 5 mg/L HA at lower Cu concentrations, but growth was better at pCu=6.0 at the higher HA concentation than it was in the presence of 5 mg/L HA. Probit analysis indicated EC_{50}'s of pCu=6.46 and 6.26 for the 5 and 10 mg/L concentrations of HA, respectively.

RSL/Cu

The HA/Cu bioassays revealed that MAAP medium could be used to test the effects of organic ligands on metal detoxification to the test alga. Figures 5.9a, b, and c show the effects of various additions of RSL to MAAP medium on algal growth in the presence of various Cu concentrations. Desalted 1:4 (shale:deionized water) RSL extract was applied at 10 and 50 percent concentrations, and a 2:1 extract was applied at 5 percent concentration in the final MAAP medium. At the 10 percent concentration, all growth parameters were significantly enhanced over the control cultures (without RSL or Cu) at low Cu concentrations, with all parameters showing a statistically significant decline when pCu drops below 8 (Table 5.6). Growth was virtually halted at a pCu of 7.0. At 50 percent RSL concentration, growth was halted at some concentration above pCu=7.0, and the growth rate and lag phase parameters in Table 5.6 indicate that pCu=7.0 was more inhibitory than pCu=8. The 5 percent application of the more concentrated RSL showed evidence for a statistically

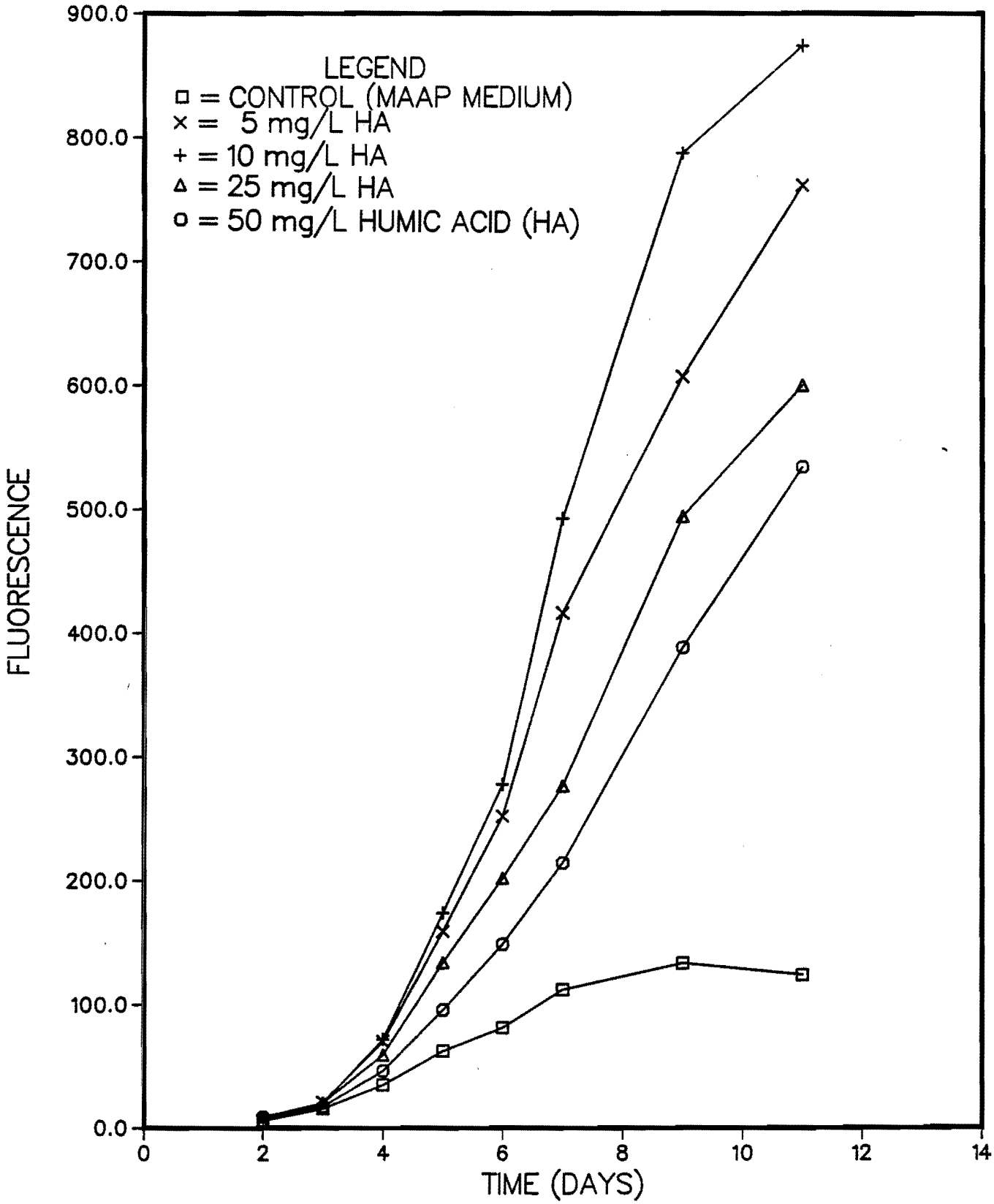

Figure 5.7. Growth responses of S. capricornutum to different concentrations of humic acid in MAAP medium.

Table 5.5. Responses of S. capricornutum to different concentrations of humic acid (HA), with and without copper spikes in terms of maximum standing crop (MSC), day on which 1/2 MSC occurred, and growth rate at 1/2 MSC.

Treatments	Fluorescence at Maximum Standing Crop (MSC)		Day on which 1/2 MSC occurred		Growth Rate at 1/2 MSC (Fluorescence/day)	
Control[b]	133.5	A	5.6	A	12.6	A
5 mg/L HA	760.9	C	6.8	A B	55.7	D
10 mg/L HA	873.6	C	6.7	A B	64.8	E
25 mg/L HA	599.7	B	7.2	B	41.7	C
50 mg/L HA	533.8	B	7.6	B	35.0	B
Control	133.5	A B	5.6	B	12.6	B
5 mg/L HA	760.9	D	6.8	B	55.7	D E
5 mg/L HA + pCu 8.0	835.4	D	6.5	B	63.8	F
5 mg/L HA + pCu 7.3	615.3	C D	5.9	B	52.2	D
5 mg/L HA + pCu 7.0	803.0	D	6.5	B	62.1	E F
5 mg/L HA + pCu 6.3	426.4	C	8.7	C	24.4	C
5 mg/L HA + pCu 6.0	139.6	B C	6.2	B	11.1	B
5 mg/L HA + pCu 5.0	0.9	A	1.0	A	0.4	A
Control	133.5	B	5.6	B	12.6	B
10 mg/L HA	873.6	E	6.7	B	64.8	G
10 mg/L HA + pCu 8.0	714.1	D	6.4	B	55.5	F
10 mg/L HA + pCu 7.3	738.4	D	5.6	B	44.2	E
10 mg/L HA + pCu 7.0	757.4	D	6.7	B	56.6	F
10 mg/L HA + pCu 6.3	476.6	C	6.9	B	34.8	D
10 mg/L HA + pCu 6.0	391.7	C	8.8	C	22.4	C
10 mg/L HA + pCu 5.0	1.8	A	1.0	A	0.9	A

[a]Within each metal treatment, responses labeled with the same letter (e.g. A, B, or C) are not significantly different based on the Duncan Multiple Range Test (DMRT).

[b]Control = modified algal assay procedure (MAAP) medium.

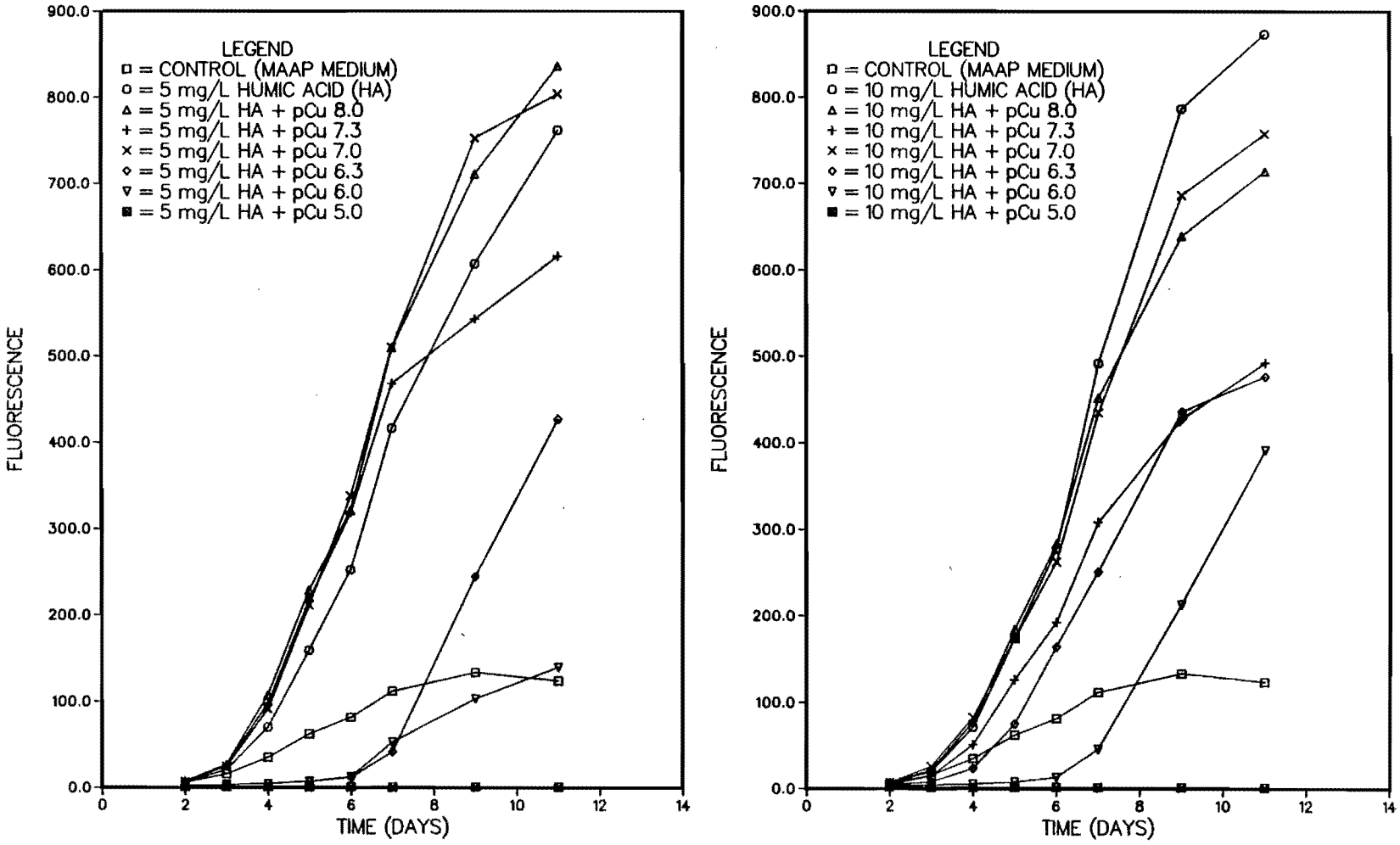

Figure 5.8. Growth responses of S. capricornutum to different concentrations of copper in the presence of a) 5 mg/L HA and b) 10 mg/L HA in MAAP medium.

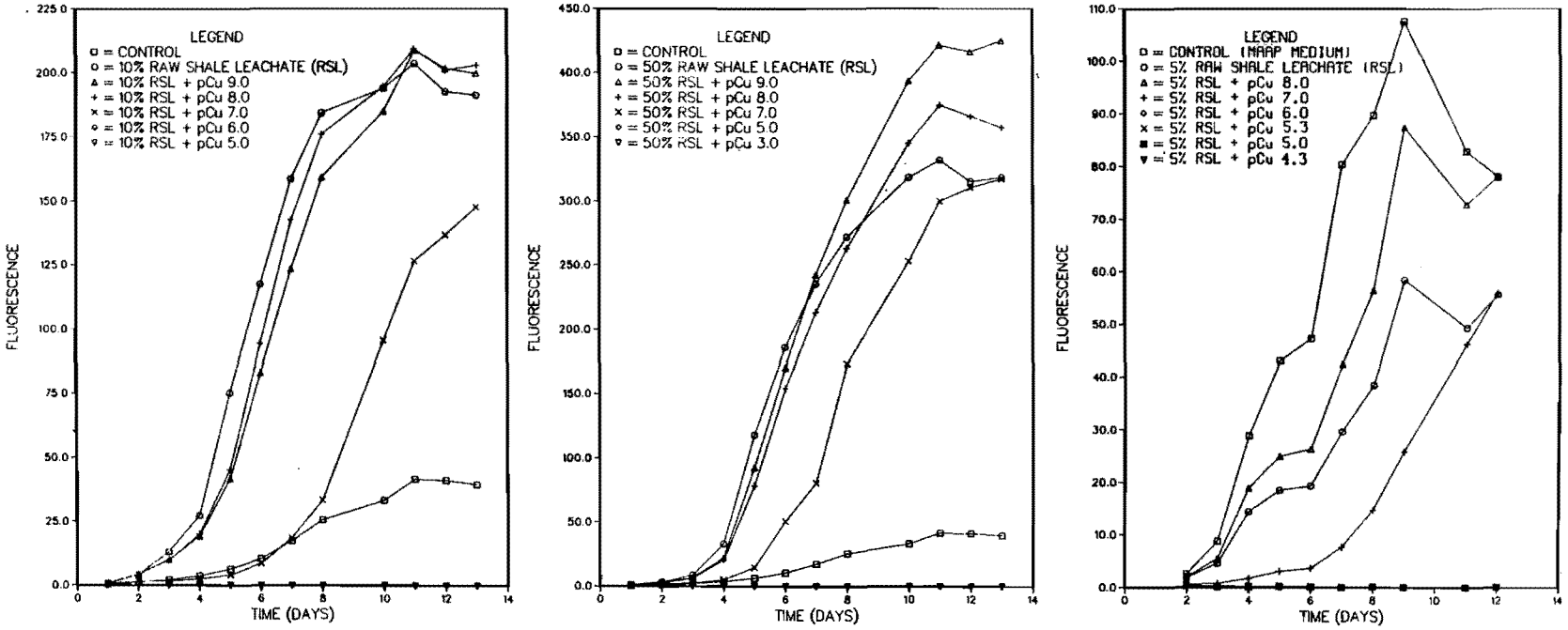

a) 10 percent RSL (1:4)

b) 50 percent RSL (1:4)

c) 5 percent RSL (2:1)

Figure 5.9. Growth responses of S. capricornutum to different copper concentrations with raw shale leachate (RSL) in MAAP medium.

Table 5.6. Responses of S. capricornutum to different concentrations of raw shale leachate (RSL), and to different concentrations of Cu (II) containing 10, 50, and 5 percent RSL in terms of maximum standing crop (MSC), day on which 1/2 MSC occurred, and growth rate at 1/2 MSC.

Treatments	Fluorescence at Maximum Standing Crop (MSC)		Day on which 1/2 MSC occurred		Growth Rate at 1/2 MSC (Fluorescence/day)	
Control[b]	41.5	A	7.6	B	2.7	A
10% RSL (1:4)[c]	203.4	C	5.6	B	18.1	C
10% RSL + pCu 9.0	208.6	C	6.6	B	16.2	C
10% RSL + pCu 8.0	209.2	C	6.2	B	16.8	C
10% RSL + pCu 7.0	147.6	B	10.0	C	7.6	B
10% RSL + pCu 6.0	0.4	A	0.5	A	0.4	A
10% RSL + pCu 5.0	0.3	A	0.8	A	0.2	A
Control	41.5	A	7.6	C D	2.7	A
50% RSL (1:4)	331.7	B	5.7	B	29.1	C
50% RSL + pCu 9.0	424.6	C	6.6	B C	32.4	D
50% RSL + pCu 8.0	374.4	B C	6.6	B C	28.5	C
50% RSL + pCu 7.0	317.2	B	8.2	D	19.7	B
50% RSL + pCu 5.0	0.4	A	0.5	A	0.4	A
50% RSL + pCu 3.0	0.5	A	0.5	A	0.5	A
Control	107.6	B	5.5	B	10.1	D
5% RSL (2:1)[d]	58.5	A B	7.2	C	4.2	B
5% RSL + pCu 8.0	87.4	B	7.2	C	6.1	C
5% RSL + pCu 7.0	56.0	A B	8.4	C	3.4	B
5% RSL + pCu 6.0	0.4	A	1.0	A	0.2	A
5% RSL + pCu 5.3	0.4	A	1.0	A	0.2	A
5% RSL + pCu 5.0	0.4	A	1.0	A	0.2	A
5% RSL + pCu 4.3	0.3	A	1.0	A	0.2	A

[a]Within each metal treatment, responses labeled with the same letter (e.g. A, B, or C) are not significantly different based on the Duncan Multiple Range Test (DMRT).

[b]Control = modified algal assay procedure (MAAP) medium.

[c]RSL (1:4) = raw shale leachate extracted with 1 part of shale and 4 parts of deionized water.

[d]RSL (2:1) = raw shale leachate extracted with 2 parts of shale and 1 part of deionized water.

significant reduction in growth rate for pCu below 7.0. The corresponding EC_{50}'s for the 10, 50, and 5 percent RSL additions were 6.84, 6.69, and 7.00, respectively, thus suggesting that the higher RSL concentration increased detoxification of Cu. The comparative effect of the different ligands on Cu toxicity will be discussed more thoroughly below.

RSL/Cd and RSL/Ni

The effects of RSL on Cd and Ni toxicity are shown in Figures 5.10 and 5.11, and Tables 5.7 and 5.8. At 10 percent RSL, Cd became markedly inhibitory as pCd dropped below 7.0, but some growth still occurred at pCd=6.3. Similar results were obtained at 50 percent RSL additions. These data contrast with the lowered growth at pCd=7.0 encountered in the absence of RSL (Table 5.1) and suggest the possibility of Cd detoxification through binding. MSC decreased significantly in the presence of Ni at pNi values below 7.0 in the presence of 10 percent RSL, with growth virtually stopping at pNi=6.0. There is evidence of a continuum of effect on the growth rate at 1/2 MSC between pNi 7.0 and 5.3 (Table 5.8). The growth response data at 10 percent RSL are similar but less clear-cut on the basis of the DMRT. Comparison of the RSL/Ni data with those in Table 5.1 shows little evidence for Ni complexation. The corresponding EC_{50}'s are pCd=6.53 and 7.71, and pNi=7.07 and 6.93 for the 10 and 50 percent RSL treatments, respectively.

SSL/Cu and SSL/Cd

The effects of the Paraho spent shale leachates described previously on algal growth in the presence of Cu and Cd are shown in Figures 5.12 and 5.13, and Tables 5.9 and 5.10, respectively. The larger size fractions (SSL_1 and SSL_2) can be seen to detoxify Cu at concentrations as high as pCu=7.0 to the levels of the no-metal control. Significant depression of the MSC can be seen to occur at pCu values less than 9.0 in the smallest size fraction, the UM2 filtrate (SSL_3). This result suggests that the Cu-binding capacity of the SSL resides in the larger (>UM2) size fraction. It also suggests that SSL is at least as effective as RSL in binding Cu. Although MSC was not affected by Cd in the presence of any of the Cd concentrations tested, pCd=7.0 depressed the growth rate at 1/2 MSC and increased the lag time, relative to pCd>7.0, with none of the SSL fractions having any apparent effect. Cd binding is apparently not sufficiently strong in the SSL to overcome the toxicity at pCd=7.0 (cf. Table 5.1).

Summary and Comparison of MAAP Results

A significant problem arises in comparing the DMRT data on the effects of the various metals in the presence and absence of the various ligands because it was very difficult to prejudge the concentrations of metal to be tested in the various bioassays. In each case, the goal was to vary the range of metal concentrations tested to cover a range from no response to complete cessation of growth. Because of limitations placed by the size of the experiments, the greater range meant less precise information in the region of the EC_{50}. This reduced the power of the data to demonstrate the statistical significance of the effect of a ligand on metal detoxification. For example, pCu=7.3 was not tested in the RSL/Cu bioassay, so it is not possible to compare the DMRT results between Cu alone (Table 5.1) and Cu in the presence of RSL in reducing growth rates. However, there was a significantly greater growth at pCu=7 in the presence of 5 percent RSL than in the absence of an organic ligand. In the latter case, growth was virtually halted (Table 5.1).

EC_{50} values, based on probit analysis, allow quantitative comparison among the various ligand treatments tested using the MAAP bioassays.

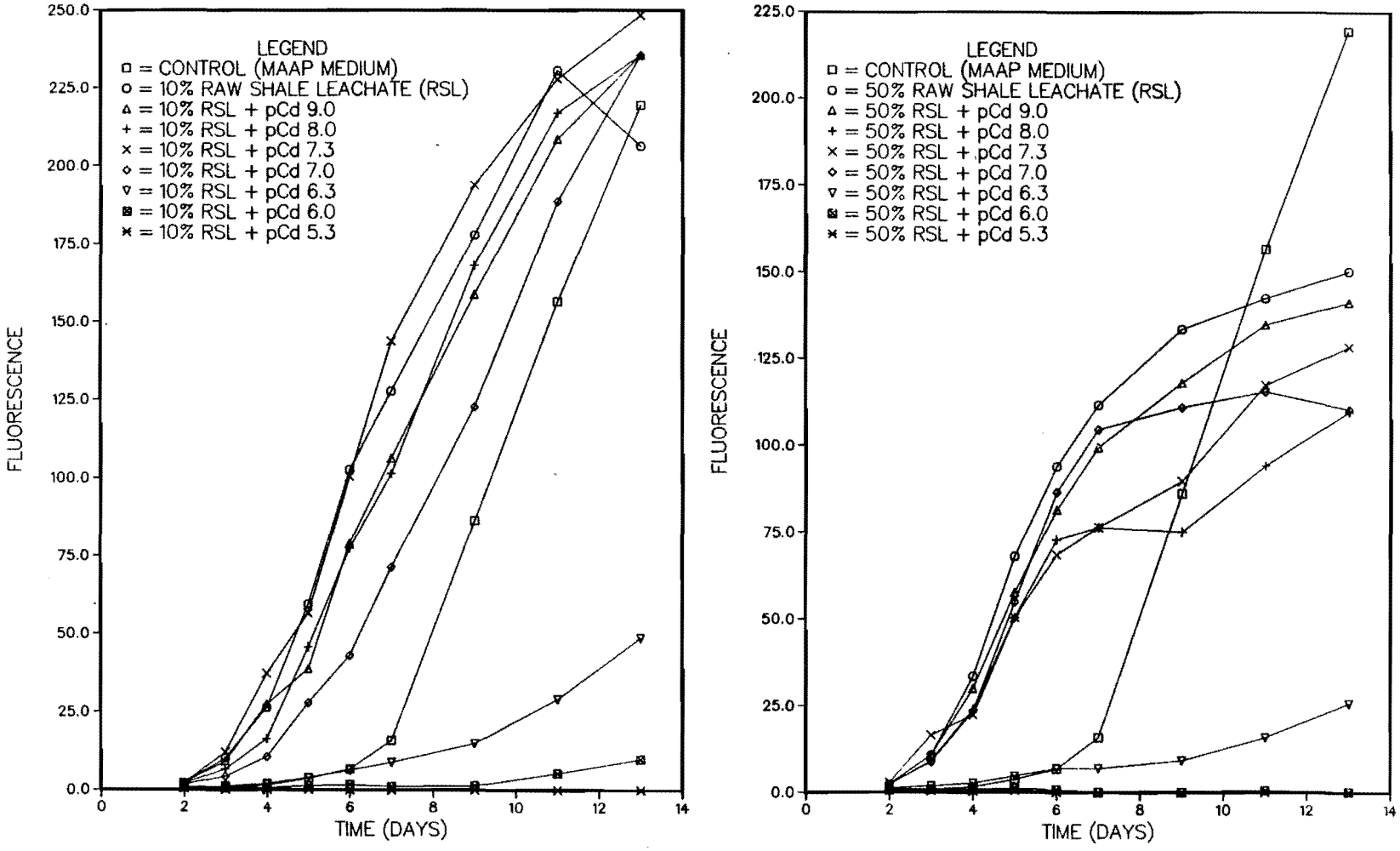

Figure 5.10. Growth responses of S. capricornutum to different cadmium concentrations in the presence of a) 10 percent RSL (1:4) and b) 50 percent RSL (1:4) in MAAP medium.

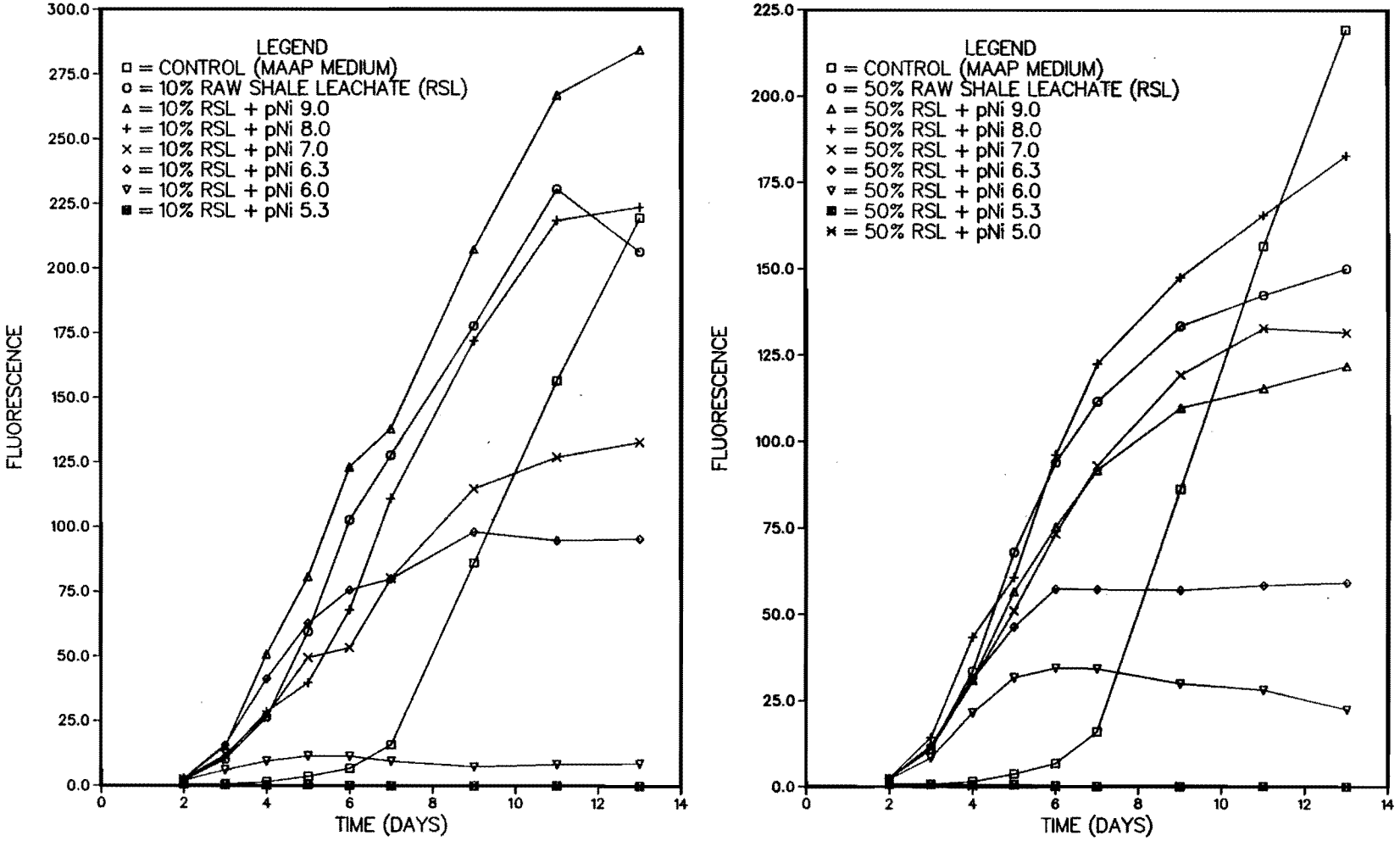

Figure 5.11. Growth responses of S. capricornutum to different nickel concentrations in the presence of a) 10 percent RSL (1:4) and b) 50 percent RSL (1:4) in MAAP medium.

Table 5.7. Responses of S. capricornutum to different concentrations of Cd (II) in the presence of 10 and 50 percent raw shale leachate (RSL) in terms of maximum standing crop (MSC), day on which 1/2 MSC occurred, and growth rate at 1/2 MSC.

Treatments	Fluorescence at Maximum Standing Crop (MSC)		Day on which 1/2 MSC occurred		Growth Rate at 1/2 MSC (Fluorescence/day)	
Control[b]	219.4	B	10.1	C D	11.2	B
10% RSL (1:4)[c]	230.5	B	6.7	B	17.6	D
10% RSL + pCd 9.0	235.4	B	7.6	B C	16.0	C D
10% RSL + pCd 8.0	235.5	B	7.4	B	15.9	C D
10% RSL + pCd 7.3	248.3	B	6.7	B	18.6	D
10% RSL + pCd 7.0	235.4	B	9.0	B C D	13.4	B C
10% RSL + pCd 6.3	48.8	A	10.4	D	2.4	A
10% RSL + pCd 6.0	9.8	A	10.4	C D	0.5	A
10% RSL + pCd 5.3	0.4	A	1.1	A	0.2	A
Control	219.4	C	10.1	C	11.2	B
50% RSL (1:4)	150.1	B C	5.4	B	14.0	C
50% RSL + pCd 9.0	141.2	B C	5.5	B	12.7	B C
50% RSL + pCd 8.0	109.7	B	5.5	B	10.2	B
50% RSL + pCd 7.3	128.2	B	5.8	B	11.0	B
50% RSL + pCd 7.0	115.5	B	5.2	B	11.2	B
50% RSL + pCd 6.3	25.6	A	8.6	C	1.5	A
50% RSL + pCd 6.0	1.1	A	1.1	A	0.5	A
50% RSL + pCd 5.3	0.8	A	1.0	A	0.4	A

[a]Within each metal treatment, responses labeled with the same letter (e.g. A, B, or C) are not significantly different based on the Duncan Multiple Range Test (DMRT).

[b]Control = modified algal assay procedure (MAAP) medium.

[c]RSL (1:4) = raw shale leachate extracted with 1 part of shale and 4 parts of deionized water.

Table 5.8. Responses of S. capricornutum to different concentrations of Ni (II) in the presence of 10 and 50 percent raw shale leachate (RSL) in terms of maximum standing crop (MSC), day on which 1/2 MSC occurred, and growth rate at 1/2 MSC.

Treatments	Fluorescence at Maximum Standing Crop (MSC)	Day on which 1/2 MSC occurred	Growth Rate at 1/2 MSC (Fluorescence/day)
Control[b]	219.4 D E	10.1 D	11.2 B C
10% RSL (1:4)[c]	230.5 D E	6.7 C	17.6 D E
10% RSL + pNi 9.0	284.2 E	6.9 C	20.9 E
10% RSL + pNi 8.0	223.6 D E	7.3 C	15.5 C D
10% RSL + pNi 7.0	132.8 C D	6.1 C	11.1 B C
10% RSL + pNi 6.3	98.2 B C	5.2 B C	10.4 B
10% RSL + pNi 6.0	11.5 A B	3.2 A B	1.8 A
10% RSL + pNi 5.3	0.6 A	1.0 A	0.3 A
Control	219.4 D	10.1 E	11.2 D
50% RSL (1:4)	150.1 C D	5.4 B C D	14.0 E
50% RSL + pNi 9.0	121.9 B C	5.2 B C D	11.6 D
50% RSL + pNi 8.0	182.8 C D	6.0 D	15.3 E
50% RSL + pNi 7.0	132.8 C	5.8 C D	11.6 D
50% RSL + pNi 6.3	59.2 A B	4.0 B C	7.4 C
50% RSL + pNi 6.0	34.4 A	3.9 B	4.5 B
50% RSL + pNi 5.3	1.0 A	1.0 A	0.5 A
50% RSL + pNi 5.0	0.8 A	1.0 A	0.4 A

[a]Within each metal treatment, responses labeled with the same letter (e.g. A, B, or C) are not significantly different based on the Duncan Multiple Range Test (DMRT).

[b]Control = modified algal assay procedure (MAAP) medium.

[c]RSL = raw shale leachate extracted with 1 part of shale and 4 parts of deionized water.

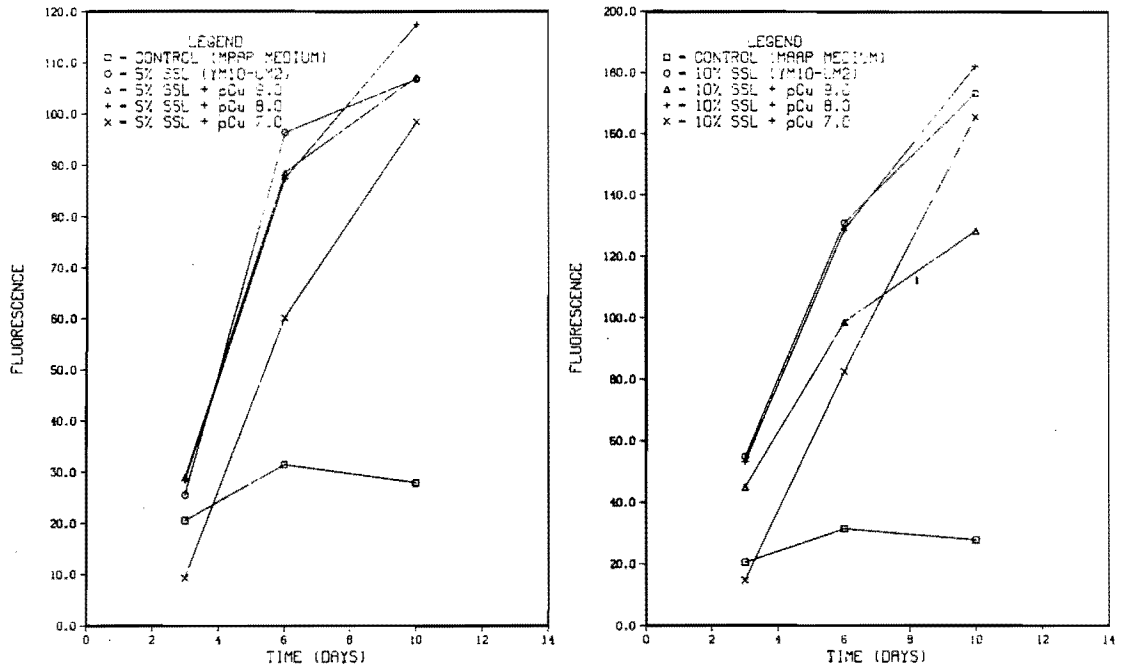

a) 5 percent SSL_1 (YM10 - UM2)

b) 10 percent SSL_1

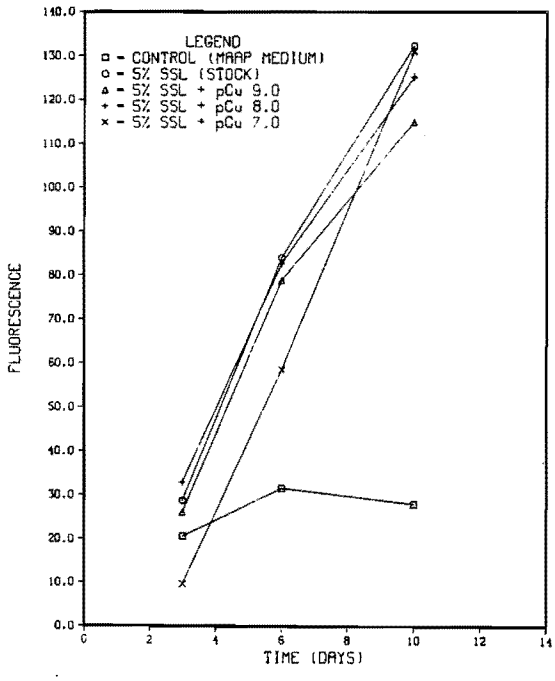

c) 5 percent SSL_2 (stock)

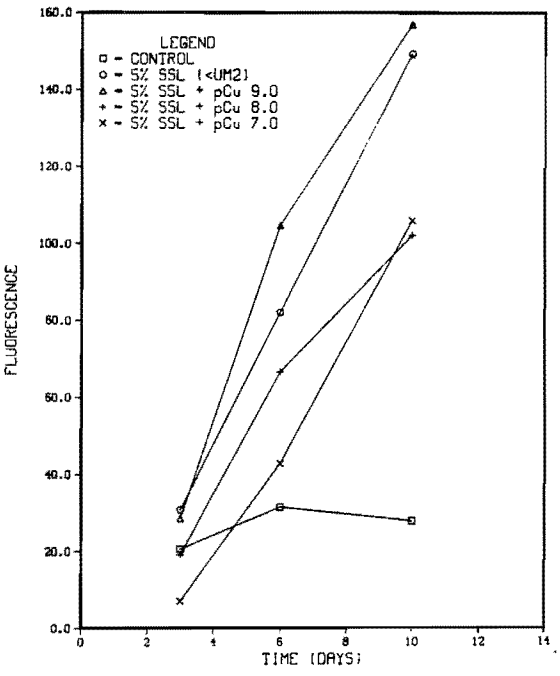

d) 5 percent SSL_3 (<UM2)

Figure 5.12. Growth responses of S. capricornutum to different copper concentrations in the presence of spent shale leachate (SSL) in MAAP medium.

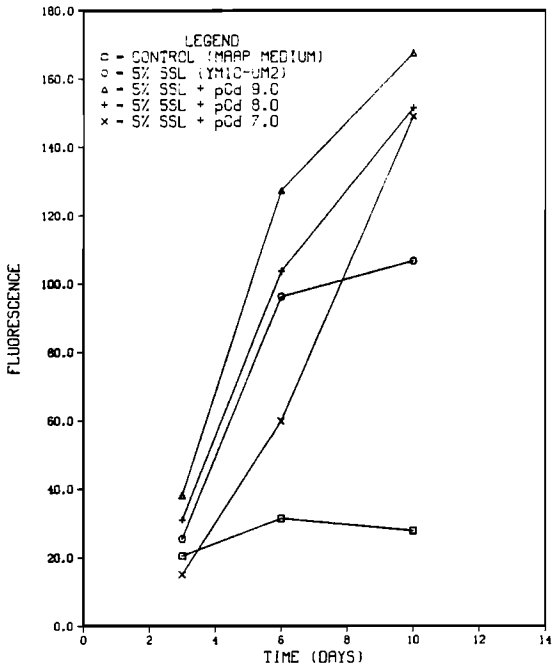

a) 5 percent SSL_1 (YM10 - UM2)

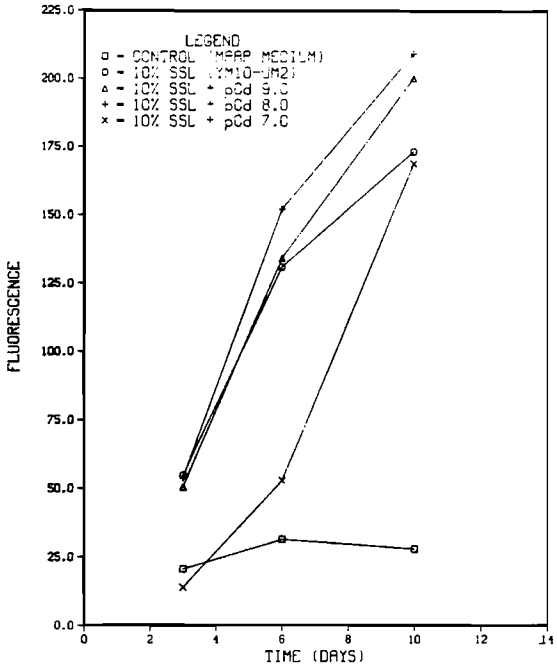

b) 10 percent SSL_1

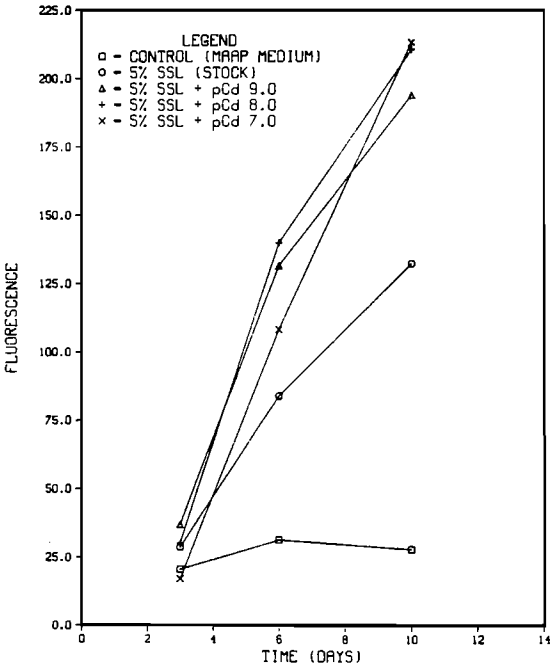

c) 5 percent SSL_2 (stock)

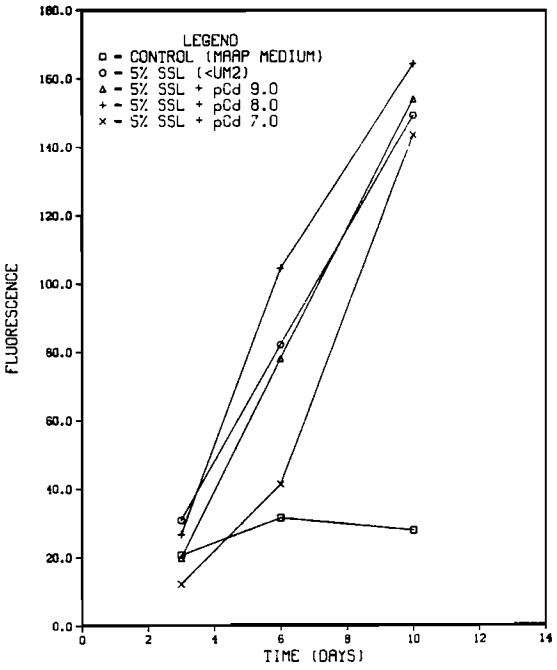

d) 5 percent SSL_3 (<UM2)

Figure 5.13. Growth responses of S. capricornutum to different cadmium concentrations in the presence of spent shale leachate (SSL) in MAAP medium.

Table 5.9. Responses of S. capricornutum to different copper concentrations in MAAP medium containing different size fractionated Paraho spent shale leachates (SSL) in terms of maximum standing crop (MSC), day on which 1/2 MSC occurred, and growth rate at 1/2 MSC.

Treatments	Fluorescence at Maximum Standing Crop (MSC)		Day on which 1/2 MSC occurred		Growth Rate at 1/2 MSC (Fluorescence/day)	
Control[b]	31.4	A	2.4	A	6.8	A
5% SSL1[c] (1:4)	122.6	B	4.7	A B	13.2	B
5% SSL1 + pCu 9.0	116.2	B	4.5	A B	13.0	B
5% SSL1 + pCu 8.0	119.4	B	6.9	B	11.2	A B
5% SSL1 + pCu 7.0	118.1	B	6.3	A B	9.6	A B
Control	31.4	A	2.4	A	6.8	A
5% SSL2[d] (1:4)	132.2	B	5.2	B	13.0	B
5% SSL2 + pCu 9.0	114.8	B	4.8	B	12.0	B C
5% SSL2 + pCu 8.0	125.1	B	4.8	B	13.2	C
5% SSL2 + pCu 7.0	134.1	B	6.5	C	10.4	B
Control	31.4	A	2.4	A	6.8	A
5% SSL3[e] (1:4)	160.8	C	5.9	B	13.6	B C
5% SSL3 + pCu 9.0	163.6	C	5.5	B	15.4	C
5% SSL3 + pCu 8.0	102.0	B	5.2	B	10.0	A B C
5% SSL3 + pCu 7.0	114.6	B	6.9	B	8.3	A B
Control	31.4	A	2.4	A	6.8	A
10% SSL1 (1:4)	173.2	B	4.4	A	20.2	B
10% SSL1 + pCu 9.0	128.4	B	5.2	A	15.2	A B
10% SSL1 + pCu 8.0	195.7	B	6.0	A	19.9	B
10% SSL1 + pCu 7.0	165.6	B	6.3	A	13.7	A B

[a]Algal responses labeled with the same letter (e.g. A, B, or C) are not significantly different based on the Duncan Multiple Range Test (DMRT).

[b]Control = modified algal assay procedure (MAAP) medium.

[c]SSL1 = Paraho spent shale leachate between YM10-UM2.

[d]SSL2 = Paraho spent shale leachate without size fractionation.

[e]SSL3 = Paraho spent shale leachate with size fractionation < UM2.

Table 5.10. Responses of S. capricornutum to different cadmium concentrations in MAAP medium containing different size fractionated Paraho spent shale leachates (SSL) in terms of maximum standing crop (MSC), day on which 1/2 MSC occurred, and growth rate at 1/2 MSC.

Treatments	Fluorescence at Maximum Standing Crop (MSC)		Day on which 1/2 MSC occurred		Growth Rate at 1/2 MSC (Fluorescence/day)	
Control[b]	31.4	A	2.4	A	6.8	A
5% SSL1[c] (1:4)	122.6	B	4.7	B	13.2	B C
5% SSL1 + pCd 9.0	168.8	B	4.7	B	18.2	D
5% SSL1 + pCd 8.0	151.4	B	4.8	B	15.6	C D
5% SSL1 + pCd 7.0	168.8	B	7.1	C	11.9	B
Control	31.4	A	2.4	A	6.8	A
5% SSL2[d] (1:4)	132.2	B	5.2	B	13.0	B
5% SSL2 + pCd 9.0	203.4	C	5.0	B	20.1	C
5% SSL2 + pCd 8.0	223.3	C	5.2	B	21.3	C
5% SSL2 + pCd 7.0	247.0	C	6.7	C	18.9	C
Control	31.4	A	2.4	A	6.8	A
5% SSL3[e] (1:4)	160.8	B	5.9	B	13.6	B
5% SSL3 + pCd 9.0	163.6	B	6.2	B	13.1	B
5% SSL3 + pCd 8.0	182.2	B	5.6	B	16.4	C
5% SSL3 + pCd 7.0	187.7	B	8.0	C	11.6	B
Control	31.4	A	2.4	A	6.8	A
10% SSL1 (1:4)	173.2	B	4.4	B	20.2	C
10% SSL1 + pCd 9.0	200.2	B C	4.8	B	21.0	C
10% SSL1 + pCd 8.0	209.2	C	4.6	B	23.2	C
10% SSL1 + pCd 7.0	195.7	B C	7.6	C	12.9	B

[a]Algal responses labeled with the same letter (e.g. A, B, or C) are not significantly different based on the Duncan Multiple Range Test (DMRT).

[b]Control = modified algal assay procedure (MAAP) medium.

[c]SSL1 = Paraho spent shale leachate between YM10-UM2.

[d]SSL2 = Paraho spent shale leachate without size fractionation.

[e]SSL3 = Paraho spent shale leachate with size fractionation < UM2.

These values are reported in Table 5.11, along with LC (lethal concentration) values, based on the lowest metal concentration at which the average fluorescence in the replicate flasks failed to reach five units. In the absence of ligands, it can be seen that Cu appears to be approximately three times as toxic as Cd, and 21 times as toxic as Ni to the test alga. Although it would appear that an order of magnitude separates the LC for the three metals, it should be noted that few intermediate concentrations (ones between pCu 7 and 8) were tested.

The presence of 5 mg/L HA increased the EC_{50} for Cu by a factor of 27, and 10 mg/L HA increased it by a factor of 42 over the no ligand control. If increasing EC_{50} with increasing HA concentration was solely the result of complexation, then 5 mg/L HA bound 96 percent of the Cu present, and 10 mg/L bound 98 percent of the Cu strongly enough to render it nontoxic.

The raw shale leachate also showed evidence for detoxifying Cu, although the effect was less pronounced than for HA even at the highest RSL concentration tested. The 1:4 leachate detoxified 91 percent of the Cu at 10 percent concentration in the MAAP medium, and 94 percent at 50 percent concentration. The 2:1 leachate, which when applied at 5 percent concentration, resulted in the lowest TOC level tested for RSL, and correspondingly detoxified only 80 percent of the Cu present in all cases, RSL decreased the apparent LC by an order of magnitude.

At the 10 percent concentration, RSL decreased the toxicity of Cd by 88 percent, but had a net deleterious

Table 5.11. Comparison of E_{50} values based on probit analysis and LC values based on lowest concentration (M/L) giving an average value of <5 fluorescence.

Ligand		Metal		
		Cu	Cd	Ni
No ligand	EC_{50}	1.31×10^{-8}[a]	3.49×10^{-8}	2.8×10^{-7}
	LC	1.0×10^{-7}	1.0×10^{-6}	1.0×10^{-5}
HA (5 mg/L)	EC_{50}	3.48×10^{-7}	N.D.	N.D.
	LC	1.0×10^{-5}		
HA (10 mg/L)	EC_{50}	5.46×10^{-7}	N.D.	N.D.
	LC	1.0×10^{-5}		
RSL (10%, 1:4)	EC_{50}	1.44×10^{-7}	2.96×10^{-7}	8.43×10^{-8}
	LC	1.0×10^{-6}	5.0×10^{-6}	5.0×10^{-6}
RSL (50%, 1:4)	EC_{50}	2.05×10^{-7}	1.95×10^{-8}	1.17×10^{-7}
	LC	1.0×10^{-6}	1.0×10^{-6}	5.0×10^{-6}
RSL (5%, 2:1)	EC_{50}	6.40×10^{-8}	N.D.	N.D.
	LC	1.0×10^{-6}		

[a]Mean of 2 values

effect on growth at the 50 percent concentration. RSL increased the toxicity of Ni to the algae at the lowest concentration tested. For all but the 10 percent RSL/Cd treatment, RSL increased (Ni) or had no effect (Cd) on the LC.

The data in Table 5.11 are consistent with the hypothesis that RSL acts as an ligand strong enough to detoxify Cu to algae, as has been shown for humic substances in lake water (e.g. Gachter et al. 1978). The data suggest that even though Cd may be bound to some extent, any such binding is insufficient to detoxify Cd at high concentrations. Indeed Cd toxicity may be enhanced by the RSL, either through toxicity of the diafiltered RSL itself or through reduced availability of a trace nutrient because of chelation at the higher RSL concentration. No evidence was found that RSL works to detoxify Ni, it merely amplifies the toxicity of this metal. Although no quantitative comparison can be made on the basis of EC_{50} values between RSL and SSL, the data in Table 5.9 clearly indicate that the cultures were not affected by Cu concentrations of pCu=7.0, relative to growth at pCu= 9.0, in the presence of the larger organic size fractions. Similar results were observed for Cd, which suggests that SSL may have more affinity for the latter metal than for Cu. These data suggest that at least 90 percent of the Cu and 30 percent of the Cd was bound by the SSL ligands.

The data in Table 5.11 can be used to estimate minimum complexation capacities for each ligand by subtracting the EC_{50} of the appropriate control from that for each ligand treatment. The resulting values are tabulated in Table 5.12, along with ranges observed for CC in the ISE binding titrations. Minimum CC's based on MAAP bioassays are well within the range of the CC values predicted using ISE titrations, and indicate occupation of 10 percent of CC_{MAX} for HA. For RSL, CC_{MIN} values appear to be more in line with those from the titrations of the RSL from the upflow columns than those based on titrations of the batch extract. Similar analysis from MAAP bioassay for Cd indicates a minimum CC of 2.61×10^{-7} M Cd/mg DOC, or a Cd:C ratio of 0.31 percent. It should be borne in mind that the ISE titration on undiafiltered leachate represents the residual CC, not already occupied by Cu (although the proportion of occupied sites is low). Unfortunately CC_{MAX} cannot be implied from the EC_{50} data, because the free Cu concentration is determined by the product of the total ligand concentration and the K_f^c, which the MAAP bioassays do not estimate independently.

The data in Table 5.11 can be used in conjunction with the CC data from the binding experiments to test the internal consistency of the binding model. If the free metal ion concentration at the EC_{50} corresponding to the presence of a particular ligand can be taken as the EC_{50} in the absence of the ligand, then the concentration of the metal-ligand complex is the difference between the values of EC_{50} in the presence and absence of the ligand. The free ligand concentration then can be calculated as the difference between the CC, as determined by one of the binding techniques described in the previous chapter, and the concentration of the metal-ligand complex. Such calculations have been done for HA and RSL, the only ligands for which both binding analyses and EC_{50}'s were available, and the results are displayed in Table 5.13.

Log K_f^c values for HA ranged from 6.77 to 6.54, depending on whether an EC_{50} of 0.98×10^{-8} or 1.62×10^{-8} (the values obtained in two separate bioassays) were used to represent the free Cu concentration in the absence of any added ligand. The bioassay results are somewhat higher than the log K_f^c value of 6.23 determined using the Ruzic plot, and fell somewhere in between the strong and weak site values determined by Scatchard analysis, both

Table 5.12. Minimum complexation capacities of various ligands based on EC_{50} estimated from MAAP bioassays.

Ligand	mole Cu/L	mole Cu/mg TOC	mole Cu/mole C (%)
HA			
5% (MAAP)	3.27×10^{-7}	1.31×10^{-7}	0.16
(ISE)	6.15×10^{-6}	1.23×10^{-6}	1.5
10% (MAAP)	5.33×10^{-7}	1.07×10^{-7}	0.13
(ISE)	1.32×10^{-5}	1.32×10^{-6}	1.6
RSL			
5% (MAAP)	5.09×10^{-8}	5.99×10^{-8}	0.072
10% (MAAP)	1.31×10^{-7}	1.31×10^{-7}	0.16
50% (MAAP)	1.92×10^{-7}	3.84×10^{-8}	0.046
50% (ISE)[a]	8.25×10^{-6}	2.66×10^{-6}	3.2
100% (ISE)[b]	3.16×10^{-6}	3.33×10^{-8}	0.04
100% (ISE)[c]	6.40×10^{-6}	3.46×10^{-7}	0.42

[a]50% UF diafiltered RSL (1:4 batch) in MAAP medium (DOC = 6.2 mg/L)
[b]Fraction 1 (RSL_1), upflow column
[c]Fraction 3 (RSL_3), upflow column

based on ISE titrations. Inasmuch as most of the CC is exerted in the region of the EC_{50}, the log K_f^c would be expected to represent the weighed average of the intrinsic K_f^c values for each binding site on the molecule. At 10 mg/L HA, K_f^c, estimated using the bioassay technique, overestimated the K_f^c by a factor of only 3.0, again falling somewhere between the K_f^c values for the "strong" and "weak" binding sites determined by Scatchard analysis. Considering that the bioassays were run in MAAP medium, rather than in the deionized water used in the ISE titration, the overestimation is actually somewhat greater, no correction has been made for competing cations at ligand binding sites.

In the Scatchard analysis, the number of intrinsically different binding sites is assumed to be two. A more reasonable concept may be to assume a large number of sites with a virtual continuum of K_f^c values, only some of which are affected by metal binding on sites with stronger affinity for the metal (Perdue and Lytle 1983, Tuschall and Brezonik 1983a). Therefore, the reasonable agreement between the single, operationally derived Ruzic value and the bioassay results, suggests that a simple binding analysis performed by ISE or other means may allow a reasonable estimate to be made of the order of magnitude of effect of a ligand on bound metal toxicity in a culture.

The log K_f^c values for RSL in the bioassay experiments can be seen to decrease with increasing concentration of ligand for the 1:4 leachate applications. For the binding analyses per-

Table 5.13. Comparison of log conditional formation constants, log K_f^c, for Cu-humic acid and Cu-raw shale leachate determined by bioassays (EC_{50}) and chemical means.

CC	Ligand	Bioassay	Binding Analysis		
			Ruzic	Strong[a]	Weak[a]
ISE	HA				
	5 mg/L	6.54-6.77	6.23	7.73	4.89
	10 mg/L	6.41-6.64	6.04	8.65	5.74
	RSL (1:4)				
	10%	6.49-6.73			
	50% MAAP	5.95-6.18	5.20	5.96	5.10
	50% (based on 100)	4.69-4.93	4.91	6.96	4.52
	RSL (2:1)				
	5%	6.36-6.64			
DPASV	HA				
	10 mg/L	7.92	7.53	8.78	6.83
	RSL (1:4)				
	50%	7.00	6.26	6.20	

[a]Based on Scatchard analysis.

formed only on the 100 percent RSL, it was assumed that the ratio of CC to TOC was the same as that in the diluted extracts, and for the 50 percent RSL in MAAP the binding capacity was adjusted upward by 10/6.2 to account for the differences in TOC between the batch of RSL used for the bioassay and that used in the binding titration. The corresponding results indicate quite good agreement between the K_f^c determined on the undiafiltered 100 percent RSL and that determined in the bioassays at the higher (50 percent) application rate. This would be expected on the basis that CC is not a linear function of ligand concentration, as can be argued from colloid chemistry considerations (e.g. Langford et al. 1983), and as was shown for HA above. However, the 50 percent RSL in MAAP titrations results in a substantial (5x) underestimation of K_f^c, relative to the bioassay results. In either case, however, the K_f^c is considerably higher than that for the heterocyclic nitrogen compounds in retort water (e.g. Stanley et al. 1981).

Possible reasons for the apparent discrepancy between the K_f^c (and CC) values determined for the 50 percent RSL can be divided into factors involving the titrations and those involving the

bioassays. The differences in the intrinsic K_f^C values in the two media can be caused by ionic strength, competing cations, ligand concentration, pH, or differences in the ligands present in the two RSL extracts. There is also some error (±10 percent) on the basis of trial calculations in fitting the titration potential data to a Ruzic plot, based on the number of points taken at the end on the titration to calculate the calibration factor for the electrode. There is also the worrisome problem of having to manipulate the potential data at all in order to produce a reasonable titration curve. Errors in the bioassay EC_{50} values may stem from the presence of enhancement of growth at low metal concentrations, but a potentially greater problem arises because of the small number of metal concentrations in the probit plot that actually determine the EC_{50} value. Further work should be done at pCu concentrations in the region of the EC_{50} using more than three replicate cultures, in order to sharpen the general conclusions reached in this preliminary study.

It was noted in Chapter IV and by Tuschall and Brezonik (1981) that DPASV produces low estimates of CC and K_f^C if the metal-ligand complex under consideration is reducible at the mercury electrode. The K_f^C bioassay values were recalculated using the corresponding CC values based on DPASV binding analysis and are tabulated below the ISE-derived values in Table 5.13. The corresponding results for 10 mg/L HA are quite good, showing a similar order of overestimation of the DPASV-derived K_f^C (2.3 times larger than the DPASV value) as was shown for the ISE-based analysis. The K_f^C estimated by the bioassay for the 50 percent RSL application was 5.5 times higher than the DPASV estimated value, which is considerably worse than the ISE analysis, based on the 100 percent RSL titration, but much better than the agreement with the 50 percent RSL in MAAP titration.

In general, the CC and K_f^C values determined using the various complexometric titrations would produce estimates of the free copper ion concentration that are in the correct order of magnitude of those "responded to" by Selenastrum in the MAAP medium. This is true even when the actual values of CC and K_f^C are incorrect (which they appear to be in offsetting ways) by more than an order of magnitude. These data demonstrate that, while concordance between bioassay data and binding parameters based on complexometric titrations is necessary to confirm the correctness of the latter, it is not a sufficient condition. This observation stems, of course, from the interaction between the total ligand concentration and K_f^C in determining the concentration of the free metal ion. The effect of "correcting" the complexometric titration curves is to decrease the CC and increase the K_f^C. This leads to a model in which a "low" equilibrium Cu concentration would be maintained for a "short" time as Cu is added to a receiving water. The alternative (higher CC and lower K_f^C) would result in free Cu ion concentration control sequentially by HA, oil shale ligands, and finally inorganic ligands such as $CO_3^=$ or OH^-, with each controlling ligand exhibiting a $[Cu^{++}]$ plateau with the concentration increasing from one plateau to another. Although the latter case cannot be ruled out, we believe that the inability to account for a complexing mechanism resulting in a high CC and low K_f^C favors the alternate interpretation. Ultimately, the utility of such titrations depends on the magnitude or error tolerable in predicting [Cu] in a receiving water.

Although it would seem that the potential errors in predicting free copper ion concentration would increase with increasing ionic strength, the 100 percent RSL titration produced a relatively good estimate of [Cu] again, despite the fact that the CC and K_f^C values individually are in error. At

present, however, it would appear that complexometric titrations of oil shale leachate give only a highly empirical estimate of [Cu] that could only be used for crude estimates of impacts of shale leachates on phytoplankton. Of the three types of titrations studied, ISE titrations would appear to be superior.

CHAPTER VI

SUMMARY AND CONCLUSIONS

This study set out to determine the potential for metal binding by organic ligands associated with oil shale leachate and the subsequent effect of the bound metals on phytoplankton growth in stream and reservoirs downstream from sources of leachate. The task left is to summarize and interpret the results obtained from the complexometric titrations and algal bioassays in a brief discussion of the implications of this laboratory work for protection of waters potentially impaired by runoff from shale piles.

Complexometric Titrations

Commercially available humic acid (HA) was examined, along with leachates from laboratory extraction of unretorted Mahogany Zone oil shale (RSL) in deionized water, using a variety of commonly titration techniques to determine the complexation capacities (CC) and conditional formation constants (K_f^c) for copper-organic complexes in water. Ultrafiltration titrations displayed good agreement between the CC values for HA and those reported for natural humic acids in the environment, 2.5×10^{-6} M Cu/mg TOC, although the K_f^c (pH=7) was somewhat lower, $10^{6.31}$. UF titration of an electrodialyzed RSL leachate buffered with $NaHCO_3$ failed to yield meaningful binding parameters, apparently because of precipitation of a copper hydroxy or carbonate salt on the UF membrane.

Ion selective electrode (ISE) titration, using copper as the titrant showed good agreement between the CC (1 mole/mole) and K_f^c ($10^{7.54}$) values reported for a model ligand, EDTA, measured by other workers using similar techniques, although neither value for K_f^c corresponds to the values of 1.00 and $10^{12.9}$ commonly utilized at the titration pH. Both HA and raw shale leachate (RSL) titrations, however, failed to reach a binding plateau. Instead, they showed a pattern that suggested either complexation by a ligand present at high concentration, but with a low K_f^c, or a reduced potentiometric response of the electrode due to poisoning of the electrode surface with an organic or inorganic precipitate. When adjustments were made for this decreased response, the resulting data provided reasonable CC and K_f^c values for HA, 2.5×10^{-6} M Cu/mg TOC and $10^{6.04}$–$10^{6.23}$ respectively, and indicated a stoichiometry of 15:1000 for copper and organic carbon in the HA ligand. The binding parameters were somewhat concentration dependent, and the K_f^c values could be divided into strong (log K_f^c = 7.7–8.6) and weak (log K_f^c = 5.7–5.9) sites using Scatchard analysis.

Titration of two leachate fractions from crushed RSL extracted with deionized water in an upflow column revealed lower CC values than those observed for HA, ranging from 3.3×10^{-8} to 3.5×10^{-7} M/mg TOC. The corresponding K_f^c values were $10^{5.97}$ and $10^{4.92}$, respectively and the Cu:C stoichiometries ranged from 0.4–4:1000. A similar titration of another RSL obtained by batch deionized water extraction of a different oil shale sample revealed an apparent CC of 4.7×10^{-5} M/mg TOC, which cannot be attributed to an organic ligand because of the unrealistic Cu:TOC stoichiometry (568:1000). Consequently, another titration was performed on a second 1:4

batch RSL leachate in MAAP medium which yielded a CC of 2.66 x 10^{-6} M Cu/mg TOC, which results in a Cu:C stoichiometry somewhat lower than HA, i.e. 0.2:1000. The corresponding K_f^c was $10^{5.20}$.

Differential pulse anodic stripping voltammetry (DPASV) was also evaluated using both HA and RSL as ligands and copper as the titrant. Cyclic voltammograms suggested that, in both cases, the Cu-ligand complex was being reduced at the mercury electrode, thus resulting in underestimates of CC and K_f^c. Titration of EDTA yielded a CC of 1 mole Cu/mole EDTA, but the K_f^c was only $10^{5.5}$-$10^{5.7}$, which is two orders of magnitude lower than that observed using ISE. The corresponding CC and K_f^c values for HA and the RSL that gave the spurious CC value in the ISE titration were 2 x 10^{-7} M/mg TOC and $10^{7.53}$, and 2.7 x 10^{-7} M/mg TOC and $10^{6.4}$, respectively. The similar orders of magnitude in the HA and RSL values further suggest the inaccuracy of the CC value for the batch-extracted RSL ISE titration reported above.

Taken as a whole, the results of the various complexometric titrations indicate that the techniques employed for binding analyses involving natural organic ligands in soft, heavily humified waters or soil extracts are not easily applied to oil shale leachates. For example titrations with model ligands (EDTA and HA) in deionized water generally gave results in agreement with those reported by other workers using slightly different HA sources (e.g. natural water) or techniques. However, complexometric titrations of oil shale leachates not diafiltered to remove inorganic salts resulted in precipitation and other interactions of copper within or on the ultrafiltration membranes, or on reservoir, titration cell, and ISE surfaces. Selection of the correct titrant concentration is critical and difficult to prejudge. Metal detection techniques are either expensive (carbon furnace atomic absorption), insensitive (Cu-ISE), or slow and inaccurate (DPASV) for application at the low concentration levels necessary for analyzing binding capacities at ambient ligand concentrations (i.e. without preconcentration which may alter binding sites).

Although many of the difficulties discussed above can be overcome in the research laboratory, it is unlikely that a precise and accurate standard method can be developed for routine use in a small onsite monitoring laboratory. However, modifications of the titrations studied here might produce useful order-of-magnitude estimates for binding parameters and give some insight as to the potential for large scale environmental impacts downstream. For example, in the case described here, the titrations were sufficiently informative to rule out small heterocyclic nitrogen species as the dominant factor in metal binding, as has been proposed for retort water.

Algal Bioassays

MAAP bioassays employing Selenastrum capricornutum in standard EPA AAP medium, modified by excluding EDTA and the trace metal solution (MAAP), were run using various concentrations of Cu, Cd, and Ni alone and amended with HA, RSL, and Paraho spent shale leachate (SSL), both whole, but diafiltered to remove salts and low-molecular weight organics, and also size-fractionated using ultrafiltration membranes. The results of the titrations indicated that the metals in the medium were toxic in the order Cu > Cd >> Ni in the absence of organic ligands, with corresponding EC_{50}'s of $10^{-7.56}$, $10^{-7.35}$, and $10^{-6.35}$ M/L, respectively.

Raw shale leachate, diafiltered to remove inorganic nutrients and toxicants, showed greatly improved growth over a control receiving no RSL. Size fractionation revealed the growth-enhancing organic to be present in the >UM2 UF size fraction. The <UM2 fraction, which includes inorganic salts

(EC=320 μmho/cm), was inhibitory to the algae. Paraho retorted shale leachate was stimulatory in all size fractions, including the <UM2 filtrate, thus suggesting that some toxicant may be removed from the latter fraction during retorting. Humic acid was highly stimulatory at low concentrations in the absence of added metals (5-10 mg/L) but somewhat less stimulatory at higher concentrations (25-50 mg/L).

In the presence of added metals, HA reduced Cu toxicity to the test alga by a factor of more than 40 (at 10 mg/L HA). Raw shale leachate also detoxified copper by a factor of 16 at 5 mg/L TOC, which is equivalent to the TOC concentration in 10 mg/L HA. Paraho retorted shale also detoxified copper, but the magnitude cannot be calculated from the data. Raw shale leachate detoxified cadmium by a factor of 8 at low application rates (1 mg/L TOC), but increased the toxicity at higher applications in the presence of added cadmium. The raw shale leachate increased the toxicity of added nickel at all application rates of the ligand. Retorted shale leachate also showed evidence of detoxified cadmium to a small and unquantifiable extent.

The MAAP bioassay results suggest that oil shale leachates may act in a manner similar to natural humic matter in water by binding copper strongly enough to reduce its toxicity to phytoplankton. Cadmium may be affected to a lesser extent, but nickel is not. The complexation capacities on a mole organic carbon basis appears to be lower for the raw shale leachate than for humic acid, which suggests that leachate from shale piles would have to contribute at least as much TOC to streams as would natural HA production for significant effects to be observed on copper and metal cycling downstream.

Thermodynamic Modeling

The results of the bioassay experiments indicated that the binding parameters determined by ISE titration for humic acid were adequate for predicting the approximate degree of algal response to free copper ion in the culture medium. Application of the binding parameter data from one RSL ISE titration revealed concordance between the predicted CC and K_f^c values and bioassay results, despite the determination that the binding capacity value was too high based on theoretical reasoning. An additional ISE titration of a second batch of RSL showed a reasonable CC, but the corresponding K_f^c overestimated the free copper ion concentration by an order of magnitude. It is not known, however, whether the organic composition of the two batches of extract were different with respect to ligand concentration. It is noted that agreement between bioassay data is a necessary, but not sufficient, condition for confirmation of the binding titration results.

The results of the thermodynamic modeling suggest that binding constants (CC and K_f^c) determined using one of the several complexometric techniques may be useful, even if they are individually incorrect, provided that their product is correct. In other words, the operationally derived CC may be higher than the actual value by a factor of ten, but if the operationally determined K_f^c is correspondingly low by the same factor, the predicted free copper (or other metal) ion concentration will be virtually identical over the range of most ligands and total copper concentrations in natural waters. It may be worthwhile to review the literature on humic and fulvic acids to see whether much of the variability in complexation capacity can be explained on the basis of compensating variations in K_f^c.

Environmental Implications for Oil Shale Storage

The results of this study suggest that raw and spent oil shale leachates contain organic ligands that are capable

of altering the toxicity of some trace metals to algae. At extremely low trace metal concentrations (unlikely to be characteristic of most reservoirs), these ligands may increase the availability of trace metal nutrients in solution by sequestering them against precipitation, but not algae uptake. As in the case of natural humic and fulvic acids, copper is bound sufficiently tight to detoxify the metal to algae. This factor is probably more significant in selecting for or against copper-sensitive species such as bloom-forming blue-green algae in reservoirs, rather than in reducing or enhancing gross photosynthetic rates or total algal standing crop biomass at ambient total copper concentrations in most reservoirs. It may be particularly significant in the effectiveness of copper sulfate application to control algal blooms in reservoirs used for municipal and industrial water.

The relative importance to the receiving waters of oil shale organic ligands versus background concentrations of natural humic and fulvic acids is difficult to forecast for the projected context of a fully developed oil shale industry. Shale piles will generally be designed to minimize runoff, although initial leachate fractions caused by an unanticipated overtopping of the designed containment facility may have quite high TOC concentrations (>80 mg/L) and presumably correspondingly high binding capacities. If such events are not frequent, the organic ligands from the shales should not cause problems significantly different in kind from those associated with the natural products of vegetative decomposition. Indeed, the toxic nature of the smallest size fraction of the raw oil shale leachate would probably impair algal growth more than would metal binding by organic ligands.

Recommendations for Further Research

Based on the results of the exploratory studies reported here, further research into oil shale ligand-metal interactions should follow two different thrusts: 1) developing better quasi-thermodynamic models relating metal-ligand chemistry to algal bioavailability, and 2) characterizing the particular ligand chemistry of various leachates and process waters associated with an in-place, commercial scale industry. The first category should be pursued immediately, and might well best proceed using complex model ligands as well as providing insights into the environmental impacts and behavior of both natural and man-made organic ligands in natural waters. Although some research of this nature is occurring, the thrust is largely analytical at this time, and the biological component needs to be more strongly integrated. The second principal thrust should coincide with development of a commercial scale industry, using samples gathered from on site shale piles, retorts operating in non-experimental modes with shale from on-site mines, and samples gathered from waste and cooling ponds. The variability resulting from sources of raw shale, weathering, retort conditions, and laboratory extraction procedures makes it virtually impossible to conduct cost-effective research into environmental effects of a full scale industry based on a few drums of material.

Theoretical work should emphasize:

1. Titrations of model ligands in increasingly complex milieux, in order to determine effects on binding capacity and K_f^c of competing cations, pH, competing ligands, and precipitation.

2. Better and more efficient methods for controlling and detecting free metal ion concentrations during complexometric titrations.

3. Bioassays emphasizing more metal concentrations in the vicinity of the

EC_{50}, increased number of replicates, different metal ions, and different test algae, including locally isolated strains.

4. Effects of competing metal ions on K_f^C and CC in both titrations and bioassays. The importance of Fe versus toxic metals should be emphasized in the latter.

Further work on a commercial-scale industry should emphasize:

1. Leachates from raw shale piles and spent shale, retort water (above ground and in situ), groundwater and water in receiving streams.

2. Cu, Cd, and Pb.

3. Samples collected in the field.

SELECTED BIBLIOGRAPHY

Adams, V. D., and V. A. Lamarra. 1983. Aquatic resources management of the Colorado River ecosystem. Ann Arbor Science, Ann Arbor, Michigan.

Adhikari, M., G. Chakrabarti, and G. Hazra. 1977. Measurement of stability constant of humic acid metal complexes. Agrochimica 21:134-139.

Allen, H., R. Hall, and T. Brisbin. 1980. Metal speciation: effects on aquatic toxicity. Environ. Sci. Technol. 14:441-443.

Amicon Corporation. 1977. Binding analysis by ultrafiltration. Publication No. 459. Amicon Corporation, Danvers, Massachusetts.

Anderson, D. M., and F. M. Morel. 1978. Copper sensitivity of Gonyaulax tamarensis. Limnol. Oceanogr. 23:283-295.

American Public Health Association (APHA), American Water Works Association, Water Pollution Control Federation. 1980. Standard methods for the examination of water and wastewater. 15th ed. American Public Health Association, Washington, D.C. 1134 p.

Avdeef, A., J. Zabronsky, and H. H. Stuting. 1983. Calibration of copper ion selective electrode response to pCu 19. Anal. Chem. 55:298-304.

Bartlett, L., F. Rabe, and W. Funk. 1974. Effects of copper, zinc, and cadmium on Selenastrum capricornutum. Water Res.8:179-155.

Bentley-Mowat, J., and S. Reid. 1977. Survivial of marine phytoplankton in high concentrations of heavy metals, and uptake of copper. J. Exp. Mar. Biol. Ecol. 26:249-264.

Bhat, G., R. Saar, B. Smart, and J. Weber. 1981. Titration of soil-derived fulvic acid by copper (II) and measurement of free copper (II) by anodic stripping voltammetry and copper (II) selective electrode. Anal. Chem. 53:2275-2280.

Boyle, E. 1979. Copper in natural waters, p. 77-88. In J. Nriagu (Ed.). Copper in the environment. Wiley-Interscience, New York, New York.

Buffle, J., F. L. Greter, and W. Haerdi. 1977. Measurement of complexation properties of humic and fulvic acids in natural waters with lead and copper ion-selective electrodes. Anal. Chem. 49:216-222.

Chaberek, S., and A. E. Martell. 1959. Organic sequestering agents. Wiley, New York, New York.

Chau, Y. K., R. Gachter, and S. C. Lum. 1974. Determination of the apparent complexing capacity of lake waters. J. Fish. Res. Bd. Can. 31:1515-1519.

Chiaudani, G., and M. Vighi. 1978. The use of Selenastrum capricornutum batch cultures in toxicity studies. Mitt. Int. Ver. Limnol. 21:316-239.

Christ, R. 1981. Nature of bonding between metallic ions and algal cell walls. Environ. Sci. Technol. 15:1212-1217.

Christman, R., and E. Gjessing. 1983. Aquatic and terrestrial humic materials. Ann Arbor Science, Ann Arbor, Michigan.

Cleave, M. L., V. D. Adams, and D. B. Porcella. 1979. Effects of oil shale leachate on phytoplankton productivity. Water Quality Series UWRL/Q-79/05. Utah Water Research Laboratory, Utah State University, Logan, Utah.

Cleave, M. L., D. B. Porcella, and V. D. Adams. 1980. Potential for changing phytoplankton growth in Lake Powell due to oil shale development. Environ. Sci. Technol. 14:683-690.

Davey, E. W., M. J. Morgan, and S. J. Erickson. 1973. A biological measurement of copper complexation capacity of seawater. Limnol. Oceanogr. 18:993-997.

Davies, A. 1976. An assessment of the basis for mercury tolerance in Dunaliella tertiolecta. J. Mar. Biol. Assoc. U. K. 56:39-57.

Dempsey, B., and C. O'Melia. 1983. Proton and calcium complexation of four fulvic acid fractions, p. 239-274. In R. Christman and E. Gjessing (Eds.).. Aquatic and terrestrial humic materials. Ann Arbor Science, Ann Arbor, Michigan.

Emery, T. 1982. Iron metabolism in humans and plants. American Scientist 70:626-632.

Ernst, R., H. E. Allen, and K. H. Mancy. 1975. Characterization of trace metal species and measurement of trace metal stability constants by electrochemical techniques. Water Res. 9:969-979.

Figura, P., and B. McDuffie. 1979. Use of Chelex resin for determination of labile trace metal fractions in aqueous ligand media and comparison of the method with anodic stripping voltammetry. Anal. Chem. 51:120-125.

Fish, R. 1980. Speciation of trace organic ligands and inorganic and organometallic compounds in oil shale process waters, p. 385-391. In J. Gary (Ed.). Thirteenth Oil Shale Symposium Proceedings. Colorado School of Mines, Golden, Colorado.

Fitzwater, S., G. Knauer, and J. Martin. 1982. Metal contamination and its effect on primary productivity measurements. Limnol. Oceanogr. 27:544-551.

Fox, R. 1977. Report of baseline water quality investigations of the White River in western Colorado. EPA-988/2-77-011. U. S. Environmental Protection Agency. Region VIII. Denver, Colorado.

Fruchter, J., and C. Wilkerson. 1981. Characterization of oil shale retort effluents, p. 31-63. In K. K. Petersen (Ed.). Oil shale: the environmental challenges. Colorado School of Mines Press, Golden, Colorado.

Gachter, R., J. S. Davis, and A. Mares. 1978. Regulation of copper availability to phytoplankton by macromolecules in lake water. Envir. Sci. Technol. 12:1416-1421.

Gamble, D. S., A. W. Underdown, and C. H. Langford. 1980. Copper(II) titration of fulvic acid ligand sites with theoretical, potentiometric, and spectrophotometric analysis. Anal. Chem. 52:1901-1908.

Giddings, J. 1981. Toxicity of shale oil to freshwater algae: comparisons with petroleum and coal-derived oils, p. 189-199. In W. Griest, M. Guerin, and D. Coffin

(Eds.). Health effects of oil shale development. Ann Arbor Science, Ann Arbor, Michigan.

Giddings, J., and J. Washington. 1981. Coal liquifaction products, shale oil, and petroleum. Acute toxicity to freshwater algae. Environ. Sci. Technol. 15:106-108.

Giesy, J. P. Jr., L. A. Briese, and G. J. Leversee. 1978. Metal binding capacity of selected Maine surface waters. Envir. Geol. 2:257-268.

Giesy, J. P., Jr., G. J. Leversee, and D. R. Williams. 1977. Effects of naturally occurring aquatic organic fractions on cadmium toxicity to Simocephalus serrulatus (Daphnidae) and Gambusia affinis (Poecilridae). Water Res. 11:1013-1020.

Griest, W. H., M. R. Guerin, and D. L. Cottin. 1981. Health effects investigation of oil shale development. Ann Arbor Science, Ann Arbor, Michigan.

Gulledge, W. P., and W. C. Webster. 1981. Analysis of leachates from selected fossil energy wastes for certain EPA criteria pollutants, p. 185-194. In L. P. Jackson and C. C. Wright (Eds.). Analysis of waters associated with alternative fuel production. ASTM STP 720. American Society for Testing and Materials, Philadelphia, Pennsylvania.

Harrison, W., R. Eppley, and E. Renger. 1977. Phytoplankton nitrogen metabolism, nitrigen budgets, and observations on copper toxicity: controlled ecosystem pollution experiment. Bull. Mar. Sci. 27:44-57.

Hertz, H., J. Brown, S. Chesler, F. Guenther, L. Hilpert, W. May, R. Parris, and S. Wise. 1980. Determination of individual organic compounds in shale oil. Anal. Chem. 52:1650-1657.

Hewlett, P. S., and R. L. Plackett. 1979. The interpretation of quantal responses in biology. University Park Press, Baltimore, Maryland.

Hinchee, R. 1983. Groundwater movement of mutagenic compounds in spent oil shale. PhD Dissertation, Utah State University, Logan, Utah.

Huntsman, S., and W. Sunda. 1980. The role of trace metals in regulating phytoplankton, p. 285-328. In I. Morris (Ed.). The physiological ecology of phytoplankton. University of California Press, Berkeley, California.

Ingle, S. E., J. A. Keniston, and D. W. Schults. 1980. REDEQL-EPAK, aqueous chemical equilibrium computer program. EPA-600/3-80-049. U.S. Environmental Protection Agency, Corvallis, Oregon.

Jackson, G. A., and J. J. Morgan. 1978. Trace metal-chelator interactions and phytoplankton growth in seawater media: theoretical analysis and comparison with reported observations. Limnol. Oceanogr. 23:268-282.

Klotz, I. M. 1982. Numbers of receptor sites from Scatchard graphs: facts and fantansies. Science 217:1247-1249.

Langford, C. H., D. S. Gamble, A. W. Underdown, and S. Lee. 1983. Interaction of metal ions with a well characterized fulric acid, p. 219-239. In R. F. Christman and E. T. Gjessing (Eds.). Aquatic and terrestrial humic materials. Ann Arbor Science Publishers, Inc., Ann Arbor, Michigan.

Leckie, J., and J. Davis III. 1979. Aqueous environmental chemistry

of copper, p. 89-122. In J. Nriagu (Ed.). Copper in the environment, Part I. Ecological cycling. Wiley, New York, New York.

Leenheer, J. A. 1981. Comprehensive approach to preparative isolation and fractionation of dissovled organic carbon from natural waters and wastewaters. Environ. Sci. Technol. 15:578-587.

Leenheer, J. A., T. I. Noyes, and H. A. Stuber. 1982. Determination of polar organic solutes in oil-shale retort water. Environ. Sci. Technol. 16:714-723.

Leischman, A., J. Green, and W. Miller. 1979. Bibliography of literature pertaining to the genus Selenastrum. EPA-600/9-79-021. U.S. Environmental Protection Agency, Corvallis, Oregon.

Lowenbach, W. 1978. Compilation and evaluation of leaching test methods. EPA-600/2-78-095. U. S. Environmental Protection Agency: Washington, D.C.

Maciorowski, A., J. Sims, L. Little, and E. Gerrard. 1981. Bioassays-procedures and results. Jour. Wat. Poll. Cont. Fed. 53:974-993.

Maciorowski, A., L. Little, R. Sims, and J. Sims. 1982. Bioassays-procedures and results. Jour. Wat. Poll. Cont. Fed. 54:830-849.

Mantoura, R. F. C., A. Dickson, and J. P. Riley. 1978. The complexation of metals with humic materials in natural waters. Estuar. Coast. Mar. Sci. 6:387-408.

Mantoura, R. F. C., and J. P. Riley. 1975. The use of gel filtration in the study of metal binding by humic acids and related compounds. Analytica Chim. Acta 78:193-200.

Mayer, S., and S. Gloss. 1980. Buffering of silica and phosphate in a turbid river. Limnol. Oceanogr. 25:12-22.

McCrady, J. K., and G. A. Chapman. 1979. Determination of copper complexing capacity of natural river water, well water and artificially reconstituted water. Water Res. 13:143-150.

McKnight, D. M. 1981. Chemical and biological processes controlling the response of a freshwater ecosystem to copper stress: a field study of the $CuSO_4$ treatment of Mill Pond Reservoir, Burlington, Massachusetts. Limnol. Oceanogr. 26:518-531.

McKnight, D. M., and F. M. M. Morel. 1978. Release of weak and strong copper-complexing agents by algae. Limnol. Oceanogr. 24:823-836.

McKnight, D. M., and F. M. M. Morel. 1980. Copper complexation by siderochromes from filamentous blue-green algae. Limnol. Oceanogr. 26:62-71.

Messer, J. J. 1983. Geochemically alkaline snowpack in the mountains of northern Utah. Atmos. Environ. (in press).

Messer, J. J., J. M. Ihnat, B. Mok, and D. Wegner. 1983. Reconnaissance of sediment-phosphorus relationships in Upper Flaming Gorge reservoir. Water Quality Series, UWRL/Q-83/02, Utah Water Research Laboratory, Utah State University, Logan, Utah.

Messer, J., and C. Liff. 1982. Oil shale. In J. Messer and F. Post (eds.). Impacts of western coal, oil shale, and tar sands development on aquatic environmental quality: a technical information matrix. Vol. 3. UWRL/P-82-04.

Utah Water Research Laboratory, Logan, Utah.

Miller, W., J. Green, and T. Shiroyama. 1978. The Selenastrum capricornutum Printz algal assay bottle test. EPA-600/9-78-018. U. S. Environmental Protection Agency, Corvallis, Oregon.

Morel, F., J. Reuter, D. Anderson, and R. Guillard. 1979. Aquil: a chemically defined phytoplankton culture medium for trace metal studies. J. Phycol. 15:135-141.

Neubecker, T. A., and H. E. Allen. 1983. The measurement of complexation capacity and conditional stability constants for ligands in natural waters. Water Res. 17:1-14.

Orion Research, Inc. 1977. Instruction manual for cupric ion electrode. Cambridge, Massachusetts.

Payne, A., and R. Hall. 1978. Application of algal assays in the evaluation of new detergent materials. Mitt. Int. Ver. Limnol. 21:507-520.

Perdue, E., and C. Lytle. 1983. A critical examination of metal-ligand complexation models: application to defined multiligand mixtures. p. 295-314. In R. Christman and E. Gjessing [eds.]. Aquatic and terrestrial humic materials. Ann Arbor Science, Ann Arbor, Michigan.

Petersen, R. 1982. Influence of copper and zinc on the growth of freshwater alga, Scenedesmus quadricaudata: the significance of chemical speciation. Environ. Sci. Technol. 16:443-447.

Pickering, W. 1979. Copper retention by soil/sediment components, p. 217-254. In J. Nriagu (Ed.). Copper in the environment. Part I. Ecological Cycling. Wiley, New York, New York.

Ramamoorthy, S., and D. J. Kushner. 1975. Heavy metal binding components of river water. J. Fish. Res. Bd. Can. 32:1755-1776.

Raspor, B. 1980. Distribution and speciation of cadmium in natural waters, p. 147-237. In J. O. Nriagu (Ed.). Cadmium in the environment. Part 1: Ecological cycling. Wiley and Sons, New York, New York.

Redente, E., W. Ruzzo, C. Cook, and W. Berg. 1981. Retorted oil shale characteristics and reclamation, p. 169-200. In K. Petersen (Ed.). Oil shale: the environmental challenges. Colorado School of Mines Press, Golden, Colorado.

Riley, R., K. Shiosaki, R. Bean, and D. Schoengold. 1979. Solvent solubilization, characterization, and quantitation of aliphatic carboxylic acids in oil shale retort water following chemical derivatization with boron trifluoride in methanol. Anal. Chem. 51:1995-1998.

Rosell, R. A., A. M. Miglierina, and L. Q. De Novilla. 1977. Stability constants of some complexes of Argentine humic acids and micronutrients, p. 15-21. In Soil organic matter studies. International Atomic Energy Agency, Vienna, Austria.

Rosotti, F. J. C., and H. Rosotti. 1961. The determination of stability constants. McGraw-Hill, New York, New York.

Rushforth, S., J. Brtherson, N. Fungladda, and W. Evenson. 1981. The effects of heavy metals on attached diatoms in the Uintah Basin of Utah. Hydrobiologia 83:313-323.

Ruzic, I. 1980. Personal communication to Thomas A. Neubecker, Human and Environmental Safety Department, The Procter & Gamble Company, Ivorydale Technical Center, Cincinnati, Ohio.

Saar, R., and J. Weber. 1982. Fulvic acid: modifier of metal-ion chemistry. Environ. Sci. Technol. 16:510A-516A.

Sakshaug, E. 1980. Problems in methodology of studying phytoplankton, p. 57-94. In I. Morris (Ed.). The physiological ecology of phytoplankton. University of California Press, Berkeley, California.

Scatchard, G. 1949. The attractions of proteins for small molecules and ions. Anal. N. Y. Acad. Sci. 51:660:672.

Scheinberg, I. H., R. A. Weisiger, J. L. Gollan, and R. K. Ockner. 1982. Scatchard plots. Science 215:312-313.

Schwarzenbach, G. 1957. Complexometric titrations. Pitman Press, London, England.

Selby, D. A., J. M. Ihnat, D. Hancey, F. J. Post, and J. J. Messer. 1983. Effects of cadmium on streams and irrigated agriculture in the presence and absence of raw oil shale leachate. Utah Water Research Laboratory, Utah State University, Logan, Utah. (in preparation).

Shuman, M. S. 1969. Nonunity electrode reaction orders and stationary electrode polarography. Anal. Chem. 41:142-146.

Shuman, M. S., and J. L. Cromer. 1979. Copper association with aquatic fulvic and humic acids. Estimation of conditional formation constants with a titrimetric anodic stripping voltammetry procedure. Envir. Sci. Technol. 13:543-545.

Shuman, M. S., and G. P. Woodward. 1973. Chemical constants of metal complexes from a complexometric titration followed with anodic stripping voltammetry. Anal. Chem. 45:2032-2035.

Shuman, M. S., and G. P. Woodward. 1977. Stability constants of copper-organic chelates in aquatic samples. Envir. Sci. Technol. 11:809-813.

Sillen, L. G., and A. E. Martell. 1964. Stability constants of metal-ion complexes. Spec. Publs. Chem. Soc. 17:754.

Skulberg, O. [Ed.]. 1978. Symposium: Experimental use of algal cultures in limnology. Mitt. Int. Ver. Limnol. 21:1-607.

Slawson, G. 1979. Groundwater quality monitoring of western oil shale development: identification and priority ranking of potential pollution sources. EPA-600/7-79-023. U.S. Environmental Protection Agency, Las Vegas, Nevada.

Smith, R. G. 1976. Evaluation of combined applications of ultrafiltration and complexation capacity techniques to natural waters. Anal. Chem. 48:74-76.

Stanley, J., M. Conditt, and R. E. Sievers. 1982. Trace elements and organic ligands in oil shale waste. Progress Report: 1980-1981. Department of Chemistry, University of Colorado, Boulder, Colorado.

Steeman-Nielsen, E., and H. Bruun-Laursen. 1976. Effects of $CuSO_4$ on photosynthetic rate of phytoplankton in four Danish lakes. Oikos 27:239-242.

Stevenson, F. J. 1977. Nature of divalent transit on metal complexes of humic acids as revealed by a

modified potentiometric titration method. Soil Sci. 123:10-17.

Stevenson, F. J. 1982. Humus chemistry: genesis, composition, reactions. John Wiley & Sons, New York, New York.

Stumm, W., and J. J. Morgan. 1982. Aquatic chemistry. Second Edition. John Wiley & Sons, New York, New York.

Sunda, W. G., and R. R. Guillard. 1976. The relationship between cupric ion activity and the toxicity of copper to phytoplankton. J. Mar. Res. 34:511-529.

Sunda, W. G., and J. M. Lewis. 1978. Effect of complexation by natural organic ligands on the toxicity of copper to a unicellular alga, Monochrysis lutheri. Limnol. Oceanogr. 23:870-876.

Takamatsu, T., and T. Yoshida. 1978. Determination of stability constants of humic acid metal complexes. Agrochimica 21:134-139.

Thomas, W. H., and D. L. R. Seibert. 1977. Effects of copper on the dominance and the diversity of algae: controlled ecosystem pollution experiment. Bull. Mar. Sci. 27:23-33.

Tuschall, J. R. Jr., and P. L. Brezonik. 1980. Characterization of organic nitrogen in natural waters: Its molecular size, protein content, and interactions with heavy metals. Limnol. Oceanogr. 25:495-504.

Tuschall, J. R. Jr., and P. L. Brezonik. 1981. Evaluation of the copper anodic stripping voltammetry complexometric titration for complexing capacities and conditional stability constants. Anal. Chem. 53:1986-1989.

Tuschall, J. R. Jr., and P. L. Brezonik. 1983a. Application of a continuous-flow ultrafiltration procedure and competing ligand differential spectroscopy to measurement of heavy metal complexation by natural water organic matter. Anal. Chim. Acta (in press).

Tuschall, J. R. Jr., and P. L. Brezonik. 1983b. Complexation of heavy metals by aquatic humus: a comparative study of five analytical methods. p. 275-294. In R. Christman and E. Gjessing (eds.). Aquatic and terrestrial humic materials. Ann Arbor Science, Ann Arbor, Michigan.

Tuschall, J. R. Jr., and P. L. Brezonik. 1983c. Hazards in treating binding data with graphical methods. Science (in press).

Vuceta, J., and J. J. Morgan. 1978. Chemical modeling of trace metals in fresh waters: role of complexation and adsorption. Environ. Sci. Technol. 12:1303-1309.

Wagemann, R. 1980. Cupric ion-selective electrode and inorganic cationic complexes of copper. J. Phys. Chem. 84:3433-3436.

Weber, J. 1983. Metal ion speciation studies in the presence of humic materials, p. 315-332. In R. Christman and E. Gjessing (Eds.). Aquatic and terrestrial humic materials. Ann Arbor Science, Ann Arbor, Michigan.

APPENDICES

Appendix A

Extraction and Chemistry of Shale Leachates

Table A.1. Summary of the characterizations for the raw oil shale leachates (RSL).

Shale:Dl-H_2O Ratio	Raw Shale Leachates				
	1:4 (Dark)	1:4 (Dark)	1:1 (Shaked)	2:1 (Shaked)	2:1 (Dark)
Na (mg/L)	40.9	42.8	-	-	-
K (mg/L)	4.68	5.21	-	-	-
Ca (mg/L)	45.6	47.2	156.8	200.6	626.4
Si (mg/L)	-	-	9.3	11.7	13.7
Ca Hardness (mg/L $CaCO_3$)	114	118	391.2	500.5	1562.8
Mg Hardness (mg/L $CaCO_3$)	49	49	232.68	490.58	577.93
Total Hardness (mg/L $CaCO_3$)	163	167	623.88	991.08	2140.73
O-PO_4 (µg/L)	8.0	9.4	182.2	9.5	2.5
T-P (µg/L)	19.12	23.32	554.02	17.62	3.24
Cl^- (mg/L)	2.11	2.88	21.22	21.69	23.20
$SO_4^=$ (mg/L)	76.24	93.60	-	-	-
NH_3-N (mg/L)	1.82	2.21	2.41	3.09	11.41
NO_2-N (mg/L)	2.0	2.4	0.5	0.7	0.08
NO_3-N (mg/L)	1.1	2.35	9.5	16.3	42.2
TN (mg/L)	5.08	7.06	15.2	28.71	66.33
EC (µmho/cm^{25})	320	310	1271	1785	2809
pH	8.17	8.02	8.02	8.12	7.74
Alkalinity (mg/L $CaCO_3$)	71	68	-	-	-
DOC	8.6	11.8	17.5	61.8	17.0

Table A. 2. Summary of the characterization for the leaching of raw oil shale and the spent oil shale.

Parameters	RSL		SSL
	Stock	<UM2	
I. Metals			
Arsenic (µg/L)	+8	16	2
Barium (µg/L)	71	83	34
Boron (µg/L)	274	304	575
Chromium (µg/L)	<13	<13	<13
Cobalt (µg/L)	<11	<11	<11
Iron, Total (µg/L)	<9	<9	<9
Manganese (µg/L)	58	53	<16
Molybdenium (µg/L)	360	290	900
Nickel (µg/L)	<11	<11	15
Selenium (µg/L)	2	3	3
Vanadium (µg/L)	<9	<9	<9
Calcium (mg/L)	114	120	730
Potassium (mg/L)	4.7	1	22
Sodium (mg/L)	40.9	28	102
II. Nonmetals			
Alkalinity, Total as $CaCO_3$ (mg/L)	71	145	419
Ammonia, NH_3-N (mg/L)	1.82	0.59	0.85
Chloride (mg/L)	2.1	1.0	72.0
Fluoride (mg/L)	14.9	14.8	20.2
Nitrate (mg/L)	1.1		
Orthophosphorus (µg/L)	8.0	<10	<10
pH	8.2	8.4	12.1
Silica (mg/L)		7.6	3.6
Sulfate, SO_4 (mg/L)	76.2	63.2	560
Nitrite (mg/L)	2.0	0.28	
TOC	8.6		

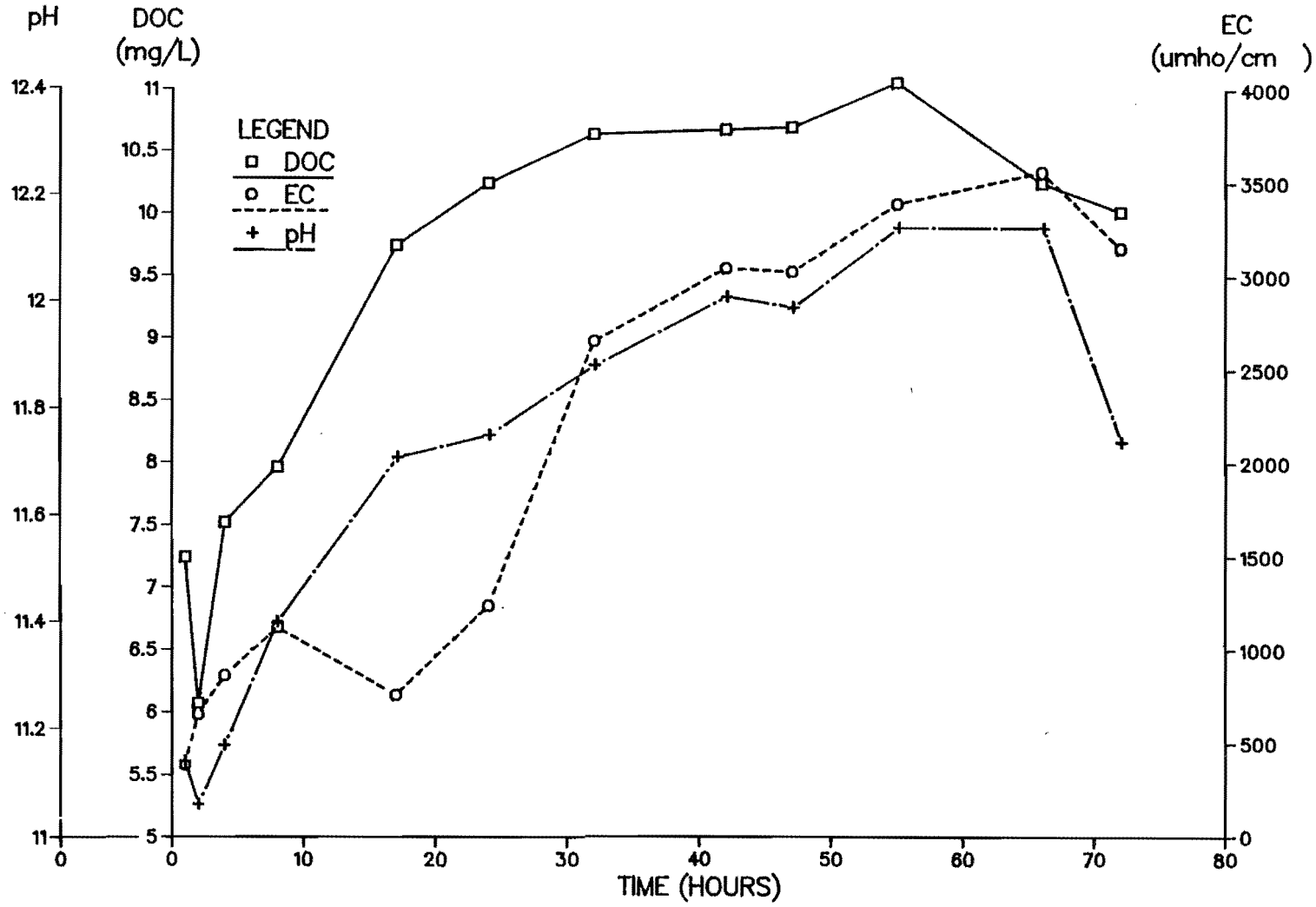

Figure A.1. Monitoring parameters used during an initial 48 hour static batch extraction of retorted (spent) oil shale leachate with shale to water ratio of 1:4.

Appendix B

Ultrafiltration

Table B.1. Flow characteristics of each type and size of the Amicon Diaflo ® ultrafiltration membrane with pressure using deionized water.

Applied Pressure (psig N_2)	Amicon Diaflo Ultrafiltration Membrane						
	UM2	UM10	YM5	YM10	YM30	PM10	XM300
5					2.00		
10	0.12[a]	0.21	0.23	0.32	4.20	4.0	4.17
20	0.22	0.44	0.48	0.68	8.2	8.3	7.60
30	0.34	0.69	0.72	1.02	11.8	12.7	10.8
40	0.43	0.90	0.94	1.39	15.2	16.9	17.6
50	0.59	1.15	1.17	1.72	17.9		
60	0.68	1.39	1.40	2.07			
70	0.77	1.61	1.61				

[a]Flowrate in mL/min.

Appendix C

Ion-selective Electrode

Table C.1. Slopes obtained from Cu-ISE calibration curves during binding studies.

pCu Range Used	Slope (mV/Log Cu)
Theoretical Nernst Response	29.5
3.00-4.00	29.8
3.00-7.00	29.6
3.00-6.00	29.3
3.00-5.00	29.8
3.00-6.00	29.2
3.00-4.00	29.5
4.00-5.00	30.7
4.10-6.00	29.7
4.16-6.00	29.6
4.18-5.82	29.9
4.22-5.70	29.9
5.00-6.00	29.9
5.00-6.00	29.55
5.00-6.00	30.8
5.00-6.00	30.2
5.00-6.00	30.6
5.00-6.00	16.7[a]
5.00-6.00	30.2[b]
5.00-6.00	30.7
6.00-7.00	26.9[c]
6.00-7.00	26.5[c]
6.00-7.00	26.2[c]
5.96-8.00	26.3[c]
6.89-8.00	26.0[c]
6.16-8.00	23.4[c]

[a]Slope after a binding titration of 10 mg/L HA.

[b]Slope before the binding titration.

[c]Cu-ISE nonlinear response below pCu 6.70.

Table C.2. Summary of results obtained from Cu-ISE complexometric titration of EDTA with copper.

pCu_T	Cu-ISE POTENTIAL (mV)	pCu_F'	pCu_F	pCu_B	$\frac{Cu_F}{Cu_B}$	$\bar{\nu}$	$\frac{\bar{\nu}}{Cu_F}$
6.303	11.9	9.663	9.727	6.303	0.377E-2	0.054	0.289E+0
6.004	13.3	9.616	9.679	6.004	0.211E-2	0.108	0.516E+0
5.830	14.2	9.585	9.649	5.830	0.152E-2	0.161	0.718E+0
5.708	15.3	9.548	9.612	5.708	0.125E-2	0.214	0.874E+0
5.613	16.2	9.518	9.581	5.613	0.108E-2	0.266	0.101E+1
5.536	17.1	9.487	9.551	5.536	0.966E-3	0.317	0.113E+1
5.471	17.3	9.481	9.544	5.471	0.845E-3	0.369	0.129E+1
5.413	18.1	9.454	9.517	5.413	0.787E-3	0.421	0.138E+1
5.366	19.2	9.416	9.480	5.366	0.770E-3	0.470	0.142E+1
5.322	20.4	9.376	9.439	5.322	0.764E-3	0.519	0.143E+1
5.283	21.4	9.342	9.405	5.283	0.755E-3	0.568	0.145E+1
5.247	22.7	9.298	9.361	5.247	0.769E-3	0.617	0.142E+1
5.214	24.0	9.254	9.317	5.214	0.789E-3	0.665	0.138E+1
5.184	25.5	9.203	9.266	5.184	0.828E-3	0.713	0.132E+1
5.156	27.2	9.146	9.209	5.156	0.886E-3	0.761	0.123E+1
5.130	29.2	9.078	9.141	5.130	0.975E-3	0.808	0.112E+1
5.106	31.5	9.000	9.063	5.106	0.110E-2	0.854	0.988E+0
5.094	33.4	8.936	8.999	5.094	0.125E-2	0.877	0.875E+0
5.083	35.8	8.855	8.918	5.083	0.146E-2	0.900	0.745E+0
5.072	38.9	8.750	8.813	5.072	0.182E-2	0.923	0.600E+0
5.062	48.9	8.411	8.475	5.062	0.387E-2	0.946	0.282E+0
5.051	88.0	7.088	7.152	5.055	0.800E-1	0.961	0.136E-1
5.041	103.9	6.550	6.613	5.053	0.275E+0	0.965	0.396E-2
5.032	110.7	6.320	6.383	5.051	0.466E+0	0.969	0.234E-2
5.022	115.2	6.168	6.231	5.050	0.659E+0	0.972	0.165E-2
5.013	118.6	6.053	6.116	5.049	0.856E+0	0.975	0.127E-2
5.004	121.3	5.961	6.025	5.047	0.105E+1	0.978	0.103E-2
4.987	125.6	5.816	5.879	5.046	0.147E+1	0.980	0.742E-3
4.970	128.8	5.708	5.771	5.045	0.188E+1	0.983	0.580E-3
4.954	131.3	5.623	5.686	5.043	0.228E+1	0.987	0.479E-3
4.939	133.5	5.548	5.612	5.043	0.270E+1	0.988	0.404E-3
4.925	135.3	5.488	5.551	5.042	0.310E+1	0.990	0.352E-3
4.911	136.9	5.433	5.497	5.041	0.350E+1	0.992	0.311E-3
4.885	139.6	5.342	5.405	5.040	0.432E+1	0.993	0.253E-3
4.860	141.7	5.271	5.334	5.038	0.505E+1	0.999	0.216E-3
4.838	143.6	5.207	5.270	5.038	0.586E+1	0.999	0.186E-3
4.817	145.2	5.153	5.216	5.038	0.663E+1	1.000	0.164E-3
4.778	147.9	5.061	5.125	5.038	0.820E+1	0.999	0.133E-3

where pCu_F' represented the free cupric ion concentration based on the uncorrected Cu-ISE calibration curve.

Table C.3. Summary of results obtained from Cu-ISE complexometric titration of 5 mg/L humic acid with copper.

pCu_T	Cu-ISE POTENTIAL (mV)	pCu_F'	pCu_F	pCu_B	$\frac{Cu_F}{Cu_B}$	$\bar{\nu}$	$\frac{\bar{\nu}}{Cu_F}$
6.000	55.8	8.248	7.968	6.005	0.109E+0	0.155	0.144E+1
5.603	88.5	7.166	6.885	5.626	0.551E+0	0.372	0.285E+0
5.303	116.3	6.245	5.965	5.410	0.279E+1	0.612	0.565E-1
5.128	129.1	5.821	5.541	5.340	0.630E+1	0.718	0.250E-1
5.004	136.1	5.590	5.309	5.301	0.982E+1	0.786	0.160E-1
4.908	140.9	5.431	5.150	5.278	0.134E+2	0.829	0.117E-1
4.830	144.5	5.312	5.031	5.262	0.170E+2	0.861	0.925E-2
4.764	147.5	5.212	4.932	5.259	0.213E+2	0.865	0.740E-2
4.708	149.7	5.139	4.859	5.238	0.240E+2	0.908	0.657E-2
4.657	151.7	5.073	4.793	5.230	0.273E+2	0.927	0.575E-2
4.613	153.4	5.017	4.737	5.218	0.303E+2	0.951	0.519E-2
4.536	156.4	4.918	4.637	5.217	0.380E+2	0.955	0.414E-2
4.471	158.8	4.838	4.558	5.212	0.451E+2	0.965	0.348E-2
4.415	160.8	4.772	4.492	5.206	0.518E+2	0.978	0.303E-2
4.366	162.5	4.716	4.435	5.197	0.577E+2	1.000	0.273E-2
4.322	164.1	4.663	4.382	5.211	0.674E+2	0.968	0.233E-2
4.247	166.7	4.577	4.296	5.218	0.836E+2	0.951	0.188E-2
4.184	168.8	4.507	4.227	5.216	0.975E+2	0.957	0.161E-2
4.130	170.6	4.447	4.167	5.221	0.113E+3	0.946	0.139E-2
4.083	172.1	4.398	4.117	5.203	0.122E+3	0.985	0.129E-2
4.041	173.5	4.351	4.071	5.221	0.141E+3	0.945	0.111E-2

where pCu_F' represented the free cupric ion concentration based on the uncorrected Cu-ISE calibration curve.

Table C.4. Summary of results obtained from Cu-ISE complexometric titration of 10 mg/L humic acid with copper.

pCu_T	Cu-ISE POTENTIAL (mV)	pCu_F'	pCu_F	pCu_B	$\frac{Cu_F}{Cu_B}$	$\bar{\nu}$	$\frac{\bar{\nu}}{Cu_F}$
6.301	13.2	9.659	9.386	6.302	0.823E-2	0.038	0.929E+1
6.000	32.7	9.013	8.741	6.001	0.182E-1	0.076	0.419E+1
5.603	58.2	8.169	7.896	5.605	0.512E-1	0.190	0.149E+1
5.303	87.8	7.189	6.916	5.314	0.250E+0	0.371	0.306E+0
5.128	107.5	6.537	6.264	5.161	0.789E+0	0.527	0.968E-1
5.004	120.0	6.123	5.850	5.071	0.166E+1	0.649	0.459E-1
4.908	129.5	5.808	5.535	5.025	0.309E+1	0.721	0.247E-1
4.830	135.5	5.610	5.337	4.993	0.453E+1	0.778	0.169E-1
4.764	140.0	5.461	5.188	4.970	0.606E+1	0.819	0.126E-1
4.708	143.6	5.341	5.069	4.956	0.771E+1	0.846	0.991E-2
4.657	146.6	5.242	4.969	4.948	0.952E+1	0.862	0.803E-2
4.613	148.7	5.173	4.900	4.928	0.107E+2	0.902	0.716E-2
4.536	152.6	5.043	4.771	4.915	0.139E+2	0.930	0.549E-2
4.471	155.7	4.941	4.668	4.909	0.174E+2	0.943	0.439E-2
4.415	158.1	4.861	4.589	4.897	0.204E+2	0.969	0.375E-2
4.366	160.2	4.792	4.519	4.893	0.237E+2	0.978	0.323E-2
4.322	162.1	4.729	4.456	4.899	0.277E+2	0.966	0.276E-2
4.283	163.6	4.679	4.406	4.889	0.304E+2	0.987	0.252E-2
4.247	165.0	4.633	4.360	4.887	0.337E+2	0.991	0.227E-2
4.184	167.4	4.553	4.281	4.886	0.403E+2	0.995	0.190E-2
4.130	169.4	4.487	4.214	4.885	0.468E+2	0.996	0.163E-2
4.083	171.1	4.431	4.158	4.883	0.531E+2	1.000	0.144E-2
4.041	172.6	4.381	4.108	4.886	0.599E+2	0.994	0.128E-2

where pCu_F' represents the free cupric ion concentration based on the uncorrected Cu-ISE calibration curve.

Table C.5. Summary of results obtained from Cu-ISE complexometric titration of the raw shale leachate extracted by batch, static 48 hours, with a shale to water ratio of 1:4 with copper.

pCu_T	Cu-ISE POTENTIAL (mV)	pCu_F'	pCu_F	pCu_B	$\frac{Cu_F}{Cu_B}$	$\bar{\nu}$	$\frac{\bar{\nu}}{Cu_F}$
5.000	53.9	8.311	7.860	5.001	0.138E-1	0.022	0.156E+1
4.700	65.3	7.934	7.482	4.701	0.165E-1	0.043	0.131E+1
4.524	72.5	7.696	7.244	4.525	0.191E-1	0.065	0.113E+1
4.400	78.4	7.500	7.049	4.401	0.225E-1	0.086	0.963E+0
4.303	81.8	7.388	6.936	4.304	0.233E-1	0.108	0.928E+0
4.224	85.8	7.255	6.804	4.226	0.264E-1	0.129	0.820E+0
4.158	90.6	7.096	6.645	4.159	0.327E-1	0.150	0.662E+0
4.100	96.0	6.917	6.466	4.102	0.433E-1	0.171	0.500E+0
4.050	101.0	6.752	6.300	4.052	0.564E-1	0.192	0.384E+0
4.004	106.0	6.586	6.135	4.008	0.746E-1	0.213	0.290E+0
3.963	111.2	6.414	5.963	3.968	0.101E+0	0.233	0.214E+0
3.926	116.8	6.229	5.777	3.932	0.143E+0	0.253	0.152E+0
3.892	121.4	6.076	5.625	3.900	0.188E+0	0.273	0.115E+0
3.860	124.8	5.964	5.512	3.870	0.228E+0	0.292	0.951E-1
3.830	129.0	5.825	5.373	3.843	0.295E+0	0.311	0.734E-1
3.803	131.4	5.745	5.294	3.817	0.334E+0	0.330	0.649E-1
3.777	133.7	5.669	5.218	3.793	0.376E+0	0.349	0.576E-1
3.752	136.0	5.593	5.142	3.771	0.426E+0	0.367	0.509E-1
3.729	138.0	5.527	5.075	3.749	0.472E+0	0.386	0.459E-1
3.708	140.7	5.437	4.986	3.731	0.556E+0	0.402	0.389E-1
3.687	141.6	5.408	4.956	3.711	0.568E+0	0.421	0.381E-1
3.667	143.3	5.351	4.900	3.693	0.621E+0	0.439	0.349E-1
3.648	144.8	5.302	4.850	3.676	0.670E+0	0.456	0.323E-1
3.630	146.5	5.245	4.794	3.661	0.736E+0	0.473	0.294E-1
3.613	147.4	5.216	4.764	3.645	0.759E+0	0.491	0.285E-1
3.596	148.6	5.176	4.724	3.630	0.804E+0	0.508	0.269E-1
3.580	149.9	5.133	4.681	3.616	0.860E+0	0.524	0.252E-1
3.565	151.1	5.093	4.642	3.603	0.915E+0	0.540	0.237E-1
3.536	153.6	5.010	4.559	3.579	0.105E+1	0.571	0.207E-1
3.509	155.7	4.941	4.489	3.556	0.117E+1	0.601	0.185E-1
3.483	157.8	4.871	4.420	3.536	0.131E+1	0.630	0.166E-1
3.459	159.4	4.818	4.367	3.516	0.141E+1	0.659	0.153E-1
3.436	160.9	4.769	4.317	3.498	0.152E+1	0.688	0.143E-1
3.415	162.4	4.719	4.267	3.481	0.163E+1	0.716	0.132E-1
3.395	163.3	4.689	4.238	3.462	0.168E+1	0.748	0.129E-1
3.375	164.2	4.659	4.208	3.444	0.172E+1	0.779	0.126E-1
3.357	166.4	4.586	4.135	3.436	0.200E+1	0.794	0.108E-1
3.339	167.5	4.550	4.099	3.422	0.211E+1	0.819	0.103E-1
3.322	168.8	4.507	4.056	3.411	0.227E+1	0.841	0.955E-2
3.306	170.0	4.467	4.016	3.400	0.242E+1	0.862	0.893E-2
3.290	171.6	4.414	3.963	3.394	0.270E+1	0.874	0.802E-2

Table C.5. Continued

3.275	172.6	4.381	3.930	3.384	0.285E+1	0.894	0.760E-2
3.261	173.5	4.351	3.900	3.374	0.298E+1	0.914	0.726E-2
3.247	174.6	4.315	3.864	3.367	0.319E+1	0.929	0.679E-2
3.234	175.4	4.289	3.837	3.358	0.332E+1	0.949	0.652E-2
3.221	176.5	4.252	3.801	3.353	0.357E+1	0.960	0.606E-2
3.208	177.6	4.216	3.764	3.350	0.385E+1	0.968	0.562E-2
3.196	178.6	4.183	3.731	3.346	0.412E+1	0.976	0.526E-2
3.184	179.3	4.159	3.708	3.339	0.428E+1	0.992	0.507E-2
3.173	180.2	4.130	3.678	3.336	0.454E+1	1.000	0.477E-2
3.162	181.4	4.090	3.638	3.338	0.501E+1	0.994	0.432E-2
3.151	182.3	4.060	3.609	3.337	0.535E+1	0.996	0.404E-2
3.141	183.3	4.027	3.575	3.339	0.581E+1	0.991	0.373E-2
3.130	184.0	4.004	3.552	3.337	0.609E+1	0.997	0.356E-2

where pCu_F' represents the free cupric ion concentration based on the uncorrected Cu-ISE calibration curve.

Table C.6. Summary of results obtained from Cu-ISE complexometric titration 50 percent UF diafiltered raw shale leachate in MAAP medium with copper.

pCu_T	Cu-ISE POTENTIAL (mV)	pCu_F'	pCu_F	pCu_B	$\frac{Cu_F}{Cu_B}$	$\bar{\nu}$	$\frac{\bar{\nu}}{Cu_F}$
7.000	68.4	7.318	7.199	7.435	0.172E+2	0.005	0.864E+0
6.700	74.0	7.132	7.014	6.988	0.943E+1	0.015	0.158E+1
6.524	78.6	6.980	6.861	6.792	0.853E+1	0.024	0.174E+1
6.400	82.0	6.867	6.748	6.658	0.812E+1	0.033	0.183E+1
6.303	84.2	6.794	6.675	6.543	0.738E+1	0.043	0.202E+1
6.224	86.3	6.724	6.606	6.458	0.711E+1	0.052	0.209E+1
6.158	88.3	6.658	6.539	6.391	0.711E+1	0.060	0.209E+1
6.100	89.9	6.605	6.486	6.331	0.699E+1	0.069	0.213E+1
6.050	91.2	6.562	6.443	6.274	0.678E+1	0.079	0.219E+1
6.004	92.3	6.525	6.407	6.223	0.656E+1	0.089	0.227E+1
5.926	95.1	6.433	6.314	6.155	0.693E+1	0.104	0.214E+1
5.860	97.6	6.350	6.231	6.101	0.741E+1	0.118	0.201E+1
5.803	99.3	6.293	6.174	6.043	0.739E+1	0.135	0.201E+1
5.753	101.1	6.234	6.115	6.000	0.768E+1	0.149	0.194E+1
5.708	102.6	6.184	6.065	5.959	0.783E+1	0.163	0.190E+1
5.648	104.9	6.107	5.989	5.913	0.840E+1	0.182	0.177E+1
5.596	106.7	6.048	5.929	5.868	0.868E+1	0.202	0.171E+1
5.536	109.1	5.968	5.849	5.824	0.944E+1	0.223	0.157E+1
5.471	111.2	5.898	5.780	5.764	0.965E+1	0.256	0.154E+1

Table C.6. Continued.

5.415	113.4	5.826	5.707	5.726	0.104E+2	0.280	0.142E+1
5.366	115.2	5.766	5.647	5.688	0.110E+2	0.305	0.135E+1
5.322	116.7	5.716	5.597	5.651	0.113E+2	0.332	0.131E+1
5.283	118.1	5.670	5.551	5.620	0.117E+2	0.357	0.127E+1
5.247	119.3	5.630	5.511	5.589	0.120E+2	0.383	0.124E+1
5.214	120.4	5.593	5.475	5.561	0.122E+2	0.409	0.122E+1
5.184	121.4	5.560	5.441	5.534	0.124E+2	0.435	0.120E+1
5.126	123.5	5.491	5.372	5.491	0.132E+2	0.480	0.113E+1
5.075	125.4	5.427	5.309	5.456	0.141E+2	0.520	0.106E+1
5.030	126.9	5.378	5.259	5.417	0.144E+2	0.569	0.103E+1
4.951	129.7	5.285	5.166	5.360	0.156E+2	0.650	0.952E+0
4.855	133.2	5.169	5.050	5.297	0.176E+2	0.751	0.842E+0
4.754	136.9	5.046	4.927	5.236	0.204E+2	0.864	0.730E+0
4.654	140.9	4.913	4.795	5.212	0.262E+2	0.912	0.568E+0
4.574	143.9	4.814	4.695	5.187	0.310E+2	0.967	0.479E+0
4.506	146.4	4.731	4.612	5.172	0.363E+2	1.000	0.409E+0
4.398	150.5	4.595	4.476	5.181	0.507E+2	0.979	0.293E+0

where pCu_F' represented the free cupric ion concentration based on the uncorrected Cu-ISE calibration curve.

Table C.7. Summary of results obtained from Cu-ISE complexometric titration of the first pore volume of raw shale leachate obtained from the upflow column (RSL_1) with copper.

pCu_T	Cu-ISE POTENTIAL (mV)	pCu_F'	pCu_F	pCu_B	$\frac{Cu_F}{Cu_B}$	$\bar{\nu}$	$\frac{\bar{\nu}}{Cu_F}$
5.303	134.7	5.636	5.511	5.724	0.163E+2	0.581	0.188E+1
5.004	146.0	5.262	5.137	5.585	0.281E+2	0.800	0.110E+1
4.830	152.4	5.050	4.925	5.540	0.412E+2	0.887	0.746E+0
4.708	156.7	4.908	4.782	5.509	0.532E+2	0.954	0.578E+0
4.613	160.1	4.795	4.670	5.523	0.714E+2	0.922	0.431E+0
4.536	162.7	4.709	4.584	5.517	0.857E+2	0.936	0.359E+0
4.471	164.8	4.639	4.514	5.494	0.955E+2	0.986	0.322E+0
4.415	166.7	4.577	4.451	5.512	0.115E+3	0.947	0.268E+0
4.322	169.7	4.477	4.352	5.502	0.141E+3	0.967	0.218E+0
4.247	172.1	4.398	4.272	5.495	0.167E+3	0.984	0.184E+0
4.184	174.1	4.332	4.206	5.492	0.193E+3	0.990	0.159E+0
4.130	175.9	4.272	4.147	5.565	0.262E+3	0.838	0.117E+0
4.083	177.3	4.226	4.100	5.497	0.250E+3	0.979	0.123E+0
4.041	178.6	4.183	4.057	5.488	0.270E+3	1.000	0.114E+0

where pCu_F' represented the free cupric ion concentration based on the uncorrected Cu-ISE calibration curve.

Table C.8. Summary of results obtained from Cu-ISE complexometric titration of the third pore volume of raw shale leachate obtained from the upflow column (RSL_3) with copper.

pCu_T	Cu-ISE POTENTIAL (mV)	pCu_F'	pCu_F	pCu_B	$\frac{Cu_F}{Cu_B}$	$\bar{\nu}$	$\frac{\bar{\nu}}{Cu_F}$
6.000	138.3	6.480	6.419	6.209	0.617E+1	0.109	0.287E+1
5.700	151.9	6.036	5.974	6.029	0.113E+2	0.166	0.156E+1
5.524	159.9	5.774	5.713	5.977	0.184E+2	0.187	0.965E+0
5.400	164.7	5.618	5.556	5.919	0.231E+2	0.213	0.768E+0
5.303	167.9	5.513	5.452	5.842	0.245E+2	0.255	0.722E+0
5.224	170.8	5.418	5.357	5.805	0.281E+2	0.278	0.631E+0
5.158	172.9	5.350	5.288	5.744	0.286E+2	0.319	0.620E+0
5.100	175.0	5.281	5.220	5.720	0.317E+2	0.338	0.559E+0
5.050	176.8	5.222	5.161	5.696	0.343E+2	0.357	0.516E+0
5.004	179.0	5.150	5.089	5.757	0.465E+2	0.310	0.381E+0
4.708	188.0	4.856	4.795	5.448	0.450E+2	0.632	0.394E+0
4.536	193.9	4.663	4.602	5.385	0.607E+2	0.729	0.292E+0
4.415	197.9	4.533	4.471	5.331	0.723E+2	0.827	0.245E+0
4.322	200.9	4.435	4.373	5.278	0.804E+2	0.934	0.220E+0
4.247	203.4	4.353	4.291	5.260	0.931E+2	0.973	0.190E+0
4.184	205.5	4.284	4.223	5.255	0.108E+3	0.984	0.164E+0
4.130	207.3	4.225	4.164	5.258	0.124E+3	0.979	0.143E+0
4.083	208.9	4.173	4.112	5.280	0.147E+3	0.930	0.120E+0
4.041	210.2	4.131	4.069	5.248	0.151E+3	1.000	0.117E+0

where pCu_F' represents the free cupric ion concentration based on the uncorrected Cu-ISE calibration curve.

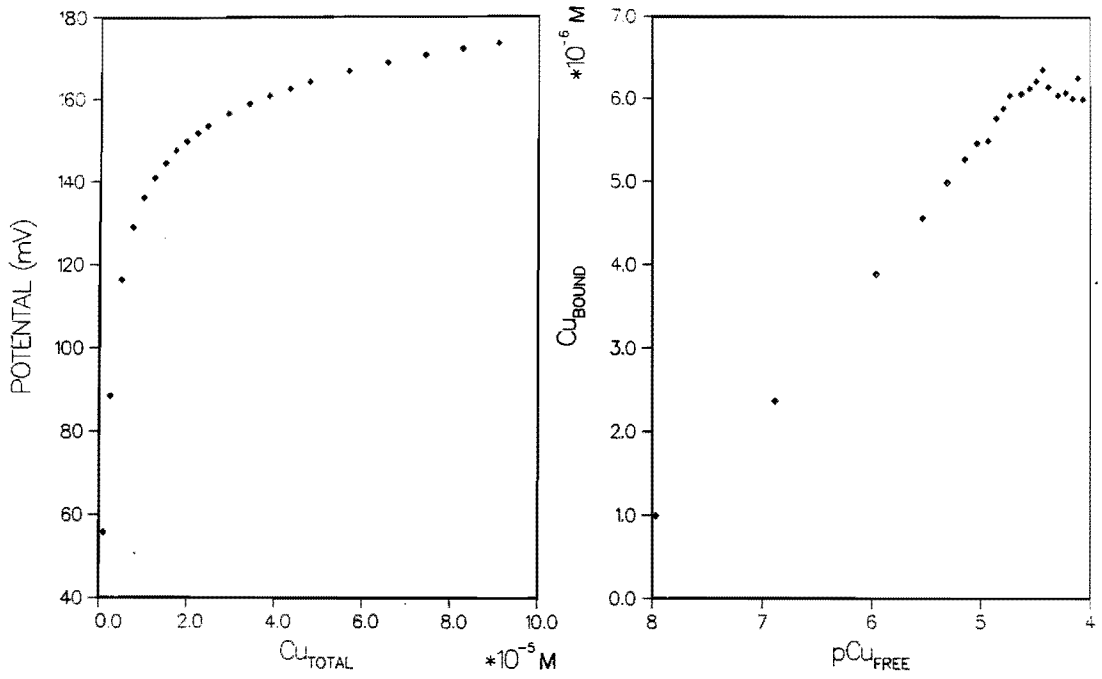

Figure C.1. Cu-ISE titration of 5 mg/L humic acid with copper: a) Cu_T vs. potential and b) Klotz plot.

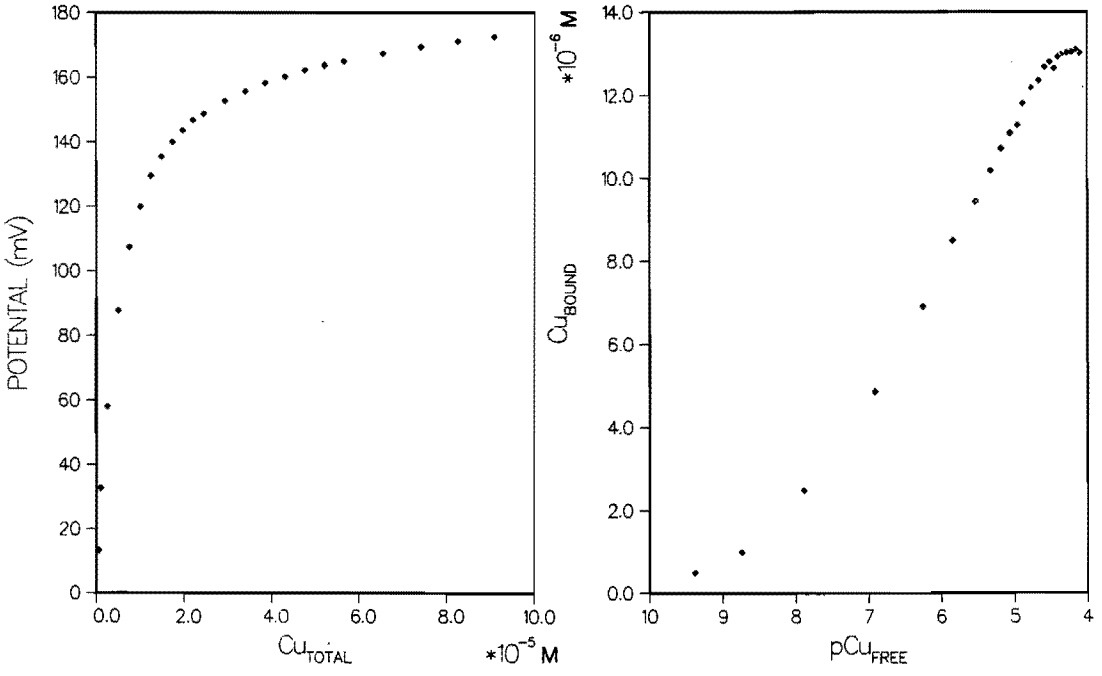

Figure C.2. Cu-ISE titration of 10 mg/L humic acid with copper: a) Cu_T vs. potential and b) Klotz plot.

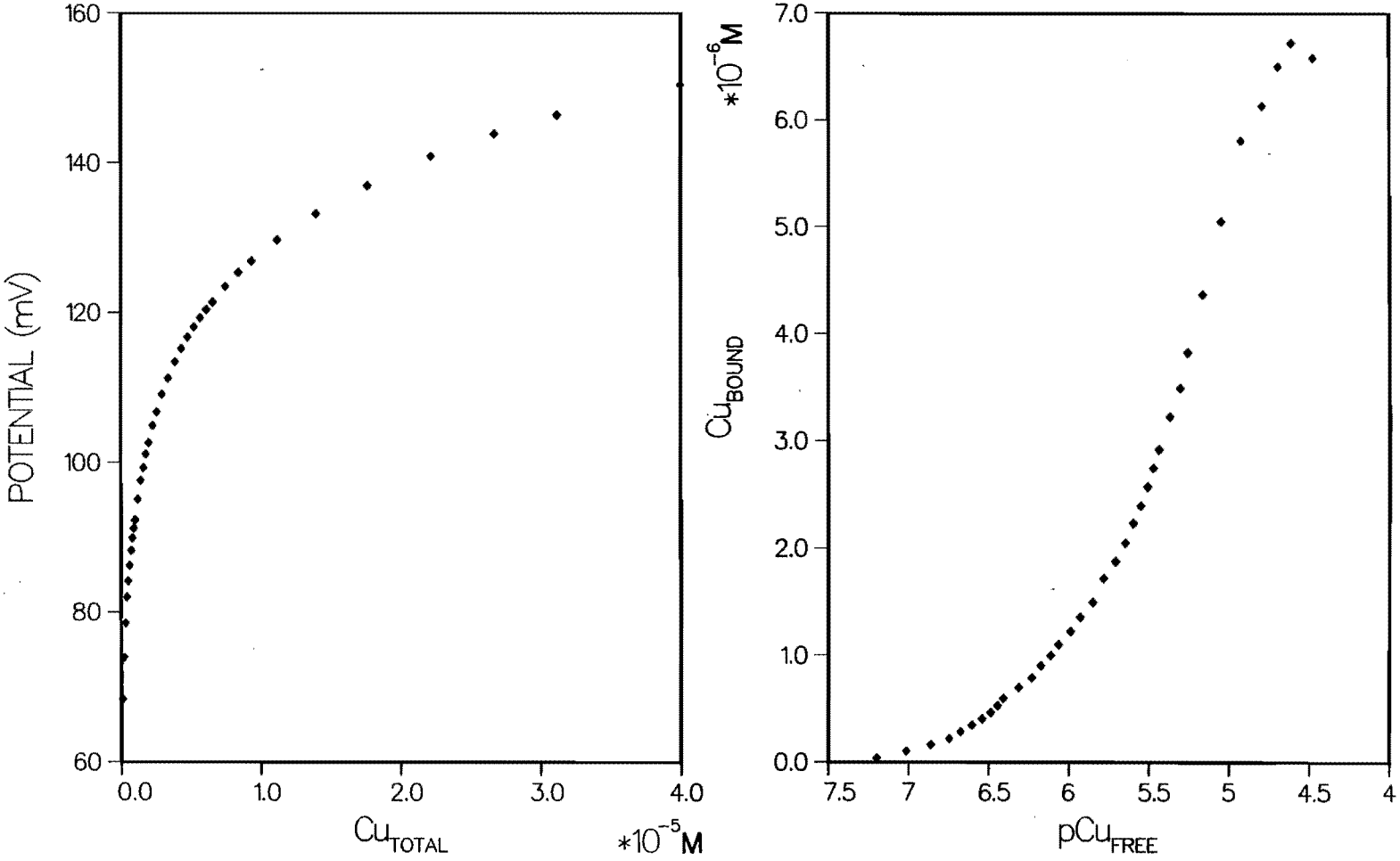

Figure C.3. Cu-ISE titration of copper with raw shale leachate (RSL) obtained from batch static 48 hr extraction: a) Cu_T vs. potential and b) Klotz plot.

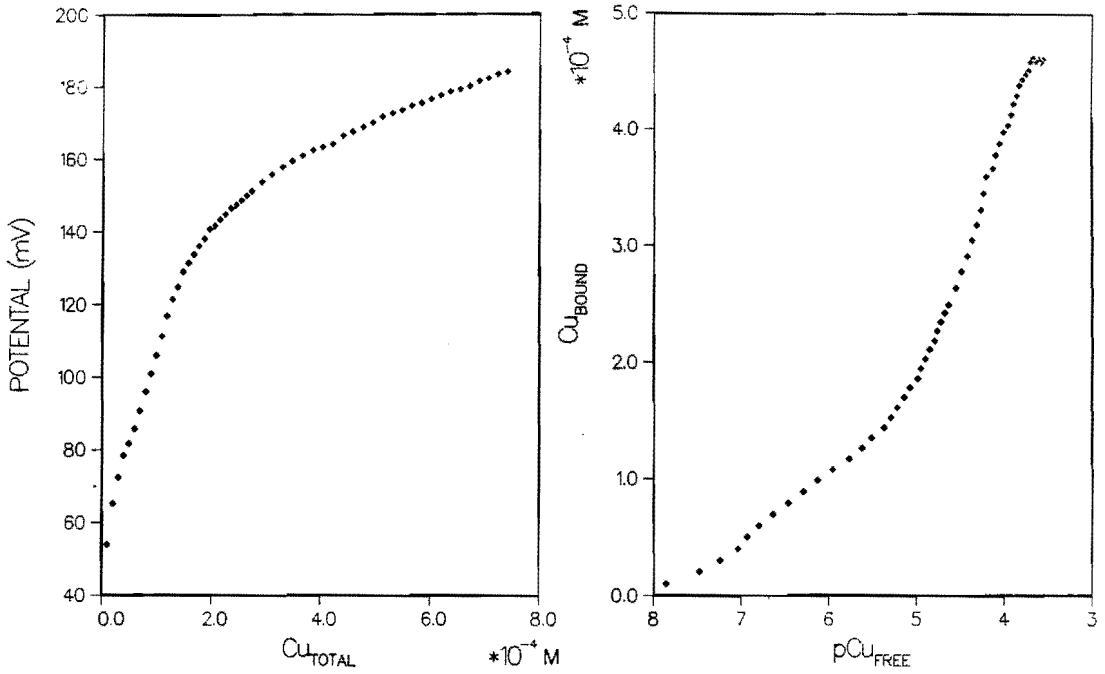

Figure C.4. Cu-ISE titration of copper with 50 percent raw shale leachate (RSL) in MAAP medium: a) Cu_T vs. potential and b) Klotz plot.

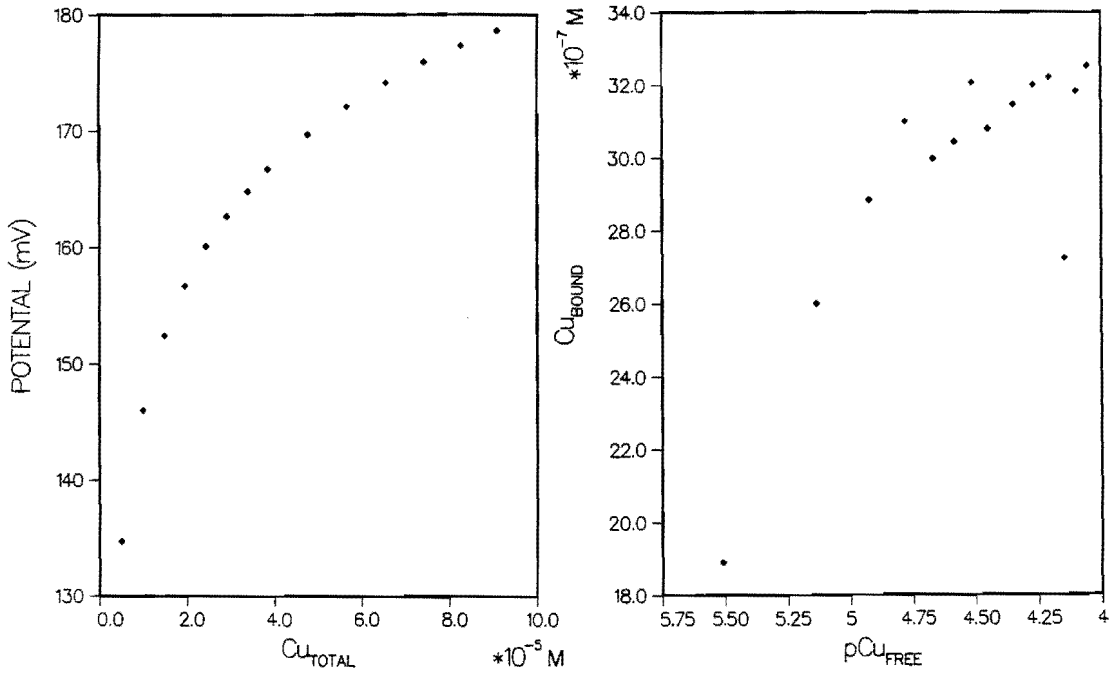

Figure C.5. Cu-ISE titration of the first pore volume of raw shale leachate (RSL_1) collected from an upflow column with copper: a) Cu_T vs. potential and b) Klotz plot.

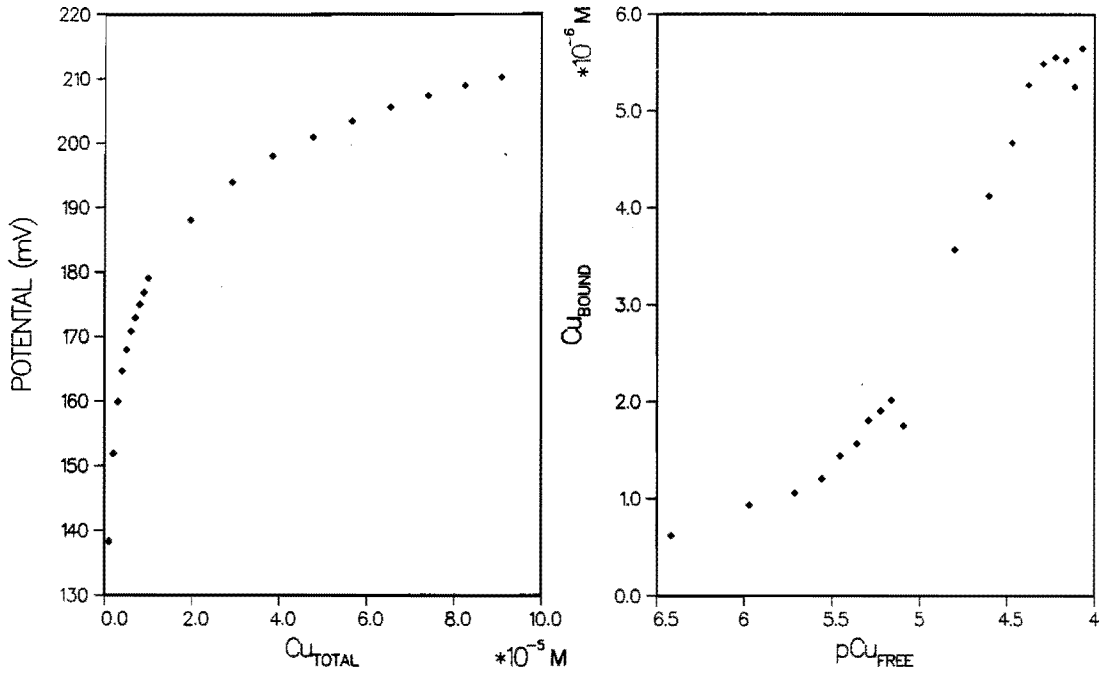

Figure C.6. Cu-ISE titration of the third pore volume of raw shale leachate (RSL_3) collected from an upflow column with copper: a) Cu_T vs. potential and b) Klotz plot.

Appendix D

Differential Pulse Anodic Stripping Voltammetry

Table D.1. Summary of results obtained from DPASV complexometric titration of EDTA with copper.

pCu_T	DPASV CURRENT (nA)	pCu_F	pCu_B	$\frac{Cu_F}{Cu_B}$	$\bar{\nu}$	$\frac{\bar{\nu}}{Cu_F}$
4.700	46.00	6.397	4.709	0.205E+0	0.196	0.488E+1
4.525	176.00	5.979	4.541	0.364E+0	0.288	0.275E+1
4.400	287.00	5.795	4.418	0.420E+0	0.382	0.238E+1
4.304	393.00	5.671	4.323	0.449E+0	0.475	0.223E+1
4.224	433.00	5.632	4.241	0.407E+0	0.574	0.246E+1
4.158	428.00	5.637	4.173	0.344E+0	0.672	0.291E+1
3.964	1626.00	5.081	3.998	0.826E+0	1.004	0.121E+1
3.926	3726.00	4.726	4.001	0.188E+1	0.998	0.532E+0
3.892	5580.00	4.552	3.999	0.280E+1	1.002	0.357E+0
3.860	7620.00	4.418	4.001	0.383E+1	0.998	0.261E+0
3.831	9700.00	4.313	4.004	0.491E+1	0.990	0.204E+0

Table D.2. Summary of results obtained from DPASV complexometric titration of 10 mg/L of humic acid with copper.

pCu_T	DPASV CURRENT (nA)	pCu_F	pCu_B	$\frac{Cu_F}{Cu_B}$	$\bar{\nu}$	$\frac{\bar{\nu}}{Cu_F}$
6.423	38.00	8.184	6.431	0.176E+0	0.930	0.142E+1
6.383	42.00	7.866	6.398	0.340E+0	1.004	0.738E+0
6.346	47.00	7.687	6.366	0.478E+0	1.078	0.524E+0
6.225	69.00	7.258	6.267	0.102E+1	1.355	0.245E+0
6.133	93.00	7.034	6.191	0.144E+1	1.614	0.175E+0
6.057	115.00	6.899	6.124	0.168E+1	1.882	0.149E+0
5.994	133.00	6.816	6.065	0.177E+1	2.158	0.141E+0
5.940	162.00	6.703	6.022	0.209E+1	2.381	0.120E+0

Table D.3. Summary of results obtained from DPASV complexometric titration of raw shale leachate (RSL) with copper.

pCu_T	DPASV CURRENT (nA)	pCu_F	pCu_B	$\frac{Cu_F}{Cu_B}$	$\bar{\nu}$	$\frac{\bar{\nu}}{Cu_F}$
5.828	29.00	6.497	5.933	0.273E+1	0.493	0.155E+1
5.776	32.00	6.479	5.872	0.247E+1	0.567	0.171E+1
5.741	66.00	6.301	5.881	0.380E+1	0.555	0.111E+1
5.652	65.00	6.302	5.762	0.288E+1	0.730	0.146E+1
5.601	124.00	6.102	5.765	0.460E+1	0.724	0.917E+0
5.555	170.00	5.991	5.753	0.578E+1	0.745	0.730E+0
5.514	184.00	5.963	5.705	0.552E+1	0.833	0.765E+0
5.477	220.00	5.896	5.685	0.615E+1	0.871	0.686E+0
5.443	259.00	5.835	5.669	0.683E+1	0.904	0.618E+0
5.412	324.00	5.748	5.681	0.858E+1	0.879	0.492E+0
5.355	406.00	5.658	5.654	0.991E+1	0.936	0.426E+0
5.329	435.00	5.630	5.630	0.999E+1	0.989	0.422E+0

Table D.4. Summary of results obtained from DPASV complexometric titration of raw shale leachate (RSL_2) with copper.

pCu_T	DPASV CURRENT (nA)	pCu_F	pCu_B	$\frac{Cu_F}{Cu_B}$	$\bar{\nu}$	$\frac{\bar{\nu}}{Cu_F}$
5.810	40.00	6.430	5.929	0.316E+1	0.370	0.996E+0
5.758	51.00	6.370	5.880	0.323E+1	0.415	0.973E+0
5.679	82.00	6.235	5.821	0.385E+1	0.475	0.816E+0
5.625	125.00	6.098	5.803	0.508E+1	0.495	0.619E+0
5.577	162.00	6.008	5.778	0.589E+1	0.524	0.534E+0
5.534	172.00	5.986	5.723	0.545E+1	0.595	0.577E+0
5.495	176.00	5.979	5.668	0.489E+1	0.676	0.643E+0
5.460	218.00	5.900	5.656	0.570E+1	0.694	0.551E+0
5.427	319.00	5.754	5.704	0.891E+1	0.622	0.353E+0
5.397	326.00	5.745	5.656	0.814E+1	0.695	0.387E+0
5.368	364.00	5.701	5.639	0.866E+1	0.722	0.363E+0
5.342	422.00	5.642	5.644	0.100E+2	0.714	0.313E+0
5.317	439.00	5.626	5.610	0.962E+1	0.772	0.327E+0

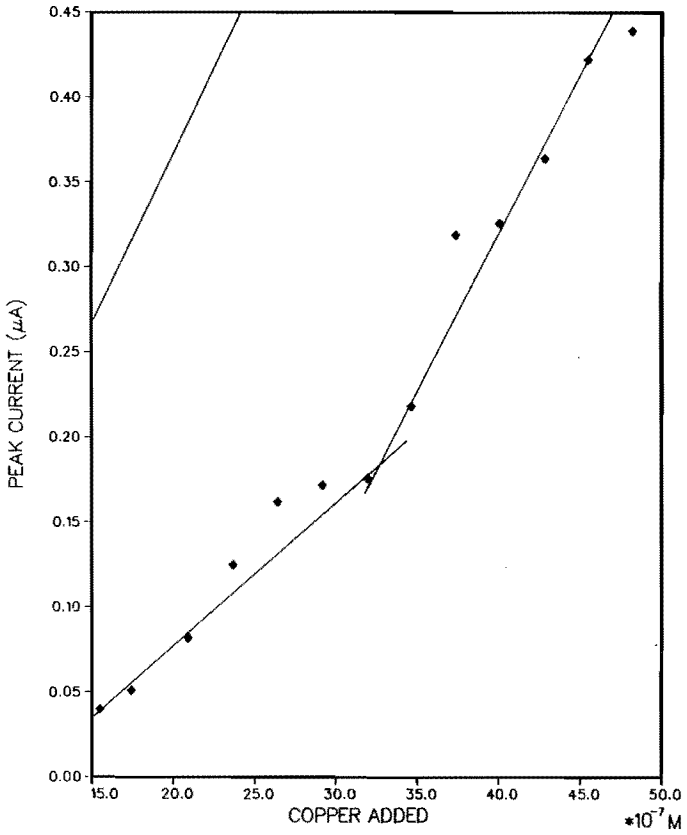

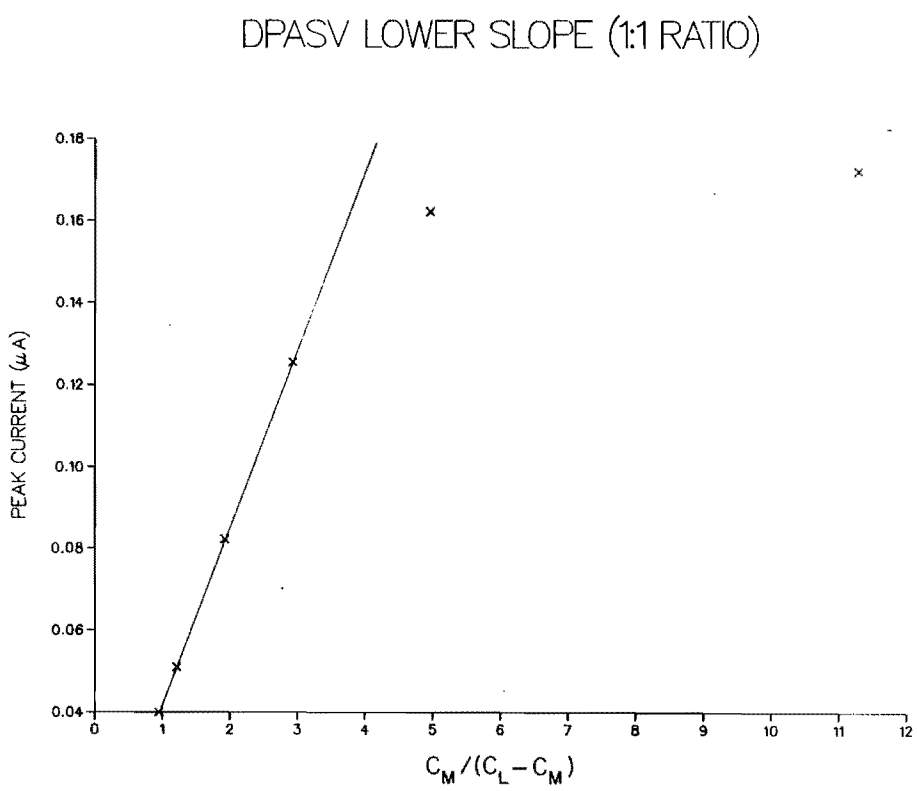

Figure D.1. DPASV complexometric titration curve for raw shale leachate (RSL) with copper: a) peak current vs. copper added and b) peak current vs. $(C_M)/(C_L-C_M)$ based on a 1:1 stoichiometry.

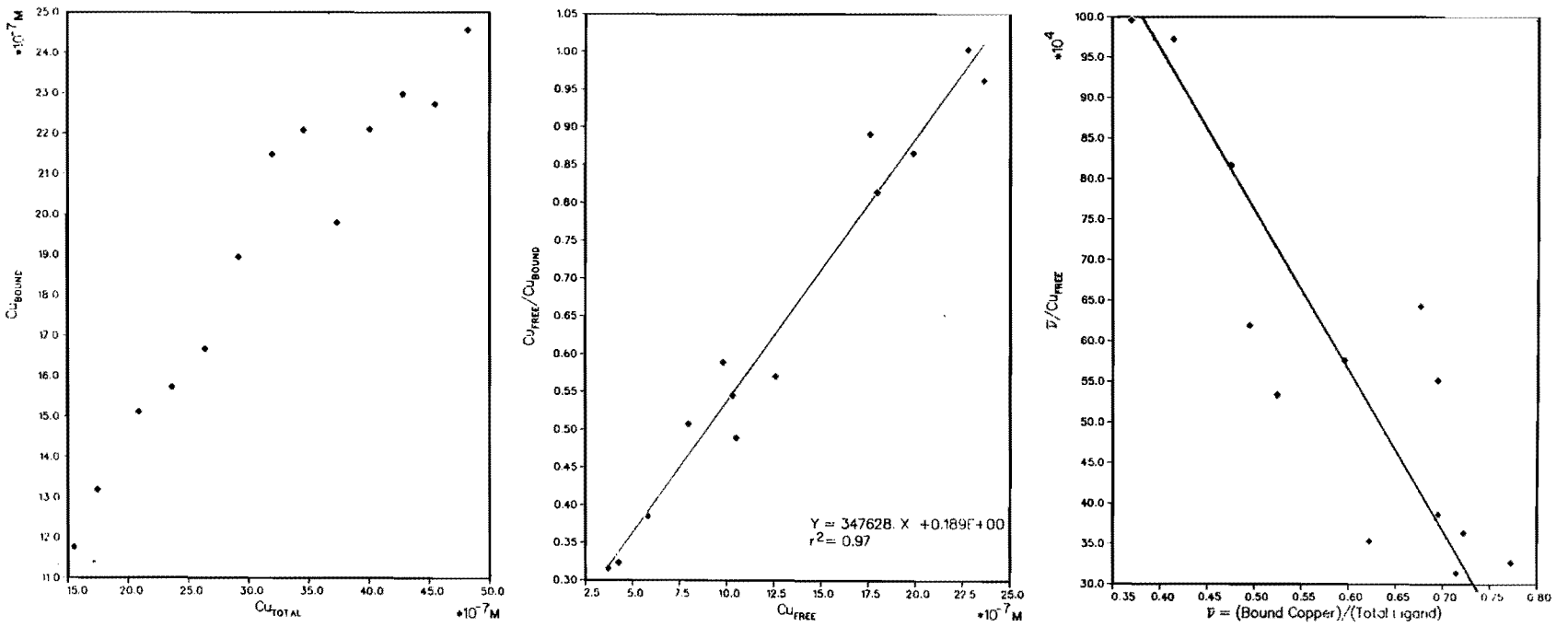

Figure D.2. DPASV titration of the raw oil shale leachate (RSL) with copper: a) Cu_T vs. Cu_{BOUND}, b) Ruzic plot, and c) Scatchard plot.

Appendix E

Algal Bioassay

Table E.1. Experimental results for the determination of copper adsorption onto borosilicate Erlenmeyer flasks in the presence of the modified algal medium (MAAP).

Cu (II) Concentration (M/L)	Soaked[a] (M/L)	Unsoaked (M/L)
10^{-4}	9.15×10^{-5}	1.45×10^{-4}
10^{-5}	8.03×10^{-6}	8.17×10^{-6}
10^{-6}	1.17×10^{-6}	1.02×10^{-6}

[a]Erlenmeyer flasks soaked with copper concentration for 48 hr, then medium was discarded, and fresh medium was added and equilibrated for 1/2 hr before detecting the concentration with Cu-ISE.

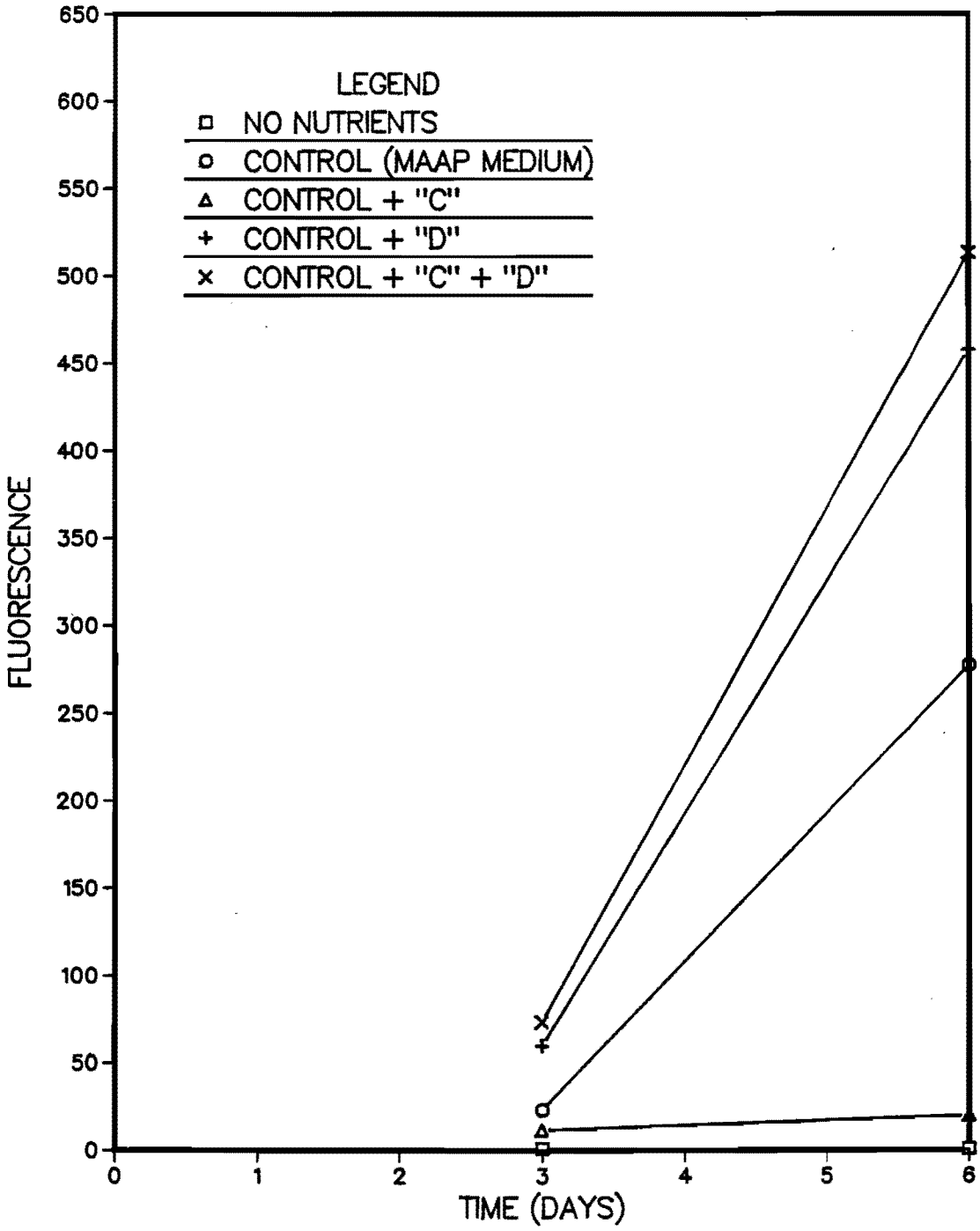

Figure E.1. Growth response of S. capricornutum in MAAP medium relative to other test media.

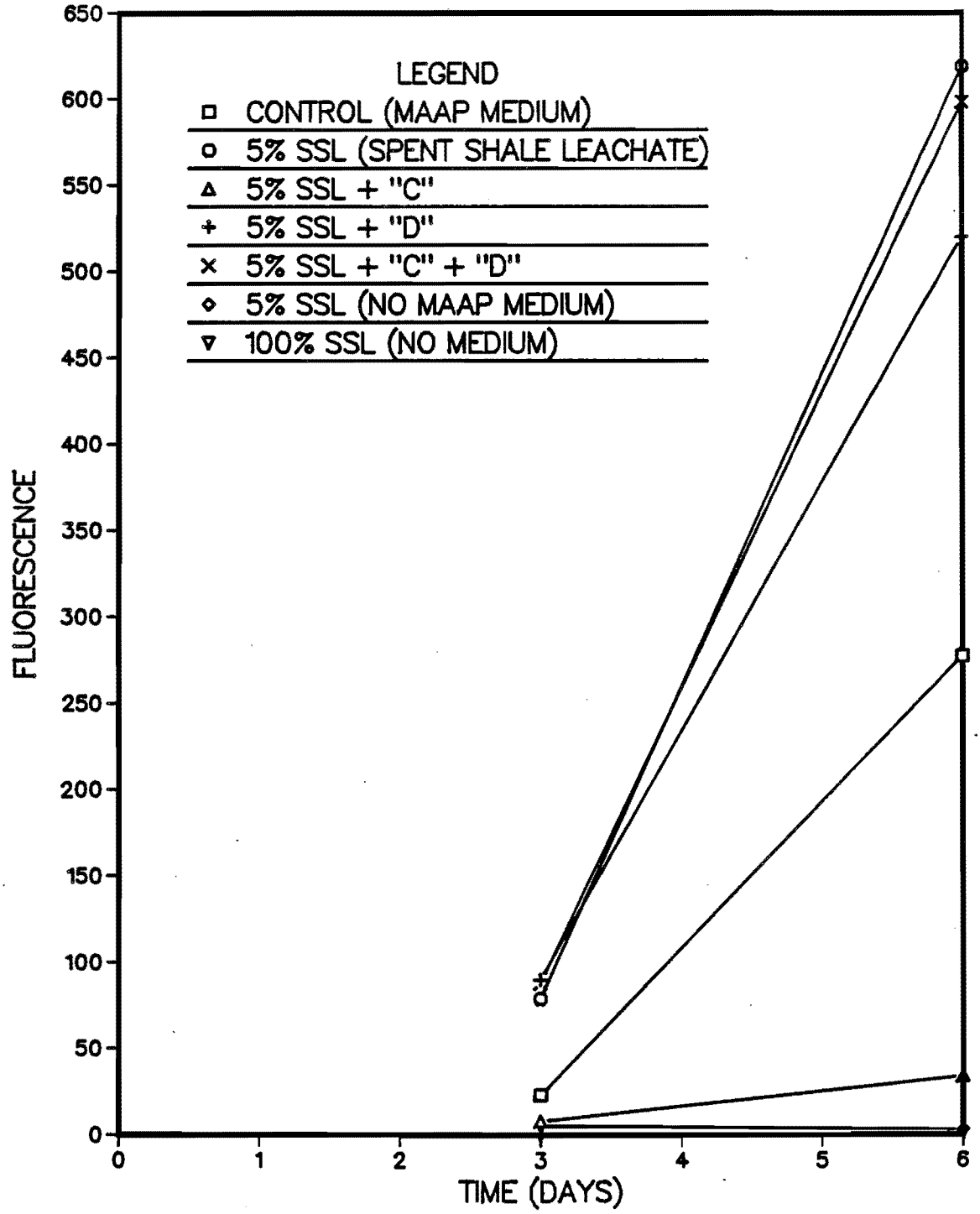

Figure E.2. Growth responses of S. capricornutum in different algal assay media containing spent shale leachate (SSL).

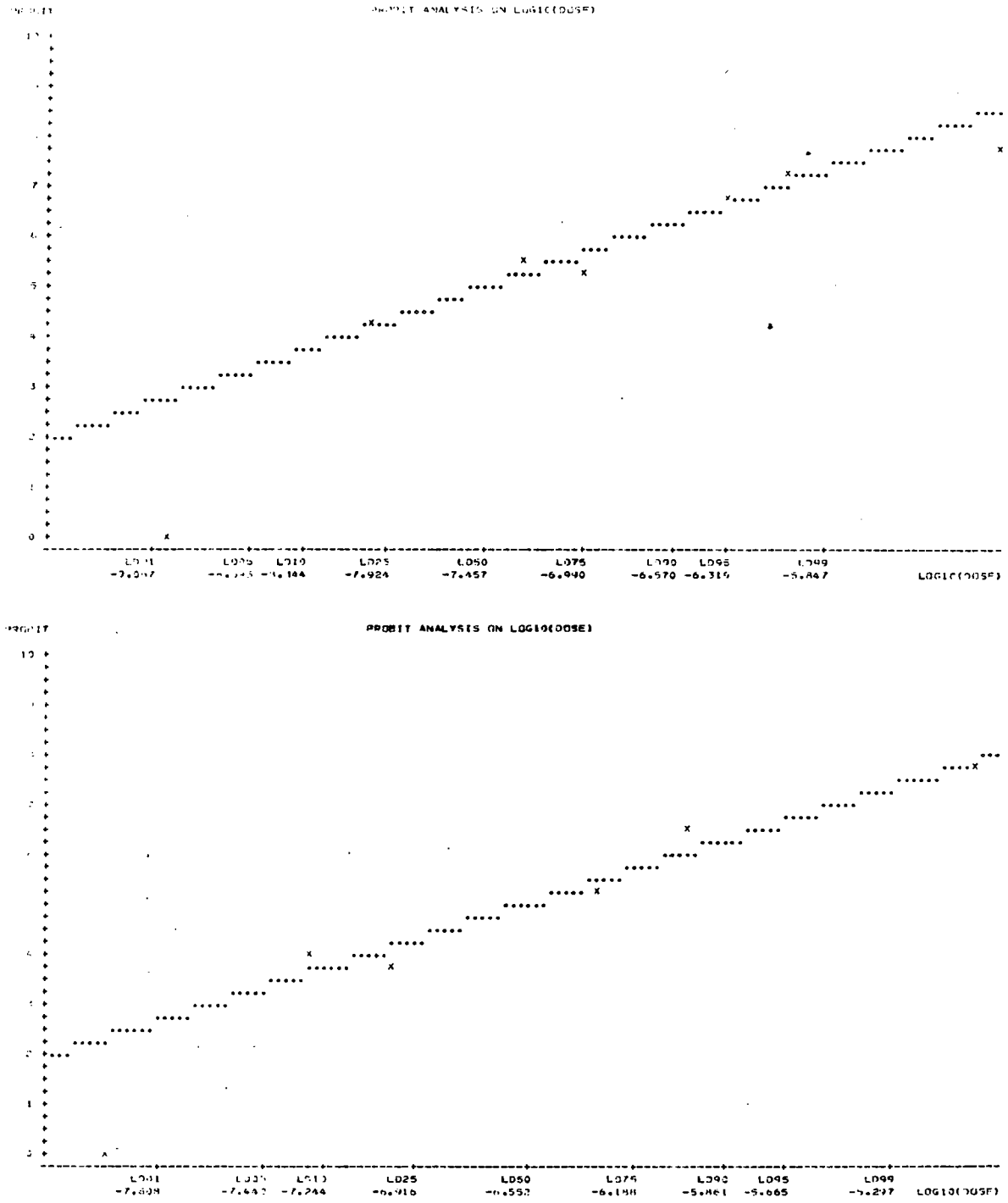

Figure E.3. Probit plots of metals: a) cadmium and b) nickel.

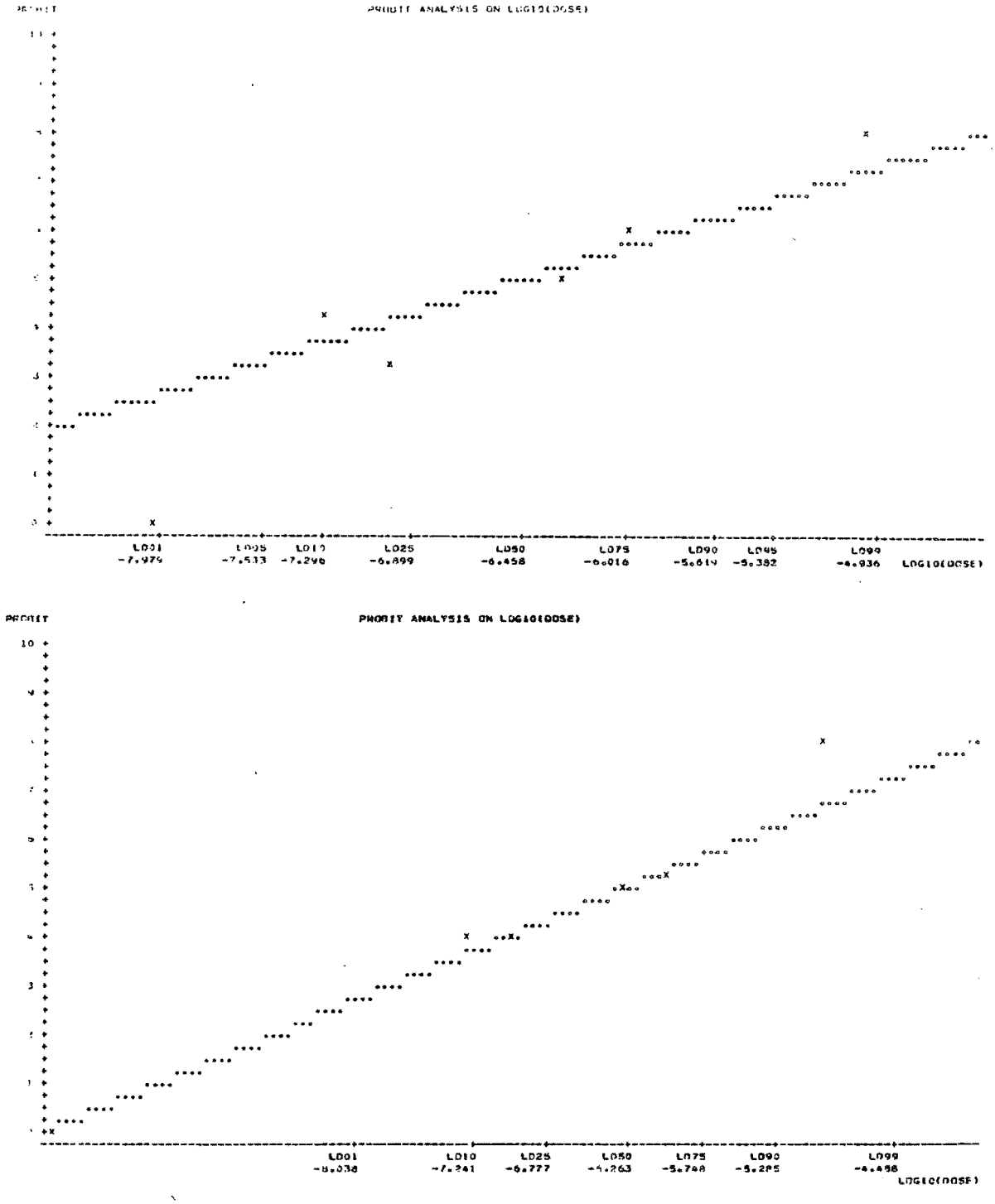

Figure E.4. Probit plots of copper with: a) 5 mg/L humic acid and b) 10 mg/L humic acid.

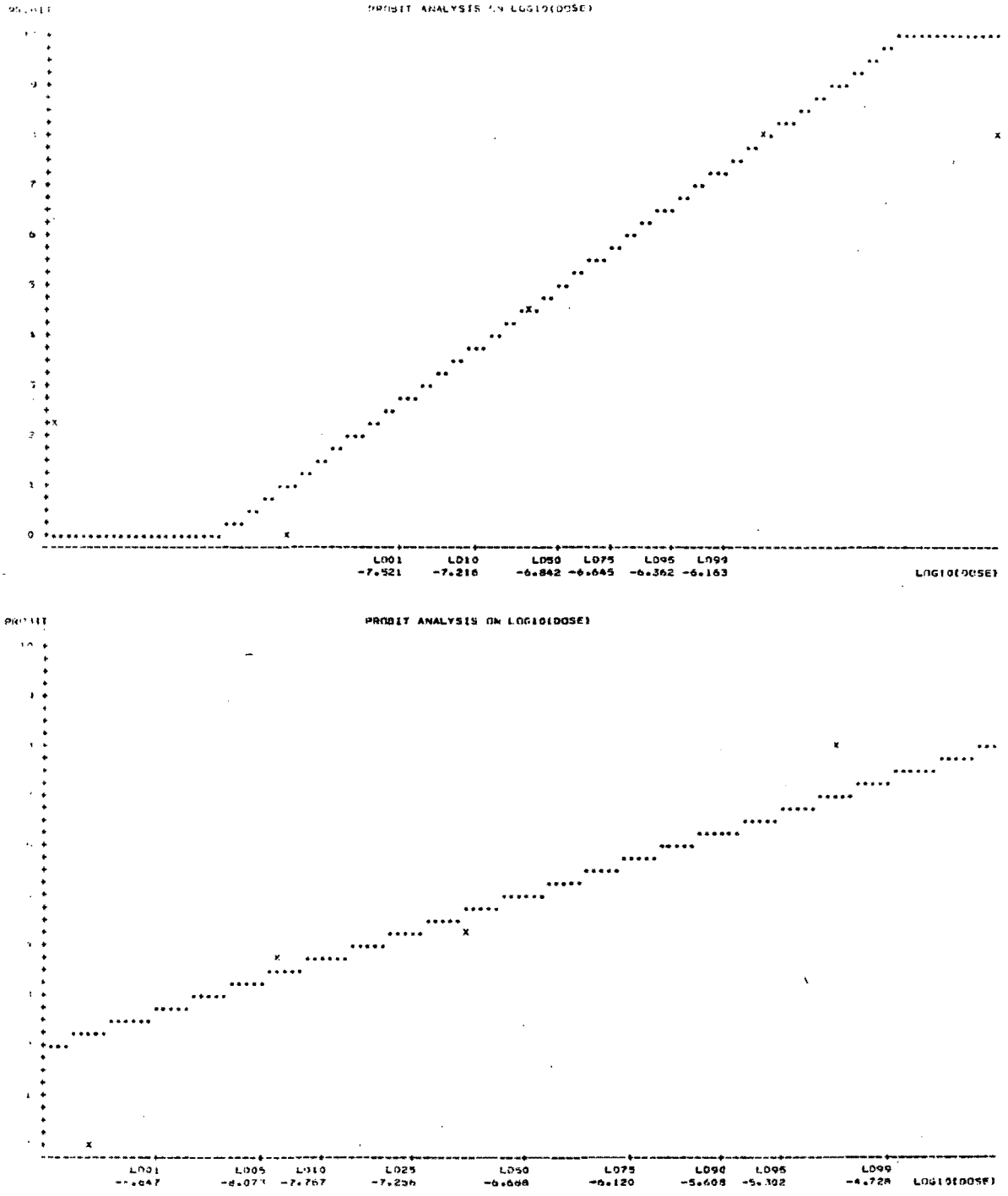

Figure E.5. Probit plots of copper with: a) 10 percent UF diafiltered raw shale leachate (RSL) and b) 50 percent of RSL.

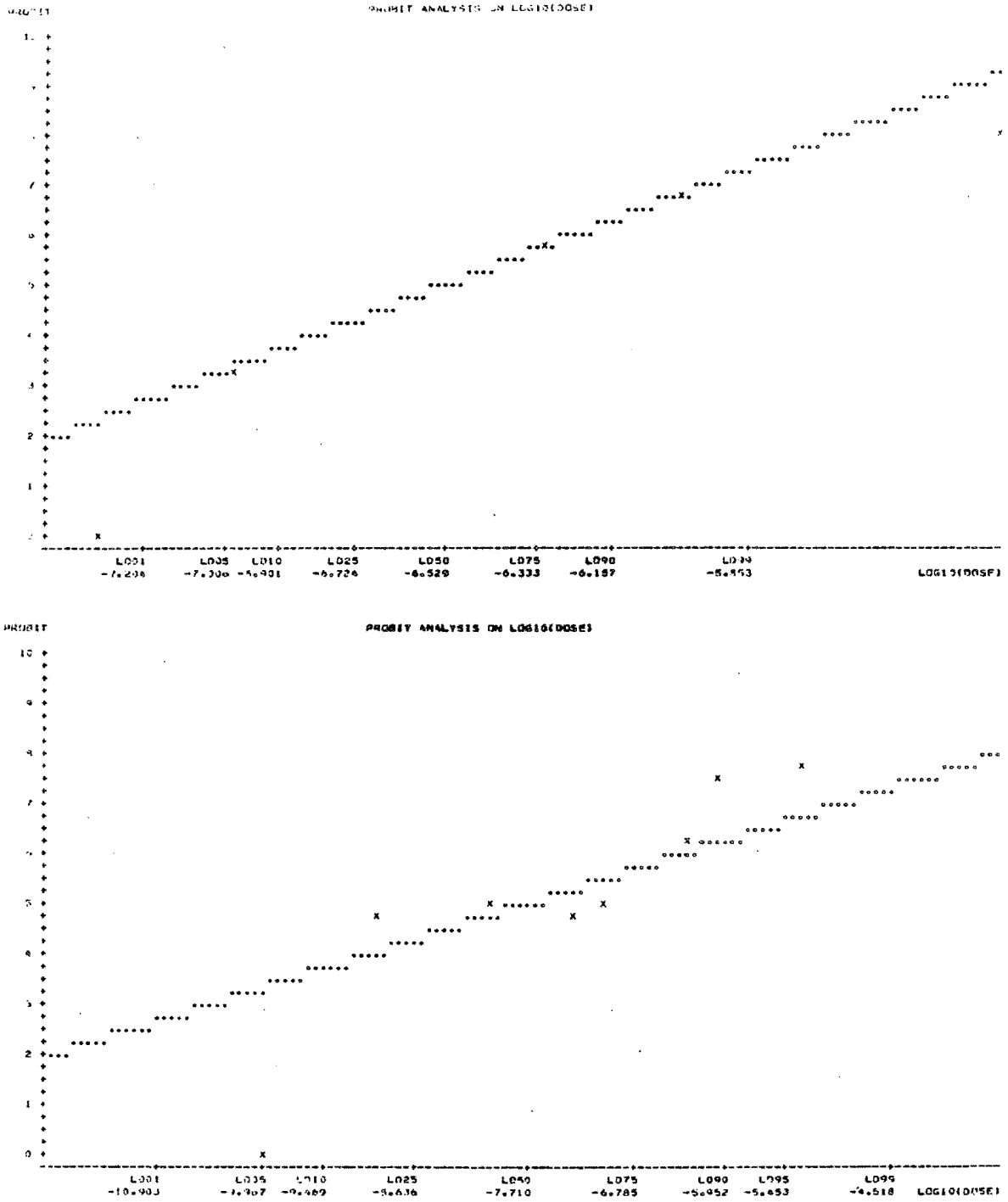

Figure E.6. Probit plots of cadmium with: a) 10 percent UF diafiltered raw shale leachate (RSL) and b) 50 percent of RSL.

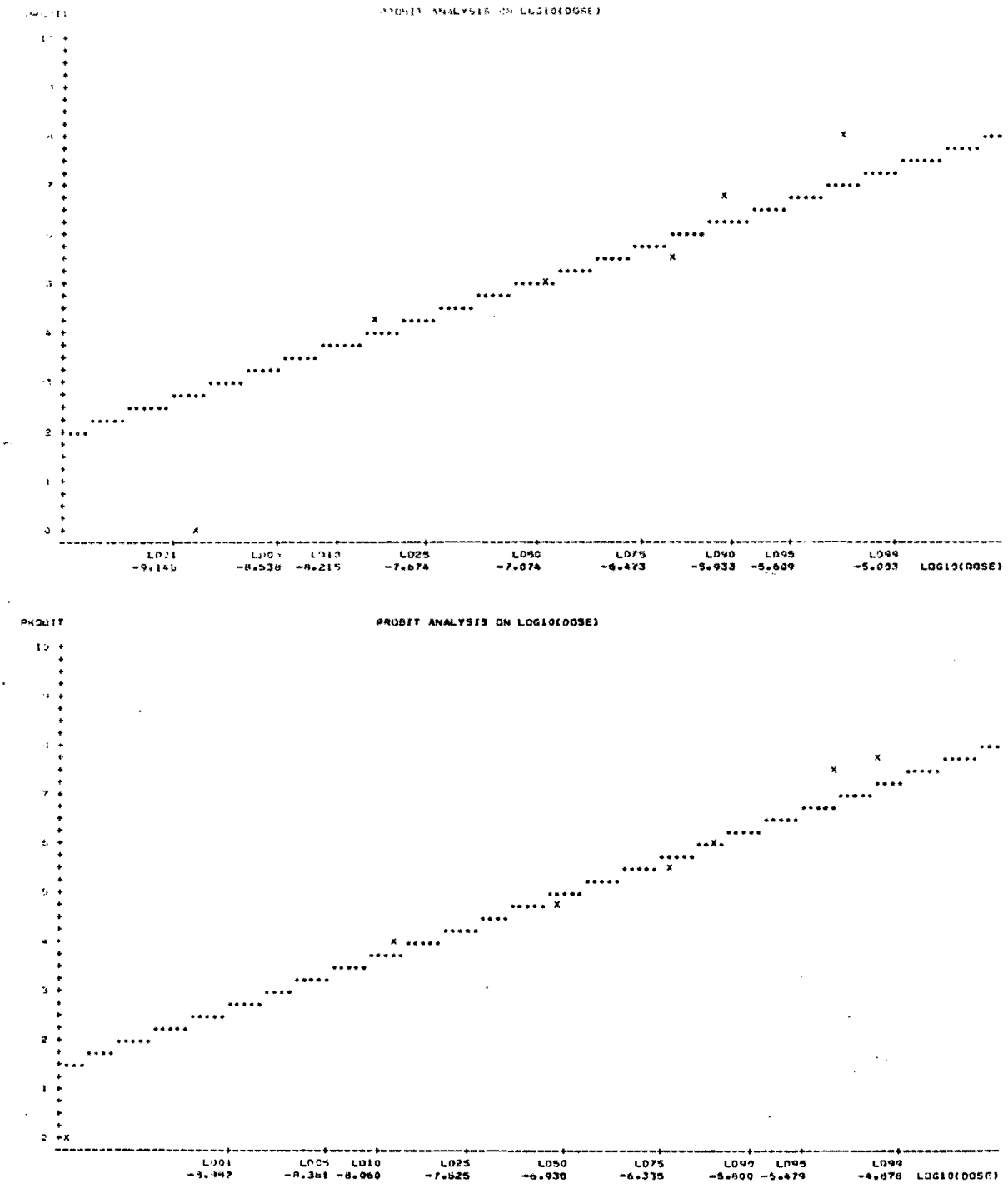

Figure E.7. Probit plots of nickel with: a) 10 percent UF diafiltered raw shale leachate (RSL) and b) 50 percent of RSL.

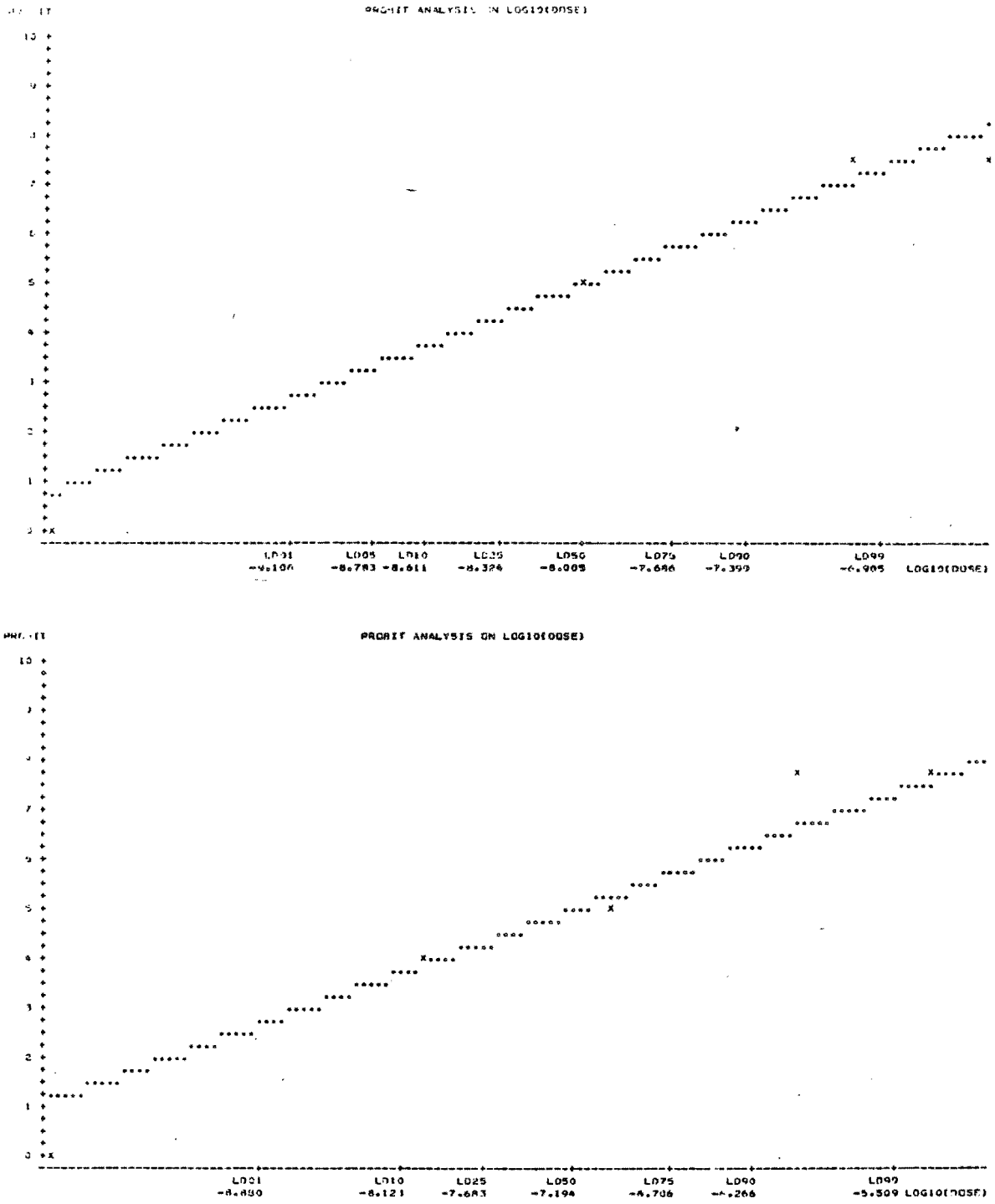

Figure E.8. Probit plots of: a) copper and b) copper with 5 percent RSL (2:1).